Characterization of a novel VAMP2 pathology in Parkinson's Disease

By

Jianqun Gao

School of Medicine

The thesis submitted in partial fulfillment of the requirement of the award of Master Degree of Neuroscience at Flinders University

July, 2015

Contents

List of Figures:

List of Tables:

Abstract

In addition to its well-established contribution to classical clinical manifestation, emerging evidence suggests synaptic degeneration may be an early event in neurodegeneration in Parkinson's disease (PD). VAMP2 (Synaptobrevin-2) is the synaptic vesicle protein that forms the SNARE complex, the protein machinery for neurotransmitter release, with the presynaptic plasma membrane-resided proteins syntax-1 and SNAP-25. The maintenance of sufficient number and functional conformation of VAMP2 on synaptic vesicles is tightly regulated for proper neurotransmitter release, and its dysfunction may contribute to neurological diseases.

By using immunohistochemistry and immunoblot, we identified the N-terminally truncated VAMP2 (tVAMP2), but not the full-length VAMP2 (fVAMP2), as an important component of Lewy bodies isolated from brains of PD and DLB (Dementia with Lewy bodies), and tVAMP2 positive-stained Lewy bodies (LBs) and Lewy neurites (LNs) were detected in various regions of PD brain. This robust immunoreactivity of tVAMP2 in Lewy pathologies was comparable to that of α-synuclein, the prominent component of Lewy bodies and Lewy neurites, both of which were pathological characteristics of PD and DLB. Furthermore, using immunofluorescence double-staining, we showed co-localization of tVAMP2 and α-synuclein in Lewy bodies and Lewy neurites, suggesting their synergetic effect on the formation of Lewy bodies and Lewy neurites. Finally, in purified Lewy bodies from PD and DLB brains, the presence of two human VAMP2 fragments (aa32-47 and aa60-83) was confirmed by mass spectrometry, while a large peptide at the N-terminus (aa2-30) was undetectable. These findings indicated the unique value of tVAMP2 in understanding the pathogenesis and pathological diagnosis of PD and DLB. Further experiments are required to identify the N-terminal truncation site.

Declaration

I certify that this thesis does not contain material which has been accepted for the award of any degree or diploma; and to the best of my knowledge and belief it does not contain any material previously published or written by another person except where due reference is made in the text of this thesis.

Jianqun Gao

Acknowledgements

First and foremost, I would like to give my sincere thanks to Dr Timothy Chataway, my principal supervisor, for all his wisdom, enthusiasm, guidance, and support over the period of my study in Flinders University. I appreciate his wonderful help in my experimental design and his valuable advices in my thesis writing. Also, I would like to thank my associate supervisor, A/Prof John Power, my former supervisor, Dr WeiPing Gai, and my assessor supervisor, Dr Hakan Muyderman, for their support and contribution in the fulfillment of my study.

To Ms Nusha Chegeni Farahani and Dr Alex Colella, I am very grateful for your great help in my experiments of gel electrophoresis and mass spectrometry. To Fariba Chegini, I cannot thank you enough for your technical support and patient guidance in my experiment. To Tong Chen, thank you for the insightful conversation every time we met along the corridor into the intricacies of VAMP2 and referring me to numerous articles about my project that I would not have otherwise taken note of.

Last, but definitely not the least, I am so grateful for the support from my family. I cannot even begin to thank you enough for the love you have shown throughout my life. Without you, I wouldn't be where I am today.

Abbreviations

α-synuclein	αSyn
AD	Alzheimer's Disease
BONT	Botulinal neurotoxins
CNS	Central Nervous System
COX	cytochrome C oxidase
CSP	Cysteine String Protein
DAT	dopamine transporter
DLB	Dementia with Lewy bodies
GCI	Glial Cytoplasmic Inclusion
GSK-3β	glycogen synthase kinase 3β
LB	Lewy body
LN	Lewy neurite
MSA	Multiple System Atrophy
NAC	nonamyloid component
PD	Parkinson's Disease
PSP	Progressive Supranuclear Palsy
REM	Rapid Eye Movement
SM protein	Sec1/Munc18-like protein
SN	substantia nigra
SNAP	Soluble N-ethylmaleimide-sensitive factor (NSF) Attachment Protein
SNAP-25	25-kDa synaptosomal-associated protein
SNARE	SNAP Receptor
TeNT	Tetanus neurotoxin
TG	neurofibrillary tangles
TH	tyrosine hydroxylase

Ub	ubiquitin
VAMP2	Vesicle Associated Membrane Protein 2

Chapter 1

Introduction

1.1 Parkinson's Disease (PD)

1.1.1 Epidemiology and Definition of PD

Parkinson's Disease (PD) is the second most frequent neurodegenerative disorder after Alzheimer's Disease and affects approximately 7 million people around the world, most of which are elderly people above the age of 50, with a prevalence of approximately 1% at age 65 and nearly 5% at age 85 [1, 2]. PD is a progressive systematic neurodegenerative disorder disrupting central and peripheral nervous systems and many other organs (e.g. spinal cord, sympathetic and parasympathetic ganglia and plexuses, the intramural enteric nervous system, the cardiac nervous system, submandibular gland, adrenals, retina, skin, and other visceral organs)[3-11] involving remarkably selective neural circuits throughout the course of the disease. There are two forms of PD which are differentiated by fundamental molecular and genetic factors. The familial form is usually early-onset PD, in which gene mutations have been identified, whereas the sporadic form is often late-onset PD, which is the most frequent type of the disease[12]. PD can be diagnosed at any age with a mean duration of 15 years from diagnosis till death[13], and the onset of symptoms may precede clinical recognition by many years[14]. Consistent with the pathology of the disease, its manifestations include motor and non-motor symptoms. The motor symptoms, which are distinctive clinically and respond well to dopamine replacement therapy, are the result of death of a substantial number of dopaminergic neurons in the substantia nigra (SN) of midbrain, especially the ventral part of the pars compacta, resulting in dysfunction of the basal ganglia, a cluster of deep nuclei that participate in the initiation and execution of movements[15]. However, the cause of neuronal death has

remained unclear till now. The clinical diagnosis of PD is principally based on the presence of one or more of the four most common motor symptoms of the disease, also called primary motor symptoms, including resting tremor, bradykinesia (slow movement), rigidity (increased muscular tone) and postural instability[16]. Parkinsonism (also known as Parkinsonian Syndrome, atypical Parkinson's, or secondary Parkinson's) is a neurological syndrome characterized by the above four main motor symptoms. Parkinsonian syndromes can be classified into four subtypes: idiopathic, acquired (e.g. cerebrovascular injury and medication induction), hereditary parkinsonism, and multiple system degeneration. In addition, PD patients may also experience other secondary motor symptoms including gait impairment (freezing of gait), micrographia, mask-like expression and unwanted accelerations[16]. Furthermore, as a result of the interference with the peripheral nervous systems, PD patients are very likely to suffer from some non-motor symptoms such as constipation[17], dementia[18], impaired olfaction (loss of sense of smell), REM (rapid eye movement) behavior disorder, mood disorders, orthostatic hypotension and depression[16]. These non-motor symptoms can be found in different systems of the body involving sensory, autonomic, emotional, behavioral and cognitive functions sometimes long before the occurrence of the motor symptoms. However, they are often unrealized or ignored by patients in the early stage of the disease, and become important contributors to overall disability, especially in the late stage, due to the fact that most of them show little or even no response to dopamine replacement therapy[19].

1.1.2 Pathological Characteristic of PD

The defining and widely-accepted pathological characteristic of PD is the formation and development of Lewy bodies (LBs) and Lewy neurites (LNs) in selective brain regions and peripheral nervous system, with or without

substantial neuronal loss or gliosis[20]. There are two types of Lewy bodies. 1. *Classic* Lewy bodies are intracytoplasmic spherical neuronal inclusions 8-30μm in diameter with a hyaline eosinophilic core, concentric lamellar bands and a narrow pale-staining halo. It stains strongly for α-synuclein which aggregates to form the fibrillar core[21]. 2. *Cortical* Lewy bodies are eosinophilic, rounded, angular, or reniform structures without a halo. The anatomical distribution of Lewy bodies and Lewy neurites and the progression of striatal dopaminergic neurons hypofunction led to a reduction of tyrosine hydroxylase (TH), the rate-limiting enzyme of dopamine synthesis which is usually strongly correlated to the manifestation, duration and severity of clinical symptoms of individuals[22]. Conversely, in the earlier stages of the disease, dopamine depletion may trigger an increase in dopaminergic cells in the striatum[23, 24] as well as the olfactory bulb [25], acting as a compensatory mechanism. Being the hallmarks of PD and other synucleinopathies, Lewy bodies and Lewy neurites are morphologically unique intraperikaryal and intraneuritic inclusions consisting of numerous proteins, with α-synuclein as the prominent component[26]. The prominence of α-synuclein in Lewy bodies may be due to the fact that α-synuclein antibodies are the most sensitive probes for detecting Lewy bodies and Lewy neurites and that its gene (SNCA) mutations and multiplications are linked to familial PDs. Alpha-synuclein pathology has been recognized in much of the neuraxis other than substantia nigra, including the peripheral cutaneous nerves, autonomic nervous system, enteric nervous system, spinal cord, lower brainstem (dorsal motor nucleus of the vagus), limbic structures (amygdala and hippocampus), and neocortex[5]. There are several other PD-susceptibility genes, including the microtubule-associated protein Tau gene (MAPT)[27], the glucocerebrosidase gene (GBA)[28], and the leucine-rich repeat kinase 2 gene (LRRK2)[29], which may also contribute to the pathogenesis of PD together with SNCA. Lewy bodies also contain many other

proteins such as ubiquitin (Ub) and phosphorylated neurofilaments, but their roles in the etiology of Parkinson's disease remain to be elucidated[30]. According to the Braak staging[31] of PD pathology, which is based on careful postmortem analysis, Lewy bodies first appear in the olfactory bulb, medulla oblongata and pontine tegmentum, with individuals being asymptomatic at this stage. As the disease progresses, Lewy bodies then spread from the lower brainstem (dorsal motor nucleus of vagus and raphe nucleus locus coeruleus) (stage 1-2) to the midbrain substantia nigra pars compacta (SN) (stage 3), progressing to supratentorial compartment (amygdala, nucleus of meynert and Hippocampus) (stage 4) and eventually in the neocortex (cingulate cortex, temporal cortex, frontal cortex, parietal cortex and occipital cortex) (stage 6)[20]. As a result, dopamine production becomes insufficient in certain neurons within parts of the midbrain. Therefore, treatments for PD are mainly through the use of L-dopa and dopamine agonists.

1.2 Other synucleopathic neurodegenerative disorders

1.2.1 Dementia with Lewy bodies (DLB)

Dementia with Lewy bodies (DLB) is a progressive degenerative dementia dominantly affecting elderly people. An epidemiologic research study among a American general population showed that the incidence rate of DLB was 3.5 per 100,000 person-years overall and increased dramatically with age and markedly higher in men[32].

The clinical symptoms of dementia with Lewy bodies overlap with Alzheimer's disease (caused by loss of cholinergic neurons)[33] and Parkinson's disease (caused by death of dopaminergic neurons)[34]. Its primary manifestation is a decline in cognition, which can cause persistent or recurring visual

hallucinations, with REM sleep behavior disorder (RBD) as a symptom often first recognized by the carer for the patient. Other symptoms of DLB include changes in thinking and reasoning, fluctuating confusion and alertness, and memory loss[35]. The time frame in which dementia symptoms appear relative to Parkinson symptoms is the diagnostic criteria for distinguishing DLB from PD. If the dementia onset is more than one year after Parkinson symptoms, the patient will be diagnosed Parkinson's disease with dementia (PDD), otherwise, if both of these two symptoms happen at the same time or within one-year time frame, the diagnosis will be DLB[36]. The anatomical pathological characterization of DLB is the presence of Lewy bodies and the aggregation of α-synuclein in neurons, which are detectable in post mortem brain histology. Therefore DLB is also classified as a synucleopathic neurodegenerative disorder.

Treatment of DLB is mainly aimed at symptom management. For example, acetylcholinesterase inhibitors, such as donepezil, rivastigmine and galantamine, are often used as the first-line therapy for cognitive symptoms of DLB[37, 38]. The treatment for motor symptoms of DLB relies on dopamine replacement therapy through the use of L-dopa.

1.2.2 Multiple System Atrophy (MSA)

Multiple system atrophy (MSA) is a sporadic, progressive degenerative neurological disorder. The incidence rate of the disease is about 0.6-0.7 per 100,000 person-years among the European general populations[39, 40], and is more common in men than in women with the ratios ranging from 1.4:1[41] to 1.9:1[42].

MSA usually progresses more quickly than Parkinson's disease. An analysis of 230 Japanese patients demonstrated that the median time from initial symptom to combined motor and autonomic dysfunction was only 2 years, and patients

with both of these two aspects present within 3 years of onset had a significantly shorter survival[43]. MSA can be classified into two clinicopathological phenotypes: predominantly parkinsonism (MSA-P) and predominantly cerebellar ataxia (MSA-C). The most common initial presentation of the disease is the appearance of an “akinetic-rigid syndrome”, which means slowness of initiation of movement. Other common manifestations of MSA include autonomic dysfunction such as genitourinary problems (erectile dysfunction, urinary incontinence or retention, constipation)[44]; parkinsonism (muscle rigidity, tremor and slow movement) and cerebella ataxia (poor coordination, unbalanced walking)[45]. The definitive diagnosis can only be made pathologically by finding abundant glial cytoplasmic inclusions (GCIs) in the central nervous system[46, 47], and α-synuclein is the major component of GCIs[48]. So together with PD and DLB, MSA also belongs to the synucleinopathies. The treatment mainly focuses on controlling symptoms. L-dopa replacement is reported effective in about 30% of patients with MSA-P, whereas there is no therapy known to be effective in treating MSA-C[49].

1.3 α-synuclein and its role in PD

1.3.1 Biological structure of α-synuclein

Synucleins are ubiquitous presynaptic proteins, namely α, β, γ- Synucleins, encoded by three genes (SNCA, SNCB and SNCG) in humans [50]. These synucleins have a common N-terminal sequence containing a varying number of repeat regions, and they differ in the C-terminal part [51]. Although in the same gene family, they function differently. Alpha-synuclein is identified as a participant in neurodegeneration-related diseases; β-synuclein is associated with neurofibrillary lesions in Alzheimer's disease and hippocampal pathology in

PD and DLB (Dementia with Lewy bodies) but not found in Lewy bodies [52], and is thought to inhibit α-synuclein aggregation [53]; while γ-synuclein may be involved in the progression of many types of cancer[54].

There are three human α-synuclein isoforms of which the full-length isoform is the most important and widely expressed [55]. Full-length α-synuclein is an abundant 14.46 kDa neuronal protein and is composed of 140 amino acids. It is localized in presynaptic terminals where it exists in equilibrium between a soluble, unfolded, monomeric cytosolic state, and an α-helical folded, multimeric membrane-bound state[56-60]. However, α-synuclein is also capable of forming a β-pleated sheet conformation that favors polymerization and aggregation into fibrils[61]. Evidence provided from disease-causing mutations, A53T and E46K, showed increased rates of fibril formation in vitro, whose structure is similar to that of the aggregated α-synuclein detected in Lewy bodies[62, 63]. α-synuclein contains an N-terminal amphipathic amino-terminal domain (residues 1-60), a hydrophobic central core (the nonamyloid component [NAC] region) (residues 61-95), and a negatively charged proline-enriched acidic C terminus (residues 96-140)[62]. The N-terminal domain has seven 11-residue repeats that can fold into alpha helices and is highly conserved among species [64]. It also contains three familial PD point mutations (A30P, A53T and E46K) [51].

1.3.2 Biological function of α-synuclein

α-synuclein is expressed throughout the central nervous system (CNS). One relatively well-studied function of α-synuclein is its role in assisting the release of neurotransmitter from synapses by acting as a chaperone for the synaptic vesicle protein Synaptobrevin-2 (also known as vesicle associated membrane protein 2, VAMP2), to form the SNARE (SNAP (Soluble

N-ethylmaleimide-sensitive factor [NSF] Attachment Protein) REceptor) complex, which mediates docking of synaptic vesicles with the presynaptic membrane during membrane fusion and endocytosis of synaptic vesicles[65]. The maintenance of active conformation of VAMP2 and sufficient number of synaptic vesicles is critical to the regulation of neurotransmitter release. A 10-fold reduction in spontaneous synaptic vesicle fusion was observed in VAMP2 knockout mice[66]. Hence, we hypothesized that the dysfunction of VAMP2 may contribute to the neurodegenerative diseases including PD.

In the formation of SNARE complexes in presynaptic terminals, α-synuclein functions as a molecular chaperone of VAMP2 by binding to the N-terminal 28 amino acids sequence of VAMP2 via its 40-residue highly acidic C-terminus binding domain. Simultaneously, α-synuclein binds to phospholipids (negatively charged anionic lipids) in the plasma membrane via its amphipathic positively-charged, 100-residue N-terminus binding domain [67]. Furthermore, Burre et al. recently demonstrated that it was the membrane-bound state and not the cytosolic unfolded state of α-synuclein that acts as a SNARE chaperone, and membrane binding causing α-synuclein to form functionally active multimers larger than octamers on the membrane surface. Also, the synaptic vesicles which α-synuclein was stably associated with had to be those docked to the presynaptic plasma membrane and engaged in SNARE complex formation [68].

1.3.3 Evidence of α-synuclein in the neuropathology in PD

Recent data suggests that the pathology of neurodegeneration process in PD is primarily due to α-synuclein aggregation related-synapse dysfunction or axon degeneration rather than neuronal loss[69, 70]. α-synuclein showed a significant role in the early onset of PD due to the observation that the missense point

mutations (A30P, E46K, A53T, H50Q, and G51D) [71-75], and duplications and triplications of the gene that encodes α-synuclein (SNCA)[76, 77] may cause α-synuclein to form amyloid-like fibrils in the pathology of PD. In addition, multiplications of α-synuclein have been found in asymptomatic carriers and accounted for approximately 2% of familial cases[78]. Furthermore, instead of soluble and non-phosphorylated α-synuclein, high concentrations of insoluble and lipid-associated phosphorylated α-synuclein at Ser129 (which caused conformational changes of α-synuclein, promoted fibril formation[79] and induced unfolded protein-mediated cell death[80]) were found accumulating in intracytoplasmic Lewy bodies and dystrophic Lewy neurites, the hallmarks observed in PD as well as other synucleinopathic neurodegenerative diseases including Alzheimer's disease (AD), multiple system atrophy (MSA) and dementia with Lewy bodies (DLB) [26, 81-84]. This suggests that α-synuclein pathology might not be caused by α-synuclein accumulation but rather by conformational changes in α-synuclein.

PD not only involves in the central nervous system, but is also associated with changes to the peripheral nervous system including the enteric nervous system[85]. It has been shown that the expression of α-synuclein varies in different regions of the central nervous system[86]. However, it is not clear whether its expression differs within different parts of organs other than the brain, such as the gut. Our group recently reported that α-synuclein was selectively expressed in the axons of cholinergic enteric neurons in the guinea pig ileum, rectum and human colon, which was related to the expression of synaptic vesicle proteins including VAMP2, synaptophysin, synaptagmin-1, 25-kDa synaptosomal-associated protein (SNAP-25) and cysteine string protein-α (CSPα) in axons[87, 88]. These findings may help to explain the mechanism of the gastrointestinal dysfunction which occurs in PD patients, which could be responsible for the frequent non-motor symptoms including

constipation. However, it was shown that α-synuclein deficiency did not contribute to the compartment-specific processes in prion disease progression that mediated synaptotoxicity and neurodegeneration[89].

Moreover, a variety of mechanisms were put forward to explain the pathology of α-synuclein in PD. It was found that in the brain of Parkinson's disease, there was cross-talk between tissue transglutaminase (tTG) and α-synuclein monomers, oligomers and aggregates[90], also, α-synuclein aggregate formation could be stimulated by increased calcium[91]. Meanwhile, it was reported that glucose starvation-induced fibrillary aggregated α-synuclein influenced dopamine transporter (DAT) in dopaminergic cells, accompanied by dopaminergic cell death[92]. Recent studies also provided evidence that α-synuclein plays a critical role in the initiation and maintenance of inflammation in PD[93], and neuroinflammatory reactions contributed to the progressive degenerative process[94]. The α-synuclein pathology may also involve the interaction between α-synuclein and other proteins such as Tau proteins. Alpha-synuclein has been shown to stimulate GSK-3β (glycogen synthase kinase 3β) induced Tau hyperphosphorylation into its pathologic form[95-97], thus causing microtubule instability that leads to loss of dopaminergic neurons in the PD brains[98]. Also, α-synuclein and Tau were found co-localized in Lewy bodies[99], suggesting a molecular mechanism in the pathology of PD.

1.4 VAMP2 and other SNARE proteins

1.4.1 Classifications of SNARE proteins

SNARE proteins are small ubiquitous proteins in a large superfamily containing more than 60 members and have been found in organisms from yeast to mammalian cells. The structure and size of these proteins can vary dramatically,

however they share a characteristic segment in their cytosolic domain called a SNARE motif, which consists of 60-70 amino acids[100] that can facilitate spontaneous and reversible assembly of t-SNARE and v-SNARE proteins into four-α-helix bundles called trans-SNARE complexes (also known as SNAREpins)[101], whereas the individual SNARE proteins are always unfolded. The predominant role of SNARE complexes is to execute and regulate vesicle fusion with the target compartment followed by the exocytosis of the intracellular cargo. According to the difference in localization, SNARE proteins are thereby classified into two categories, vesicle or v-SNARE and target or t-SNARE (table 1). v-SNAREs are generally incorporated into the membranes of transport vesicles, while t-SNAREs are mainly located in the membranes of target compartments. Another classification is based on their structural characteristics, dividing SNARE proteins into R-SNAREs and Q-SNAREs. R-SNAREs and Q-SNAREs are proteins providing arginine (R) and glutamine (Q) residues from a specific location within the primary sequence of the protein respectively to form the zero ionic layers in the assembled core SNARE complexes. Four SNARE motifs have been identified (referred to as R-, Qa-, Qb- and Qc-SNARE motifs)[100]. The four-α-helix bundle of SNARE complex contains one motif of each R/Q class (called R/Q-rule), with R-SNAREs usually corresponding to v-SNAREs, while Q-SNAREs correspond to t-SNAREs.

Table 1-1: Classifications of SNARE proteins

Classification 1	Classification 2	Location	Residue provided	Representative Proteins
v-SNARE	R-SNARE	Membranes of transport vesicles	Arginine (R)	synaptobrevin/ VAMP2
t-SNARE	Q-SNARE	Membranes of target compartments	Glutamine (Q)	Syntaxin 1, Syntaxin 4

				SNAP-25, SNAP-23

1.4.2 VAMP2 and other SNARE complex components

VAMP2 (vesicle associated membrane protein 2), also known as synaptobrevin-2, is a member of the vesicle-associated membrane protein (VAMP)/synaptobrevin family. It is a critical SNARE protein participating in the membrane fusion in many important internal processes including neurotransmitter release and insulin secretion. Mice lacking a functional VAMP2 gene cannot survive after birth, and have a significant reduction in synaptic transmission [66]. VAMP2 is classified as a R-SNARE protein or a v-SNARE protein. Structurally, VAMP2 is a single transmembrane synaptic vesicle protein composed of a relatively short cytoplasmic proline-rich N-terminal domain of 31 amino acid residues, a SNARE motif (residues 32-84), and a transmembrane (TM) domain (95-116) at the C-terminus [102]. SNARE mediated membrane fusion is a process involving multiple steps: docking, hemifusion and full (complete) fusion. VAMP2 has been identified to participate in neurotransmitter release at a stage between docking and fusion. In order to release neurotransmitter, VAMP2 associates with two other presynaptic transmembrane t-SNARE/Q-SNARE proteins, namely syntaxin and SNAP-25, to form trans-SNARE complexes between synaptic vesicle and presynaptic membrane. The formation of trans-SNARE complexes makes synaptic vesicles competent for fusion with the membrane, and subsequently facilitates exocytosis of neurotransmitter [103-105]. Meanwhile, VAMP2 also forms a distinct complex with synaptophysin. Grey et al. found that several synaptic vesicle membrane associated proteins including VAMP2, synaptophysin and the chaperone protein CSP (cysteine string protein) showed reduced expression in the progress of synaptic degeneration [106]. Outside the SNARE complex, VAMP2 exists as monomers and dimers, whereas disruption of its

dimerization does not affect its SNARE-dependent fusion activity [107]. Hence, the role of its dimerization remains unclear.

Syntaxins are a family of membrane-integrated Q-SNARE proteins with a single C-terminal transmembrane domain, a SNARE domain (known as H3 domain) and an N-terminal regulatory domain (known as Habc domain). The H3 domain binds to both SNAP-25 and VAMP2 to form the core SNARE complex, whereas the three α-helices of Habc domain can form an inactive closed syntaxin conformation which is stabilized by binding to SM (Sec1/Munc18-like) protein Munc 18-1. Moreover, syntaxins bind synaptotagmin via H3 domain in a Ca^{2+}-dependent manner in the late stage of membrane fusion.

SNAP-25 is a membrane-bound t-SNARE protein anchored to the cytosolic membrane via palmitoyl side chains in the middle of the molecule. SNAP-25 contributes two α-helices in the formation of trans-SNARE complex in neurons with another two α-helices provided by syntaxin 1 and VAMP2 respectively to facilitate the synaptic vesicle fusion with the plasma membrane [108]. SNAP-25 also interacts with synaptotagmin through its C2B domain in a Ca^{2+}-independent manner[109].

1.4.3 The cleavage of SNARE proteins by neurotoxins

SNARE-mediated docking of synaptic vesicles with the presynaptic membranes are the targets of bacterial neurotoxins responsible for botulism and tetanus which are acting as specific proteases that inhibit synaptic vesicle fusion [110-112]. That is to say, Tetanus neurotoxin (TeNT) and seven botulinal neurotoxins (BONT/A to BONT/G) can work as inhibitors of synaptic vesicle exocytosis in nerve endings [113, 114] by acting as endopeptidases and cleaving the SNARE proteins which in turn blocks the formation of the synaptic vesicle-docking fusion complex, inhibiting neurotransmitter release from nerve

endings [115-117]. Based on the different sensitivity to BONTs, the VAMP family can be classified into two isoforms: toxin-sensitive isoform (VAMP2) and toxin-insensitive isoform (VAMP7) [118] (table 1-2). However, the neurotoxins only attack the free, but not the complexed SNARE proteins, suggesting that the association among VAMP2, syntaxin 1 and SNAP-25 is quite stable and defensible[119].

Table 1-2: Neurotoxins act as endopeptidases to cleave SNARE proteins (species: rat) [114]

Neurotoxin	Target protein	Peptide Bond of Cleavage	SNARE Motif required
BONT/A	SNAP-25	Gln197-Arg198	S1,S2,S3 or S4
BONT/B	VAMP2	Gln76-Phe77	V2 motif
BONT/C	Syntaxin, SNAP-25	Lys254-Ala255 (Syntaxin 1A) Lys253-Ala254 (Syntaxin 1B) Arg198-Ala199 (SNAP-25)	Not known
BONT/D	VAMP2	Lys59-Leu60	V1 motif
BONT/E	SNAP-25	Arg180-Ile181	S1,S2,S3 or S4
BONT/F	VAMP2	Gln58-Lys59	V1 motif
BONT/G	VAMP2	Ala81-Ala82	V2 motif
TeNT	VAMP2	Gln76-Phe77	V1 motif

1.5 Mechanisms of membrane fusion in neurotransmitter release

1.5.1 Zipper Hypothesis

Before fusion, the trans-SNARE complexes anchor in opposing membranes (e.g. Synaptic vesicle membrane and target compartment), whereas after membrane fusion, the fully zippered SNARE complexes become cis-SNARE complexes. The

association and dissociation of SNARE complexes modulates fusion in an ATP-dependent manner, because a specific ATPase (NSF) catalyzes the unfolding of cis-SNARE complexes and returns them to the initial inactivated state for recycling[120, 121].

The assembly of trans-SNARE complexes is likely to form bridges between the opposing lipid bilayers of cell plasma membranes and secretory vesicles to induce their fusion[122]. In the process of assembly, the influx of calcium triggers its completion, which is regulated by an interaction between the calcium sensor, synaptotagmin, and the SNARE complex.

In the "Zipper" hypothesis, the complex assembly starts at the N-terminal of SNARE motifs towards the C-termini that anchor interacting proteins in the membrane. Firstly, SNAP-25 and syntaxin-1 form an intermediate complex at the pre-synaptic plasma membrane, which later combines synaptobrevin/VAMP2 located in the synaptic vesicle with the help of α-synuclein, and eventually becomes the complete trans-SNARE complex. Then the v-SNARE and t-SNARE proteins gradually zipper up into a four-α-helical bundle from the N-terminal membrane-distal end progressing towards the C-terminal membrane-proximal end of the heptad-repeat-containing SNARE motifs which pulls the opposing two membranes together to provide enough energy to overcome repulsive forces during fusion[123, 124] (figure 1-1). The primary function of SNARE complexes as energy generators during fusion was further confirmed physiologically by the observations that both lipid-anchored syntaxin-1 and lipid-anchored VAMP2 lacking C-terminal transmembrane regions (TMRs) still effectively stimulated spontaneous and Ca^{2+}-triggered membrane fusion, by measuring synaptic vesicle exocytosis in cultured neurons[125]. On the contrary, some early studies proved that the transmembrane regions (TMRs) of syntaxin-1 and VAMP2 were essential during membrane fusion and may cause the opening of fusion pore[107,

126, 127] and these TMRs interacted with each other[128] and formed single continuously interacting α-helices with SNARE motifs[129].

1.5.2 The role of SM proteins in membrane fusion

The clasp-shaped SM (Sec1/Munc18 -like) proteins subsequently bind to trans-SNARE complexes to play complementary roles in fusion and to ensure specificity of fusion reactions. Therefore, the cooperated SNARE and SM proteins are called intracellular membrane fusion machinery, which can activate membrane fusion when it is needed and clamp when it is not. Otherwise, the chronic imbalance in membrane fusion may contribute to the progress of some diseases such as diabetes, immune system defects and Parkinson's disease[104].
The role of SM proteins in membrane fusion was first identified by the observation that Munc 18-1 binds to synaptic t-SNARE syntaxin-1[130]. However, recently, a clearer picture of the relationship between SM and SNARE proteins has emerged from different studies, showing that SM proteins associated with both v-SNARE and t-SNARE as clasps to regulate trans-SNARE complexes spatially and temporally. The SM protein Munc18-1 blocks the formation of trans-SNARE complexes by binding to N-terminal Habc domain of syntaxin-1 in the closed syntaxin conformation (the open syntaxin conformation is active and competent to form into SNARE core complexes) [131, 132]. This kind of inhibitory effect could be mediated by the regulatory protein Munc13 or the specific binding between Munc18-1 and VAMP2 or VAMP3[133-135]. In this case, SM proteins were acting as negative regulators for membrane fusion. In addition, SM proteins play a positive role in SNARE –mediated fusion as well. It was revealed by the second mechanism of interaction between SM and SNARE proteins, in which SM protein Munc18-1 was anchored to a specific N-terminal peptide sequence of syntaxin and a membrane proximal region of VAMP2,

potentially enabling SM proteins to clasp and cooperate in trans-SNARE complex assembly and organization[136, 137]. Recently, by using a reconstituted membrane fusion assay, it was confirmed that helix 12 in domain 3a of Munc18-1 acts as a molecular switch and a folding template for VAMP2 and activated SNAREpin assembly and membrane fusion[138].

1.5.3 Clamp hypothesis

In 1992, Thomas Sudhof and Reinhardt Jahn reported that the cytoplasmic domains of synaptotagmin bound calcium at physiological concentration, indicating that synaptotagmin acts as a calcium receptor in exocytosis[139]. Later, Geppert et al reported that synaptotagmin was the main low-affinity Ca^{2+}-sensor mediating Ca^{2+} regulation of synchronous neurotransmitter release in hippocampal neurons[140]. A reversible clamping protein, known as complexin, inhibits synaptic vesicle fusion proceeding by competing with VAMP2 for binding to the C-terminal membrane proximal part of the t-SNARE[141] and by regulating the binding between calcium and the C2 domain of its sensor synaptotagmin, thereby regulating the interaction with syntaxin[142]. Simultaneously, complexin binds to the N-terminal membrane distal region of VAMP2 and syntaxin-1 SNARE motif in the SNAREpin via its central α-helix[141], so that it stabilized partially assembled SNAREpins and blocked further SNAREpin zippering. However, when calcium is added back, the SNARE complex will be released by complexin and bind to synaptotagmin, thus, the membrane fusion will restart. This suggests that synaptotagmin and complexin may be co-regulators in synaptic vesicle fusion to control the precision of timing of neurotransmitter release[143]. Furthermore, complexin acts upstream of Ca^{2+}-triggered fusion, demonstrated by the evidence that deletion of complexin in mice causes a similar phenotype to synaptotagmin deletion, suggesting that

complexin may function to activate the reaction between SNARE complexes and synaptotagmin[144] (figure 1-1). However, the precise mechanism of how complexin and synaptotagmin function on SNARE complexes in a Ca^{2+}-dependent manner remains unclear. In Drosophila, it was reported that neuronal vacuolar-type H^{+}-adenosine triphophatase V0 subunit a1 (V100) regulated SNARE complex assembly in a calcium-calmodulin-dependent manner for spontaneous neurotransmitter release[145].

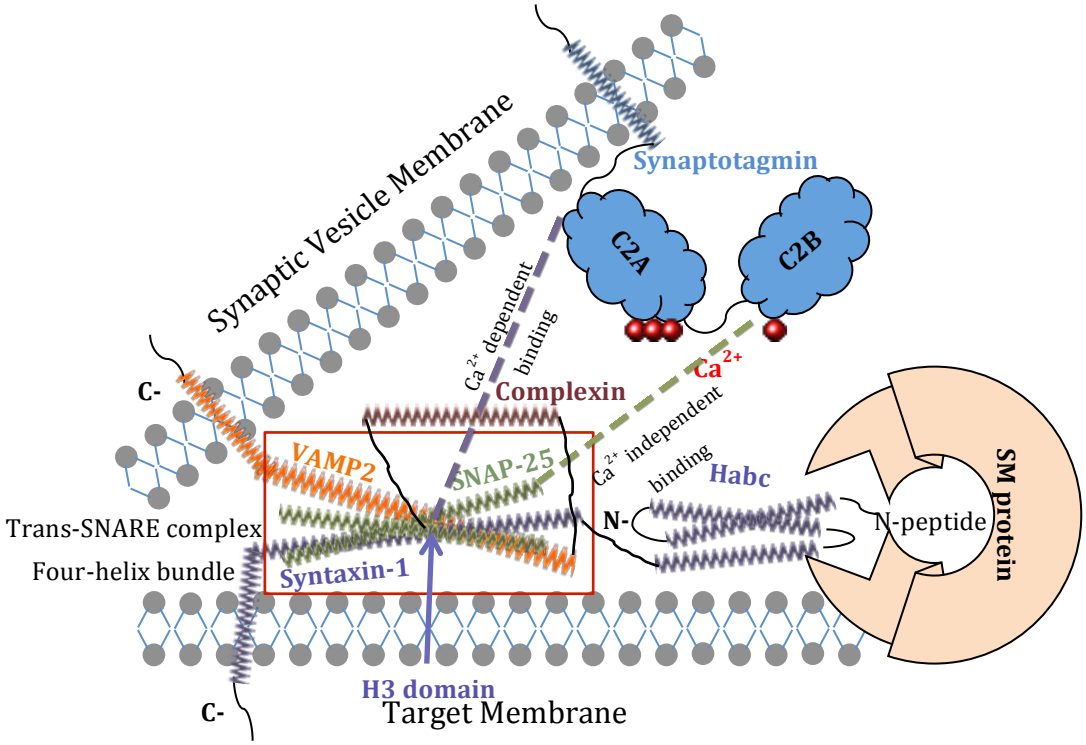

Figure 1-1: Summary of "zipper" and "clamp" hypotheses of potential mechanism of membrane fusion in neurotransmitter release. In synaptic vesicle exocytosis, syntaxin 1 (t-SNARE) and VAMP2 (v-SNARE) are anchored in opposing membranes by their C-terminal domains, while SNAP-25 is tethered to the plasma membrane via several cysteine-linked palmitoyl chains. The trans-SNARE complex is a four-α-helix bundle, with one helix contributed by syntaxin-1, one helix by VAMP2 and two helices provided by SNAP-25. The formation of the SNAREpin pulls the target plasma membrane and synaptic

vesicle membrane together to provide enough energy required by fusion, while SM proteins play a complementary role in fusion through binding to the N-peptide of Habc domain of syntaxin-1. Complexin binds to the N-terminal membrane distal region of VAMP2 and syntaxin 1 SNARE motif (H3 domain) in the SNAREpin via its central α-helix to stabilize partially assembled SNAREpins and blocks further SNAREpin zippering. When calcium is added back, the SNARE complex will be released by complexin and binds to the Ca^{2+} -sensor synaptotagmin.

1.6 The presentation, trafficking and retrieval of VAMP2

1.6.1 Evidence of α-synuclein in the regulation of SNARE complex assembly

Recently, increasing evidence showed that α-synuclein regulated SNARE complex assembly in a VAMP2-dependent manner. On one hand, triple (α, β, γ-) Synucleins knockout mice demonstrated a decrease in SNARE complex assembly and developed age-dependent neurological impairment, suggesting that Synucleins play an important role in the maintenance of normal SNARE complex assembly[67]. On the other hand, by using a single-vesicle optical microscopy system, it was detected that recombinant and native α-synuclein purified from mouse brain promoted clustering of synaptic vesicles. This kind of "clustering" was dependent on specific interactions of α-synuclein with VAMP2 as well as anionic lipids, and it could be disrupted by one of the Parkinson's disease-related point mutants of α-synuclein, A30P, which was the lipid-binding deficient mutation[146]. Although it was recently demonstrated that the multimeric membrane-bound state of α-synuclein was critical for SNARE complex assembly [68], it was also reported that full phospholipid binding was not necessary to

maintain the physiological function of α-synuclein as a SNARE protein chaperone and was only impaired when over 75% of phospholipid binding failed (e.g. helix 1 was missing)[147].

In the process of the formation of the SNARE complex, α-synuclein and cysteine string protein-α (CSPα) are acting as the chaperones to the SNARE proteins, VAMP2 and SNAP-25, respectively, in the presynaptic terminals[67, 148, 149]. When the chaperone activity of α-synuclein or CSPα was attenuated, this led to the misfolding and depletion of VAMP2 or SNAP-25 in presynaptic terminals, and subsequently to a deficit in SNARE complex assembly and neurodegeneration[67, 148-153]. Interestingly, the lethal neurodegeneration induced by knock-out of CSPα could be abolished by transgenic expression of α-synuclein, which rescues SNARE complex assembly rather than SNAP-25 levels. However, this kind of neurodegeneration would be accelerated by deletion of endogenous synucleins. These phenomena suggested a potential important interaction between CSPα and α-synuclein[151]. In another model, overexpression of fluorescent-human-alpha-synuclein on cultured hippocampal neurons from brains of transgenic mice significantly down-regulated the expression of several endogenous synaptic vesicle proteins such as VAMP2, piccolo and synpasin-1, leading to a pathologic cascade of events in α-synuclein-induced synaptic deficits[154]. Furthermore, in the study of the striatum of transgenic mice containing truncated human α-synuclein (1-120) or full length human α-synuclein, it was found that the expression of truncated (1-120) and full-length (1-140) human α-synuclein led to a redistribution of SNARE proteins related to decreased exocytosis and dopamine release, highlighting that the toxic function of α-synuclein at the synapse may be an early event in the pathogenesis of PD. This process appeared not to be affected by the last 20 amino acids of α-synuclein. The author hypothesized that the balance between monomeric α-synuclein and SNARE proteins could be critical to proper SNARE complex

assembly and function, and the increase of α-synuclein could be the reason for the formation of toxic oligomers that influence SNARE distribution and function, and consequently cause impaired exocytosis[155]. In another study, using a single-vesicle assay which could distinguish vesicle docking from fusion, it showed that α-synuclein specifically inhibited synaptic vesicle docking without interfering with vesicle fusion by binding to acidic lipid containing membranes at high concentrations or by interacting with v-SNARE at much lower concentrations. Surprisingly, C-terminal truncated α-synuclein had similar inhibitory effect as wild type, indicating that the interaction between α-synuclein and VAMP2 was not essential for its inhibitory effect on lipid mixing [156].

The mechanism of neurotoxicity caused by α-synuclein oligomerization was proposed in a variety of studies. It was reported that dopamine accelerated the formation of large α-synuclein oligomers through inhibiting fibril formation, indicating a relationship between dopamine and large α-synuclein oligomers[157]. Recently, Bong-Kyu Choi et al.[158] showed that large α-synuclein oligomers preferentially bound to the N-terminal domain of VAMP2 and prevented SNARE complex formation, which suppressed neuronal SNARE-mediated lipid mixing, revealing the inhibitory function on dopamine release and neurotoxicity of large α-synuclein. Another possibility regarding the toxicity of α-synuclein oligomers suggested the α-synuclein oligomers may directly bind to mitochondrial membranes causing mitochondrial fragmentation and neuronal cell death [159], and that the mutant and wild type α-synuclein interacted with the mitochondrial complex IV enzyme and cytochrome C oxidase (COX) to enhance mitochondrial dysfunction[160], which is the main contributor to PD[161]. On the contrary, α-synuclein monomer had an opposite effect on lipid binding even when its amount was 30-fold more than large α-synuclein oligomers[158].

1.6.2 PDK3 is another important binding partner of VAMP2

The protein kinase D (PKD) family is a newly identified serine/threonine kinase family containing 3 members: PKD1 (PKD/PKC μ), PKD2 and PKD3 (PKC ν) [162]. PKD3, a novel member of the protein kinase D (PKD) family, was identified as a binding partner of VAMP2 through yeast two-hybrid screening. It directly interacted with VAMP2 in vitro and in vivo, and partially colocalized with VAMP2 vesicles in HEK293 cells, providing the evidence that PKD3 had a functional role in facilitating the recruitment of VAMP2 vesicles to the target plasma membrane [163].

1.6.3 Proteins playing an important role in VAMP2 retrieval

1.6.3.1 Synaptophysin

Synaptophysin is another major synaptic vesicle protein to interact with VAMP2. Synaptophysin, also known as the major synaptic vesicle protein p38, is a 38 kDa synaptic vesicle glycoprotein with four transmembrane domains and cytoplasmic N- and C- termini. It forms multimers in a structurally basket-like way with a pore in the center [164]. It is a major interaction partner with VAMP2, and the complex forms between the transmembrane (TM) regions of the two proteins [165], which may be dissociated by a peptide encompassing the N-terminal of VAMP2 [166]. Unlike α-Synuclein, Synaptophysin remains in contact with VAMP2 even after its incorporation into the SNARE complex. On one hand, it suggested that Synaptophysin may regulate the availability of VAMP2 for synaptic vesicle fusion reactions based on the fact that up to 25% of VAMP2 can be associated with Synaptophysin in homo- and heteromultimers after stimulation [167]. On the other hand, the entry of VAMP2 into SNARE

complexes may be independent of Synaptophysin and complete SNARE complex assembly not only connects membranes but also drives fusion according to the studies showing that VAMP2 dissociates from Synaptophysin freely when synaptic vesicles are exposed to Syntaxin and SNAP-25, the other two SNARE complex components [168]. It is possible that overexpression of exogenous VAMP2 caused either its increased expression at the plasma membrane (which could be reduced and redistributed into intracellular compartments via the interaction of VAMP2 with Synaptophysin I without affecting the rate of VAMP2 endocytosis [169]), or its mis-sorting along the axons of the neurons (which could be corrected by coexpression of Synaptophysin I [170]). In the light of these facts, it suggests that Synaptophysin may play a role in the retrieval of VAMP2 during the endocytosis of synaptic vesicles. Some studies have shown that inefficient VAMP2 retrieval may result in an indirect and sustained influence on synaptic vesicle endocytosis, however, its long-term effect may cause the loss in the ability of neurons in neurotransmission [171, 172].

1.6.3.2 AP180

AP180 can also play an important role in VAMP2 retrieval. AP180 is a monomeric adaptor protein that plays an important part in clathrin-mediated endocytosis of synaptic vesicles. It binds membrane lipids and clathrin simultaneously to recruit clathrin to the membrane of vesicles. In Drosophila melanogaster, deletion of the AP180 homologue Like-AP180 (LAP), led to increased size but decreased number of synaptic vesicles and hence reduced transmitter release. Three vesicle proteins, Synaptotagmin I, cysteine-string protein, and neuronal synaptobrevin/VAMP, were all mislocalized to the extrasynaptic axonal regions in the mutant [173]. In HEK293 cells, knockdown of AP-180 and its ubiquitous homologue CALM (Clathrin-assembly lymphoid

myeloid leukaemia protein) caused selective surface accumulation of VAMP2. Moreover, the ANTH (AP-180 N-terminal homology) domain of AP-180 or CALM interacts directly with the N-terminal half of the SNARE motif of VAMP2 [174]. These results suggest that AP180 is required for either recycling vesicle proteins and/or maintaining the distribution of both vesicle and synaptic proteins in the nerve terminal.

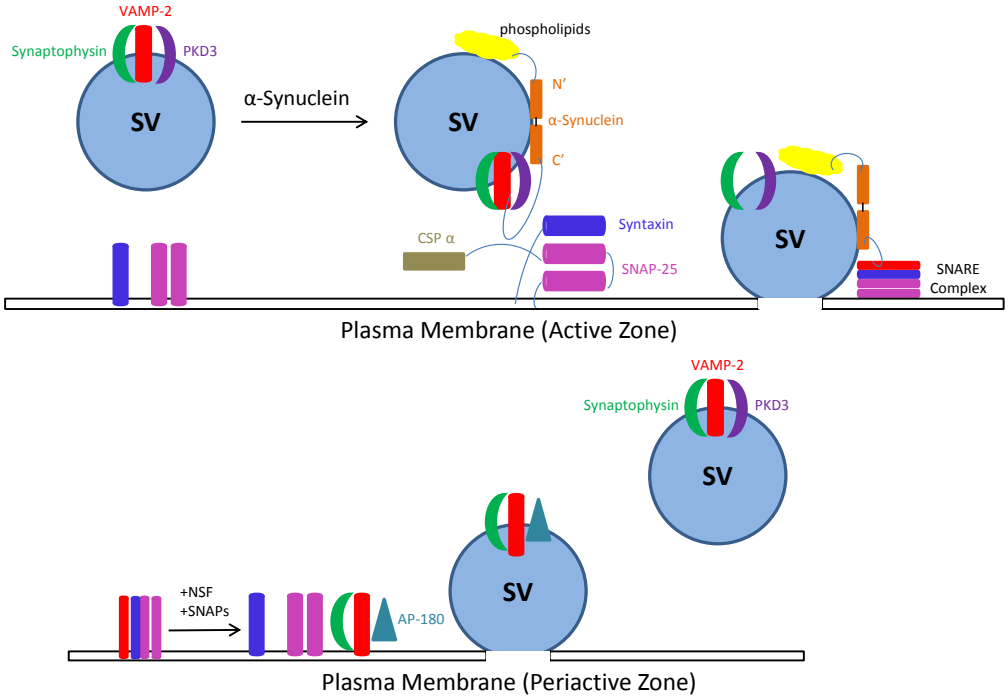

Figure 1-2: Proposed model of the presentation, trafficking and retrieval of VAMP2. VAMP2 forms a complex with Synaptophysin and PKD3 on the synaptic vesicle. Then native α-Synuclein binds to VAMP2 via its C-terminus and phospholipids via its N-terminus. CSP α acts as a chaperone to bind to SNAP-25, both of these facilitating the assembly of SNARE complexes between VAMP2, syntaxin and SNAP-25. This in turn triggers synaptic vesicle fusion with the presynaptic plasma membrane. After synaptic vesicle fusion, the SNARE complex is dissociated by N-ethylmaleimide-sensitive factor (NSF) and soluble NSF-attachment proteins (SNAPs). VAMP2 then binds to synaptophysin and AP180 to start the retrieval.

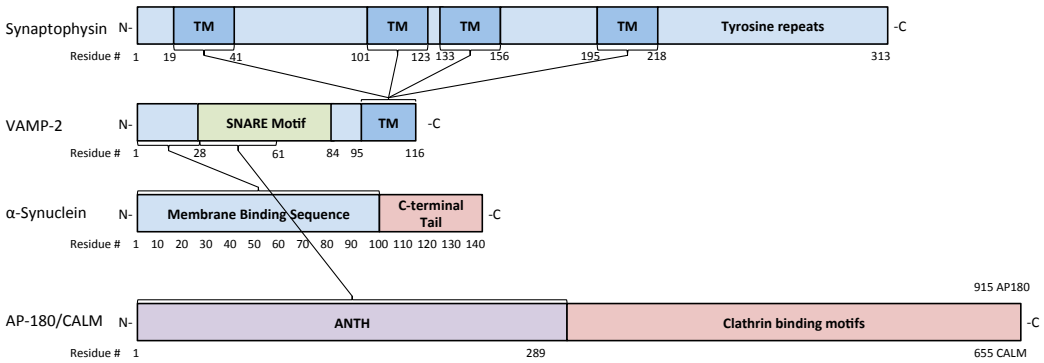

Figure 1-3: VAMP2 trafficking partners. VAMP2 forms a complex with synaptophysin by interaction with the four transmembrane motifs of synaptophysin. α-Synuclein binds to the N-terminal 28 amino acids sequence of VAMP2 via its 40-residue highly acidic C-terminus binding domain. AP-180/CALM interacts with VAMP2 via the ANTH (AP-180 N-terminal homology) domain.

VAMP1 Human

```
        10          20          30          40          50
MSAPAQPPAE GTEGTAPGGG PPGPPPNMTS NRRLQQTQAQ VEEVVDIIRV
        60          70          80          90         100
NVDKVLERDQ KLSELDDRAD ALQAGASQFE SSAAKLKRKY WWKNCKMMIM
       110
LGAICAIIVV VIVIYFFT
```

VAMP2 Human

```
        10          20          30          40          50
MSATAATAPP AAPAGEGGPP APPPNLTSNR RLQQTQAQVD EVVDIMRVNV
        60          70          80          90         100
DKVLERDQKL SELDDRADAL QAGASQFETS AAKLKRKYWW KNLKMMIILG
       110
VICAIILIII IVYFST
```

VAMP3 Human

```
        10          20          30          40          50
MSTGPTAATG SNRRLQQTQN QVDEVVDIMR VNVDKVLERD QKLSELDDRA
        60          70          80          90         100
DALQAGASQF ETSAAKLKRK YWWKNCKMWA IGITVLVIFI IIIIVWVVSS
```

Figure 1-4: Sequence of human VAMP1/2/3 homology.

1.7 Project Hypothesis

It has been demonstrated that α-synuclein facilitates SNARE complex assembly by acting as a chaperone for VAMP2. This occurs at the presynaptic plasma membrane with VAMP2 in its multimeric membrane-bound state instead of a cytosolic unfolded state, which may protect against neurodegeneration. Misfolded VAMP2 which is incorporated into neurotoxic aggregates will promote the pathology of neurodegenerative disorders such as PD. Meanwhile, the N-terminally truncated VAMP2, which lacks 28 N-terminal residues, does not bind α-synuclein, and diminishes SNARE complex assembly, which is essential for neurotransmitter release. However, the role of both full-length and truncated VAMP2 in Parkinson's disease remained unexplored. The absence of full-length VAMP2 caused by N-terminal truncation could play a role in α-synuclein aggregation and contribute to the formation of Lewy bodies and Lewy neurites, hallmarks of PD and DLB. The significance of this study is to provide the neuropathological diagnostic value of truncated VAMP2 pathology in Lewy body diseases and explore potential therapeutic value by obtaining knowledge on the mechanism of VAMP2 in participation in initiation and propagation of α-synuclein aggregation and Lewy body formation in humans. Currently, prevention of α-synuclein aggregation is a key strategy in developing modified therapies for PD.

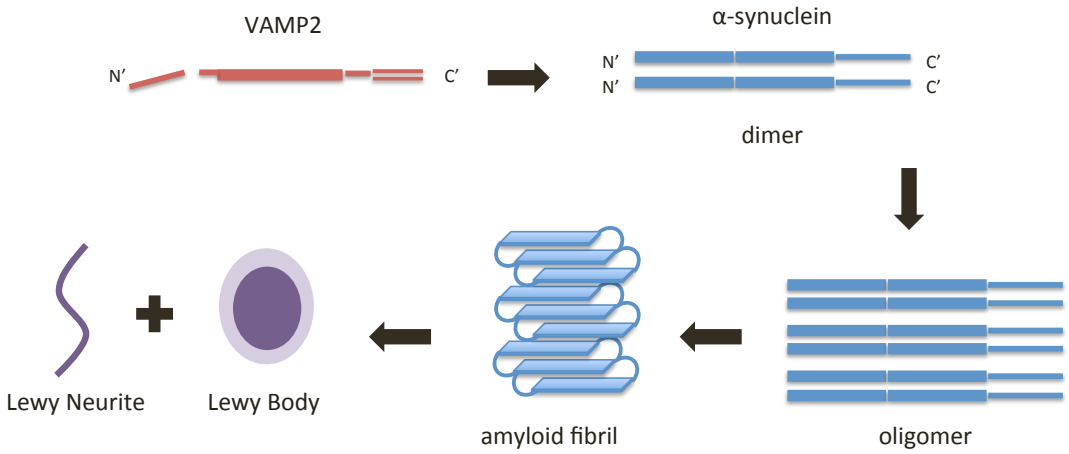

Figure 1-5: project hypothesis. The absence of full-length VAMP2 caused by N-terminal truncation could play a role in the aggregation of α-synuclein monomers to form dimers, oligomers and amyloid fibrils, and eventually contribute to the formation of Lewy bodies and Lewy neurites in PD and DLB.

1.8 Project Aims and Scope

In order to provide the evidence to our hypothesis, the project was divided into several stages:

1. To test the specificity of 2 fVAMP2, 2 tVAMP2 and 2 α-synuclein antibodies by immunostaining and immunoblot.

2. To observe the distribution of Lewy bodies and Lewy neurites in regions of neocortex and brainstem of PD or DLB brains by using immunostaining with optimized tVAMP2 and α-synuclein antibodies on free-floating sections.

3. To explore the correlation between truncated VAMP2 and α-synuclein in Parkinson's disease in vitro by dual immunofluorescence staining.

4. To characterize the specificity of truncated VAMP2 neuropathology in PD and DLB by comparison with other neurodegenerative diseases such as Alzheimer's disease (AD) and multiple system atrophy (MSA).

5. To determine the truncation site of VAMP2 by using 2D gel electrophoresis and mass spectrometry.

Chapter 2

Materials and Methods

2.1 Brains

All post mortem brain tissue was obtained from the National Health Medical Research Council (NHMRC). In total of 44 human cases were analyzed in the present study, including 10 brains of Parkinson's Disease (PD) with or without other co-morbidities, 11 brains of Alzheimer's Disease (AD) with or without other co-morbidities, 10 Dementia with Lewy bodies (DLB) with or without other co-morbidities, 3 Multiple System Atrophy (MSA), and 10 control cases with no neurological disease (Table 2-1). The medical history was available for all these cases. The control group was matched with the PD group in terms of age at death, post-mortem delay and time of section storage. Lewy bodies and Lewy neurites were observed in all cases with PD or DLB, but were absent in controls and other neurodegenerative diseases.

Table 2-1: human cases analyzed in this study

Patient ID	Sex	Age	Post-mortem delay (hr)	Neuropathological diagnosis	Region	VAMP2 Staining	α-synucle in Staining	Tau Staining
SA0053	F	86	7	AD	HIP	√	×	×
SA0068	F	83	5	AD	HIP	√	√	√
SA0078	M	59	20	AD	HIP	√	√	√
SA0123	M	80	21	AD	MT	√	√	√
SA0092	F	85	48	AD (atypical)	HIP	√	×	×
SA0060	F	71	13	AD (SDAT)	HIP	√	×	√
SA0065	M	67	61	AD (SDAT)	HIP	√	√	√

SA0143	M	84	15	AD + Brainstem LB's	BS	√	×	√
SA0072	F	84	16.5	AD + mild hypertens vasc	MF	√	√	√
SA0073	M	63	33.5	AD + other	HIP	√	×	√
SA0148	M	81	14	AD + other	HIP	√	×	√
SA0079	F	82	31	DLB	IF, ST	√, √	√, √	×, ×
SA0046	F	82		DLB	MT, IT	√	√	×
SA0069	M	69	31	DLB	ST	√	√	×
SA0094	M	74	24	DLB	MF, MT, IF	√ , √ , √	×, √, √	× , × , ×
SA0181	M	77	19	DLB + AD	MB	√	√	×
SA0052	M	67	~24	DLB + other	SF	√	√	×
SA0063	F	81	7	DLB, Infarcts	CING, IF	×, √	√, ×	×, ×
SA0083	M	80	6	DLB + AD	SF, MT, MF	√ , √ , √	√, √, √	× , × , √
SA0113	M	78	12	DLB	MF	√	√	×
SA0249	M	87	7	DLB	IF	For Lewy body purification.		
SA0061	F	62	8	MSA	MT, MF	√, √	√, √	×, ×
SA0071	F	73	5	MSA	BG, SMT	√, √	√, ×	×, ×
SA0101	M	73	20	MSA	ST	√	√	√
SA0008	F	76	22	Normal control	MT	√	√	√
SA0010	M	58	14	Normal control	BS	√	×	×
SA0011	F	88	35	Normal control	MF	×	√	×
SA0019	M	80	20	Normal control	MT, MF	√, √	√, √	×, ×
SA0020	M	70	10	Normal control	MF	×	√	×
SA0026	F	78	18	Normal control	SF	√	√	×
SA0036	F	84	15	Normal control	ST, MT	√, √	√, √	×, √
SA0038	F	86	25	Normal control	IF	√	√	√

SA0162	M	72	30	Normal control (Brain + spinal cord)	MT	√	√	×
SA0230	M	86	22	Normal control	IF	For Lewy body purification.		
SA0014	F	77	4.5	PD	ST	√	√	×
SA0015	M	78	2	PD	MF	√	√	√
SA0051	F	85	~12	PD	MT, BS	√	√	×
SA0067	F	73	21	PD	BS	√	√	×
SA0041	F	80	7	PD + AD	MT	√	√	×
SA0045	M	73	24	PD + AD	TP	√	×	×
SA0056	F	83	13	PD + Other	ST	√	√	×
SA0057	F	91	24	PD + Other	BS	√	√	×
SA0024	M	88	3	PD, NF Degen, Plaques	SF	√	√	×
SA0274	F	90	6	PD	MF	For Lewy body purification.		

AD=Alzheimer's disease; SDAT=Senile Dementia of the Alzheimer's Type; DLB=Dementia with Lewy bodies; MSA=Multiple System Atrophy; PD=Parkinson's Disease

HIP=Hippocampus; MT=Middle Temporal; BS=Brain Stem; MF=Middle Frontal; IF=Inferior Frontal; ST=Superior Temporal; MB=Midbrain; SF=Superior Frontal; CING=Cingulate; BG=Basal Ganglia; SMT=Superior Medial Temporal; TP=Temporal Planum; IT=Inferior Temporal

2.2 Immunohistochemistry

2.2.1 Free Floating/Paraffin Embedded Human Brain Section Preparation

The majority of post-mortems were performed within 48 hours after death. After removed from the skull, the brains were first flushed with 1% sodium nitrite in PBS (pH 7.4) to remove the blood, and immediately fixed by perfusion via the basilar and internal carotid arteries (for the whole brain) or through the carotid, vertebral and anterior cerebral arteries (for half brain) with 2L of fixative containing 15% formalin in 0.1M phosphate buffer (pH 7.4) for 30-45min and post-fixed for 6-12hr. After dissecting the brain into different parts, the dissected blocks were transferred into fresh fixative for 24-48 hours, then to 20% sucrose in 0.1M phosphate buffer with 0.1% sodium-azide for 2-3 days, followed by 30% sucrose in 0.1M phosphate buffer with 0.1% sodium-azide for additional 2-3d for cryoprotection, then stored at -80℃ until use. Brainstems, cerebral cortex and hippocampus were then cut transversely into sections with the thickness of 30-50μm, which were collected in a PBS-azide solution [0.1% sodium azide in PBS (pH 7.4)]. Each section was either stained directly or stored at -80℃ for future use.

For preparation of paraffin sections, brainstem blocks were embedded in paraffin and 6μm sections were obtained and placed on Superfrost slides (Menzel-Glaser, Germany) and dried overnight at room temperature. These slides were fixed by immersion in cold acetone (-20℃) for 2 minutes, followed by air drying at room temperature prior to staining.

2.2.2 Antigen Retrieval

The sections were deparaffinized in two changes of xylene for 10min each, then rehydrated in 100%, 95% and 70% ethanol for 10min each, rinsed with deionized water for 5min and incubated in TBS-azide for 5min afterwards. The sections were then placed in a plastic rack containing 250ml of sodium citrate buffer (10mM Citric Acid pH 6.0) and heated in a microwave oven to 95℃. After

cooling down to 40℃, the sections were then transfer to EDTA buffer (1mM EDTA, 0.05% Tween 20, pH 8.0) and heated again to 95℃. After cooling down, the sections were washed (2x2min) in PBST buffer (137mM NaCl, 2.7mM KCl, 10mM Sodium Phosphate Dibasic, 2mM Potassium Phosphate Monobasic, 0.1% Tween 20, pH 7.4), and then blocked with peroxidase blocking solution (3% H_2O_2 + TBS-Azide) for 10min before proceeding to the standard immunohistochemistry protocol.

2.2.3 Antibodies

Conventional histological staining protocols such as cresyl violet, haemotoxylin-eosin, Weil, Bodian, modified Bielschowsky and methenamine silver were used for all brain tissue. All primary antibodies used in immuno-staining are listed in Table 2-2. The secondary antibodies were HRP-conjugated donkey anti-mouse, donkey anti-sheep or donkey anti-rabbit from Vector Laboratories, Burlingame, Calif., USA.

Table 2-2: Primary antibodies used in this study

Antibody	Species	Poly/Mono	Epitope	Source	Dilution
VAMP1/2/3 (FL-118)	Rabbit	Polyclonal	aa 1-118 VAMP1 (h)	Santa Cruz: sc-13992	1:1k
tVAMP2	Rabbit	Polyclonal	aa 30-47	Courtesy Dr Weiping Gai	1:1k-2k
AtVAMP2	Rabbit	Polyclonal	aa 30-47	Courtesy Dr Weiping Gai	6.8-13.6ug/ml 0.34ug/ml (WesternBlot)

AfVAMP2	Rabbit	Monoclonal	aa 2-17	Biochem animal ID: 3023	1:1k
AfVAMP2	Rabbit	Monoclonal	aa 2-17	Biochem animal ID: 3024	1:1k
α-synuclein	Sheep	Polyclonal	aa 116-131	Courtesy Dr Weiping Gai	1:2k
α-synuclein 11A5	Mouse	Polyclonal	P129 synuclein	Elan	1:2k-5k
Pan synuclein	Rabbit	Polyclonal	α-, β-, γ-synuclein (h)	Abcam: ab15534	1:2k
AF Tau	Sheep	Monoclonal	aa 12-30 Tau (h)	Antibody Technology Australia	1:2k

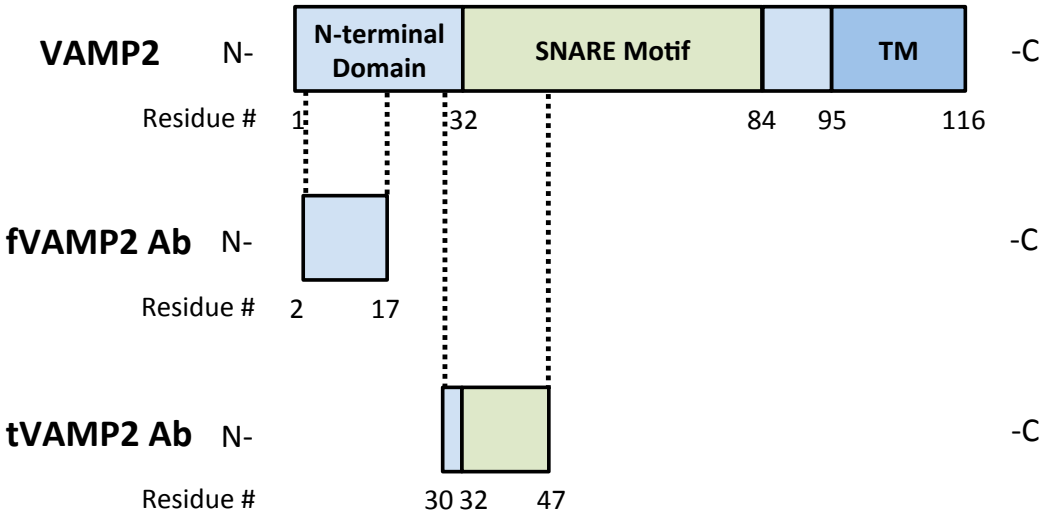

Figure 2-1: Domain structure of VAMP2 and its antibodies. tVAMP2 against aa30-47 was designed by our lab and fVAMP2 against aa2-17 was purchased from Biochem.

2.2.4 Immunohistochemistry

2.2.4.1 Immunohistochemical staining on free-floating sections

Selected free-floating sections (30-50μm thick) from brain regions of interest were placed in glass bottles or plastic containers. The sections were first incubated in 50% ethanol (3x10min), then immersed in 1% H_2O_2/50% methanol for 10min to eliminate endogenous peroxidase activity. Then tissue sections were washed in 1% normal horse serum (NHS) in TBS-azide (0.02M Tris, 0.15M NaCl, 1% Sodium Azide, PH7.4) containing 0.25% Triton X-100 (washing buffer) three times (5-10min per wash), blocked in 20% NHS and TBS-azide containing 0.25% Triton X-100 (blocking buffer) for 1 hour at room temperature in a humidified chamber in order to block non-specific antibody binding sites. This was followed by incubation with primary antibodies diluted in antibody diluent solution (1% NHS in TBS-azide containing 0.25% Triton X-100) overnight at 4℃, and rinsed in washing buffer three times (5-10min per wash). The biotin conjugated secondary antibodies were diluted in antibody diluent solution before being applied to the sections for 60-90min at room temperature. This was followed by the incubation with avidin-biotin-peroxidase complex (ABC solution) (ABC kit from Vector Laboratories, UK) for one hour and then with 3-3-Diaminobenzidine-4 HCl/H_2O_2 (DAB substrate solution) (DAB tablet from Sigma D5637, USA) solution for 5-10min or until the desired color intensity was reached according to the background staining of tissue. After the DAB reaction, the sections were mounted on Superfrost slides, air-dried, dehydrated by immersing into four changes of alcohol (70%, 95%, 100%, 100%) and two changes of xylene, 10min each, and finally cover-slipped before taking images under the light microscope (Olympus BH-2) fitted with a MicroPublisher 3.3 RTV digital camera (QIMAGING, Canada). The images were acquired using Adobe Photoshop 9.0.

2.2.4.2 Immunohistochemical staining on paraffin sections

After rehydration and antigen retrieval, the paraffin sections were incubated in (1) blocking buffer, (2) primary antibodies, (3) secondary antibodies, (4) ABC solution, (5) DAB substrate solution, using the same procedures for free-floating sections (2.2.4.1). After washing with TBS-azide for three times (2min per wash), the selected sections were counterstained by selective staining such as haematoxylin-eosin, methenamine silver or methylene blue for 30sec, followed by a quick dip in acid alcohol for destaining of background and lithium carbonate for 2min for consolidation of staining. Rinsing in dH_2O for 1min was performed after each step. Then the sections were placed on superfrost slides, air-dried, and dehydrated through three changes of 70%, 95% and 100% alcohol (10sec each), and cleared in two changes of xylene (2min each), and cover-slipped using DePex mounting medium. Sections were examined and mapped with a light microscope (Olympus BH-2) fitted with a MicroPublisher 3.3 RTV digital camera (QIMAGING, Canada) and the images were acquired using Adobe Photoshop 9.0.

2.2.5 Double Immunostaining

Smears were prepared by adding 10µl of the sample across a 10mm x 20mm area in the center of a gelatin-coated slide and spreading with pipette tip. After drying at RT, the smears were fixed in fixative buffer (2% paraformaldehyde with 0.2% picric acid in 0.1M PBS) for 10min, followed by 3 washes in washing buffer (TBS-Azide) (5min per wash). In order to block peroxidase activity, the sections were incubated in 3%H_2O_2 for 10min and then in TBS-azide for 5-10min. In order to block the non-specific binding sites, the smears were then incubated in blocking buffer (20% NHS in TBS-azaide) at RT for 1 hour, followed by

incubation with primary antibodies diluted in antibody diluent solution (1% NHS in TBS-azide) at RT overnight. The primary antibodies used were: 1) Mouse anti-α-synuclein 11A5, 1:300 dilution; 2) Rabbit anti-tVAMP2, 1:200 dilution. On the next morning, after washing 3 times with washing buffer (5min per wash), the smears were then incubated with fluorescent conjugated secondary antibodies diluted in antibody diluent solution for 60min. The secondary antibodies used were: 1) CY3 conjugated donkey anti-mouse from Jackson (713-165-147), 1:200 dilution (green); 2) Alexa Fluor 488 conjugated donkey anti-rabbit from Invitrogen (A-21206), 1:200 dilution (red); followed by another 3 washes in washing buffer. Then the smears were covered with 10 to 20μl of VectaShield mounting medium (Vector Laboratories, Catalog No. H-1200, 1.5μg/ml) to stain nuclei with DAPI (blue). The smears were then cover-slipped and sealed with nail polish. The images were captured using an Olympus BX-50 fluorescence microscope fitted with a Photometrics CoolSNAP cooled CCD camera using the following settings:

Dye	**Excitation**	**Emission**
DAPI (UV-excitable blue dye)	360-370	420-460
Alexa488 (blue-excitable green dye)	465-495	515-555
Cy3 (green-excitable red dye)	515-550	575-615

The images from each channel were colorized and merged in Adobe Photoshop 9.0 using blue for DAPI, red for Cy3 and green for Alexa488.

2.2.6 Quantification of Lesions

Free-floating sections of brainstem were immunostained with α-synuclein or tVAMP2 antibodies separately using the DAB reaction as described above. Before counting, each section was divided into twelve parts (figure 2-2). The total number of lesions in each case was the sum of that of twelve regions determined

at the magnification of 100 times under an Olympus BH-2 light microscope (Tokyo, Japan) equipped with a MicroPublisher 3.3RTV digital camera (QIMAGING, Canada).

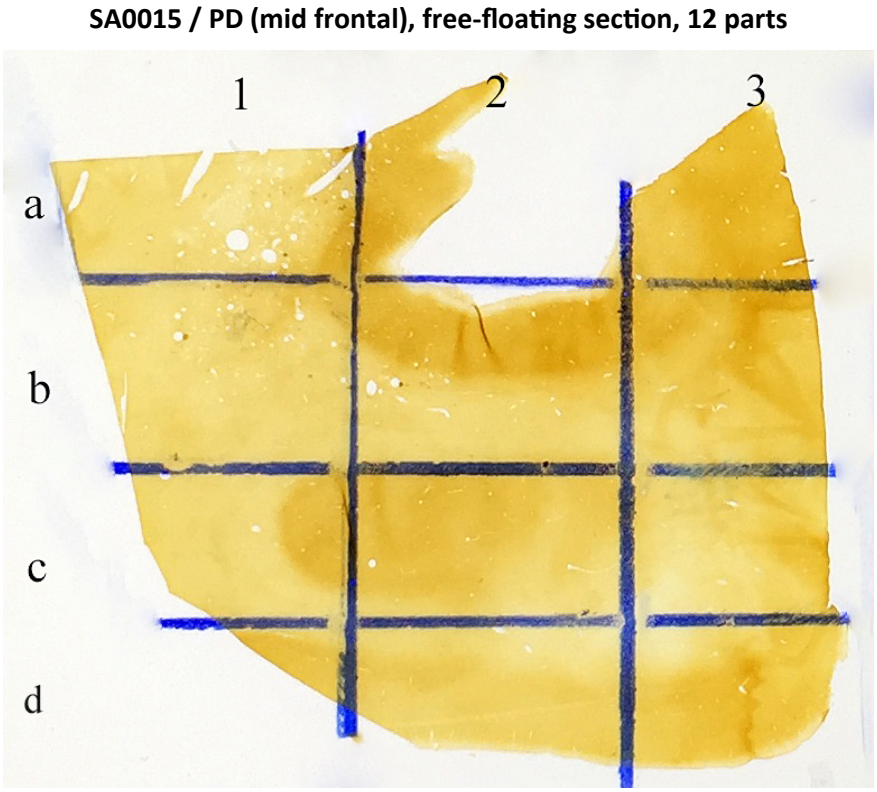

Figure 2-2: Quantification of Lewy bodies under microscope. Each slide was divided into twelve regions before counting. Lewy bodies were counted in each part under 100x magnification using an Olympus BH-2 light microscope (Tokyo, Japan). The total number of Lewy bodies was determined by the sum of the inclusions counted in all twelve regions.

2.3 Isolation of Synaptosomes and Inclusions

2.3.1 Synaptosomes Purification from Human Brain Homogenate

The brain tissue was defrosted on ice, dissected either grey matter (LBs) or white matter (GCIs), and minced with scalpel blade. The tissue (~2g) was then put into the Dounce homogenizer (Wheaton, Millville, NJ, USA) with

Homogenization Buffer (HB) (~10ml) [5mM EDTA, 1µg/ml Pepstatin, 1µg/ml Leupeptin, 0.3mM PMSF in sucrose-tris buffer (20mM Tris, 0.32M sucrose, 7.7mM sodium azide), pH 7.4], and homogenized with 10x strokes with Pestle B (loose) and 10x strokes with Pestle A (tight). The homogenized tissues from the same case were mixed together and divided into 10ml aliquots, frozen in liquid nitrogen and stored at -80°C.

Homogenized brain tissue was defrosted on ice and filtered through glass wool using a 20ml syringe, then flushed with HB and diluted to 24ml per tube of homogenate. The filtrate was divided into 3 centrifuge tubes, 8ml per tube, and centrifuged at 3000 RPM (1000x g) at 4°C for 10min (JA21 rotor). The supernatant was collected and the pellet was resuspended with another 8ml of HB and another centrifugation (3000 RPM, 4°C, 10min) performed. The pellet was used for purification of inclusions.

Table 2-3: The preparation of percoll gradient

Reagent name	**Percoll Plus (ml)**	**Percoll Buffer (ml)**	**50mM DTT (µl)**	**Total vol (ml)**
3% Percoll (vol/vol)	0.3	9.63	62.5	10
10% Percoll (vol/vol)	1	8.93	62.5	10
15% Percoll (vol/vol)	1.5	8.43	62.5	10
23% Percoll (vol/vol)	2.3	7.63	62.5	10

Four Beckman centrifuge polycarbonates tubes were prepared, and five layers (figure 2-3) were injected into each tube from top to bottom in the following

order very slowly (1ml/min) using a long needle (Teumo spinal needle, 19G x 3 1/2), 2ml per layer (figure 2-3). The tubes were centrifuged in a Ti 50 rotor using an L8 Beckman ultracentrifuge at 31000 x g (18,500rpm) at 4°C for 5min. All fractions were collected using a glass Pasteur pipette. Each fraction was diluted to 35ml with ice cold sucrose/EDTA buffer (Percoll Buffer) (1mM EDTA in sucrose-tris buffer, pH 7.4) in 35ml Nalgene tubes and then centrifuged in a JA20 rotor at 20,000 x g (12,800rpm) at 4°C for 30min. After discarding the supernatant, the pellet was once again resuspended with 35ml of sucrose/EDTA buffer and centrifuged as above. After the second centrifugation, the supernatant was removed and the pellet was resuspended in 1.5ml of ice cold TBS-azide + Protease Inhibitors (PIs) (20mM Tris, 150mM NaCl, 0.1% sodium azide, 1mM EDTA, 0.3mM PMSF, 1µg/ml Pepstatin A, 1µg/ml Leupeptin, pH7.4), centrifuged at 18,000 x g in a microfuge at 4°C for 5min, and the pellet collected and resuspended in TBS-azide + PIs for use.

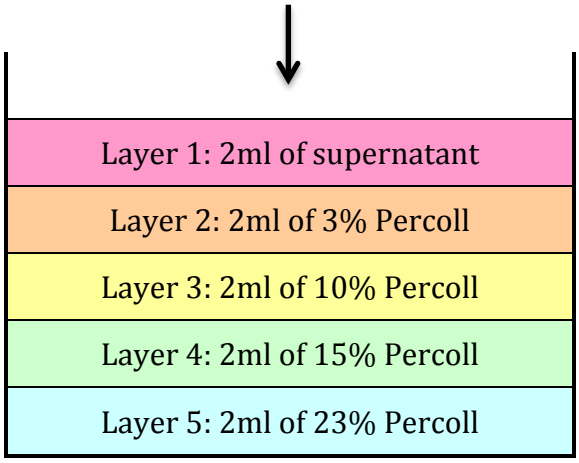

Figure 2-3: Diagram of different layers of percoll gradient injected into each tube.

2.3.2 Lewy Body Purification from Human Brain Homogenate

2.3.2.1 Brain Tissue Homogenization

The brain tissue was defrosted on ice, dissected either grey matter (LBs) or white matter (GCIs) from inclusion-rich regions and minced with a scalpel blade. After recording the weight of the tissue, it was then placed into a Dounce homogenizer with 3x volume of HB according to the weight (e.g. approx. 5g tissue + 15ml buffer), and homogenized for 10-20 strokes with Pestle B (loose) followed by 10-20 strokes with Pestle A (tight). The homogenized tissues from the same case were mixed together and divided into 10ml aliquots (each 2g of tissue was diluted with 10ml Homogenization Buffer), snap frozen in liquid nitrogen then stored at -80°C until use.

2.3.2.2 Lewy Body Purification

Day1: Semi-purifying brain homogenate by using percoll gradient

The six brain homogenate tubes were first defrosted on ice (10ml/tube, with approximately 2g of tissue), then filtered through glass wool using a 20ml syringes. The filtered homogenate was flushed and diluted with a total of 144ml homogenization buffer (24ml/tube), then the filtrate was loaded across 18 centrifuge tubes (8ml/tube), centrifuged at 3,000rpm (1,000 x g, JA21 rotor) at 4°C for 10min. After collecting and freezing supernatant, pellets were resuspended in a total of 8ml HB, centrifuged again at 3,000rpm (1,000xg) at 4°C for 10min. Then supernatant was discarded and each pellet was resuspended with 0.84ml Percoll Plus (GE Healthcare, Buckinghamshire, UK) together with 5.16ml HB (14% Percoll), followed by loading 2.4ml of 35% Percoll Plus in HB (17.5ml Percoll Plus, 32.5ml HB) at the bottom of the tube using a large syringe needle. Another centrifugation was performed at 17,500rpm (34,986xg) at 4°C for 30min, then different layers including top layer, myelin layer and UAN (Upper/Aggregates/Nuclear, fraction of interest) were collected by glass Pasteur

pipettes separately and UAN was stored overnight at 4°C for further purification.

Day2: Digestion and primary antibody incubation

The UAN fractions were diluted to 128ml with TBS-azide and split across ~16 centrifuge tubes (8ml/tube) and centrifuged at 4,000rpm (1,830 x g) at 4°C for 10min. After discarding the supernatant, the pellets from all tubes were combined and distributed into 6 tubes and resuspended in 8ml TBS-azide in each tube. After a second centrifugation at 4,000rpm (1,827 x g) at 4°C for 10min, each pellet was resuspended in 2ml TBS-azide and transferred into an eppendorf tube. The protein concentration in UAN fractions was determined by EZQ analysis after diluting (6µl UAN fraction + 15µl 4x sample buffer w/o Bromophenol Blue w/ DTT + 39µl ddH2O, vortex) and heating (at 95°C for 5min, vortex, spin down) the fraction to allow solubilisation of the protein.

DNAse digestion: in each 2ml fraction, 10µl of 1M NaOH was added to adjust pH to 8.0. After pre-warming tubes at 37°C for 10min, 4µl of diluted trypsin (0.25mg/ml) was added into each tube and vortexed briefly to lyse nuclei. The digestion reaction was immediately stopped by adding 6µl PMSF, 2µl Pepstatin and 2µl Leupeptin. DNA was digested by adding 12.25mM MgCl2 and 200µg DNase I into each tube and incubating at 37°C for 1hour. The samples were washed twice in TBS-azide via centrifugation at 4,000rpm (1,830 x g) at 4°C for 10min, and resuspended in 2ml TBS-azide.

Tryptic digestion: in each 2ml fraction, 10µl of 1M NaOH was added to adjust pH to 8.0. After pre-warming tubes at 37°C for 10min, trypsin (1mg/ml) was added into each tube to give a 1:4000 enzyme: protein ratio and incubated in a thermomixer (1400rpm) at 37°C for 5min. Previous time course experiments were performed to ensure that no decrease in the size of Lewy bodies was seen at 5min (personal communication, T Chataway, Flinders University). At the end of the 5-min incubation, the reaction was immediately stopped by protease

inhibitors (6µl PMSF + 2µl Pepstatin + 2µl Leupeptin). After digestion, the samples were washed twice in TBS-azide + PIs via centrifugation at 4,000rpm (1,830 x g) at 4°C for 10min, and resuspended in 2ml TBS-azide.

Antibody incubation: the sample in each tube was incubated with 20µg of primary antibody (sheep anti α-synuclein) at 1000rpm at 4°C overnight.

Day3: antibody capture

The sample was washed in TBS-azide for 3 times by centrifugation at 4,000rpm (1,830 x g) at 4°C for 10min and removing the supernatant, then the pellet was resuspended in 2ml TBS-azide. The primary antibody attached to inclusions was first captured by adding 15.4µl of biotin-conjugated donkey anti-sheep IgG and mixing at 1000rpm at room temperature for 1hr. After that, a 10µl aliquot was mixed with 2µl 1:400 diluted Cy3-conjugated Streptavidin (Jackson ImmunoResearch Laboratories, West Grove, PA, USA, product No. 016-160-084) and examined under fluorescent microscope to visualize antibody binding to inclusions. Then 6.68µl Dynal MyOne Streptavidin T1 Dynabeads (Invitrogen) and 10µl Dynal M-280 Streptavidin Dynabeads (Invitrogen) were added and mixed at 1400rpm at room temperature for 10min and 60min respectively. Unbound particles were gradually washed off by placing tubes containing 2ml suspension in washing buffer into an EasySep™ magnet (Stemcell Technologies, Melbourne, VIC, Australia) for 5min and removing supernatant 3 times, and final beads were gathered at the bottom of the tube by high-speed centrifugation for 4 times at 18,000 x g at room temperature (1st spin 5min, 2nd spin 5min, 3rd spin 2min, 4th spin 30sec). In order to solubilize inclusions, 80µl of Protein Extraction Buffer (TUC) (7M urea, 2M thiourea, 4% (w/v) CHAPs) was added into each tube of homogenate and vortexed until beads were fully suspended, then mixed at 1400rpm at room temperature overnight.

Day4: ultracentrifugation

The beads were removed by spinning down at 18,000 x g at room temperature for 10min and supernatant containing solubilized inclusions was transferred into Beckman centrifuge tubes for ultracentrifugation (183,000xg, 4°C, 30min) to further purify the samples for use. Protein concentration was determined by EZQ® Protein Quantitation Kit (Invitrogen) to determine the volume to use in the subsequent experiment.

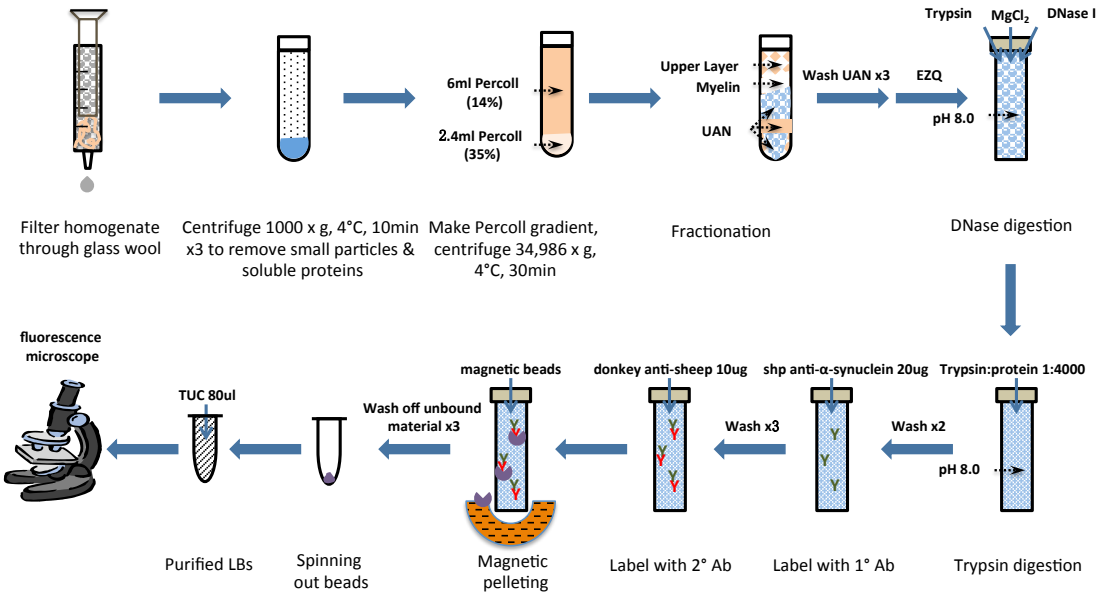

Figure 2-4: Procedures of Lewy Body purification.

2.4 Western Blot

2.4.1 EZQ Protein Quantification Assay

1µl of each standard, sample or dH_2O (as blank) was pipetted onto the assay paper on microplate in triplicate. After drying, the assay paper was removed from the microplate and the empty columns were trimmed off from the end of the paper. Then the assay paper was placed in a tray containing 40ml of methanol and placed on a rocking platform for 5min at RT. The methanol was

then removed and the assay paper was dried on low heat using an Easy Breeze Gel Dryer. Then 35ml of EZQ Protein Quantification Reagent was added into the tray and again agitated as above for 30min, followed by rinsing 3 times for 2min in 40ml of EZQ destain solution (10% methanol and 7% acetic acid in dH_2O). The assay paper was scanned in a BioRad EZ-Doc Imager and analyzed with Carestream Image analysis software.

2.4.2 SDS-PAGE

Immunoblots were used to determine the expression of proteins (α-synuclein, tVAMP2) extracted from brain tissues collected from specific regions of interest. The samples (50µg) in 2x Laemmli sample buffer (4% SDS, 10% 2-mercaptoethanol, 20% glycerol, 0.004% bromophenol blue, 0.125M Tris-HCl, pH 6.8) were loaded onto a polyacrylamide gel after they were denatured by heating at 95°C for 2min, and then electrophoresed with molecular weight markers (Bio-Rad Precision Plus Protein™ Standards, Dual Color, 10-250kD) using a SDS (sodium dodecyl sulfate)-PAGE (polyacrylamide gel electrophoresis) gel (Bio-Rad Mini-PROTEAN® TGX Stain-Free™ Precast gel, any kD™ gel) in running buffer (25mM Tris base, 190mM glycine, 0.1% SDS) at 200 Volts for approximately 30min for a 10-well gel or 300 Volts for approximately 20min for an 18-well gel. After running, the gel was imaged in a Bio-Rad Gel-Doc EZ Imager to check the electrophoresis results and quality prior to western blotting. The images of protein bands on the gels taken by the Imager were used as loading controls in the subsequent data analysis. The proteins within the gel were then transferred to a 0.2µm PVDF membrane (Bio-Rad) in a semi-dry Trans-Blot® Turbo™ Blotting System (Bio-Rad) at 25V, 1.0A for 30min. After transfer, both the gel and the membrane were imaged in the Bio-Rad Gel-Doc EZ Imager to confirm the efficiency of the transfer. The membrane was then blocked in 5%

skim milk in PBST (0.05% Twen-20) (blocking solution) for 1hr at room temperature (RT), and incubated with primary antibodies including mouse anti α-synuclein (ELAN) 11A5 antibody (final concentration at 1:2k), rabbit anti AtVAMP2 antibody (final concentration at 1:2k), rabbit anti tVAMP2 antibody (final concentration at 1:2k) or rabbit anti AfVAMP2 antibody (final concentration at 1:2k) diluted in antibody diluent solution (2.5% skim milk powder solution in PBST (0.025% Tween-20)) at 4°C overnight. The membrane was washed 3 times in PBST and incubated with species appropriate HRP-conjugated secondary antibodies for 1hr at RT. Bound antibodies were detected using ECL Substrate (Bio-Rad Clarity™ Western ECL Substrates Luminol Enhancer Solution and Stable Peroxide Solution). The membrane was exposed and imaged in a Fuji LAS-4000 Imager.

2.4.3 2D Gel Electrophoresis

Day 1: Sample Preparation and Strip Rehydration

The isolated inclusions were diluted in TUC buffer containing 0.4% DTT to make the final volume 275ul for a 13cm strip. Then 0.5% ampholytes and a trace amount (~0.5ul) of saturated bromophenol blue solution were added to the sample/buffer mixture to complete the sample preparation before 2D gel electrophoresis.

The prepared sample solutions were evenly loaded along the strip holder between the two electrodes, covered by strips and Dry strip cover fluid, 1-2ml per strip. The strip holder was then placed into the IPGphor and the rehydration was performed overnight at 20°C, 50V.

Day 2: Isoelectric Focussing (1st Dimension)

The hydrated strips were taken out and the strip holder and its lid were washed

with IPG detergent and deionized water and dried. Whatman filter paper (No 1) was cut into small pieces ("wicks") with the right size to cover the electrodes in the strip holder. The wicks were dampened with deionized water and were then placed over the electrodes in the strip holder with forceps, and the strips were returned to the strip holder and covered by 1-2ml of Dry strip cover fluid evenly afterwards. The strip holder was once again placed into IPGphor and the isoelectric focusing (IEF) was performed overnight with gradient up to 10,000Vhr until 69,893 total Vhr was reached followed by holding at 220V. The program in Ettan IPGphor 3 was set as follows:

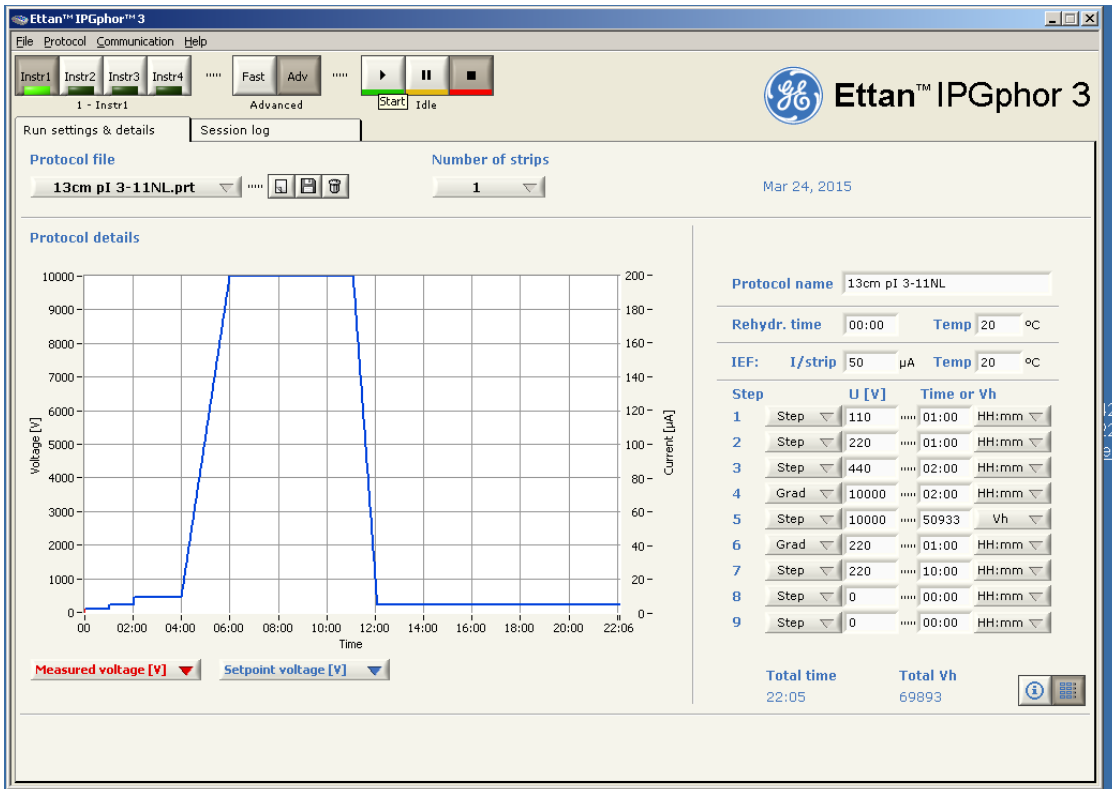

Day 3: Gel Electrophoresis (2nd dimension)

The strips were removed from the strip holder and transferred into the equilibration (EQ) tube with one end sealed with a stopper or parafilm. After adding 5ml of EQ Solution containing 1% DTT into the tube, the other end was sealed and the tube was placed on the stirrer for 15min before pouring off

Solution 1. The procedure was repeated using 5ml of EQ Solution containing 4% Idoacetamide + 20µl Bromophenol blue. The strips were then removed from the equilibration tube and placed on top of the gel, with a gel comb at the negative end of the strip for molecular weight marker (MWM). Then a layer of 1% low-melting point agarose was placed over the strip to the top of the gel plate and was cooled for ~5min until the agrose was solidified. After putting the gel plates into the tank and pouring 1X running buffer into the top and bottom compartments, the gels were run at constant voltage of 300V for approximately 20min until bromophenol blue reached 0.5cm from the bottom of the gel plates.
After running, the gel was detached from the plates and transferred into a glass dish containing fixative/destain solution (20% methanol, 7.5% acetic acid) for 30min before proceeding with either Coomassie blue or silver stain for 45-60min. After destaining until desired background gained, the gels were ready for imaging.

2.5 Mass Spectrometry

2.5.1 Coomassie Staining

After gel electrophoresis of 15ug of purified Lewy bodies along with molecular weight markers (Bio-Rad Precision Plus Protein™ Standards, Unstained, 10-250kD, Catalogue# 161-0363), the 1D gel was fixed in the fixing solution containing 40% methanol and 10% acetic acid for 1-2hr, followed by staining in Coomassie solution (2g Coomassie Brilliant Blue R250, 200ml of methanol, 50ml of glacial acetic acid, 750ml of dH_2O) for 1hr. The gel was then placed in dH_2O and heated in a microwave for 20min to washout excess stain. The gel was then transferred into destaining solution (20% methanol, 7.5% acetic acid), imaged using the BioRad Gel Doc Imager, and washed in dH_2O 3 times (30min per wash)

to remove traces of acetic acid from the fixative and prepare for trypsin digestion.

2.5.2 In-Gel Trypsin Digestion

The band or spot of interest was removed from the gel using a scalpel blade or pipette tip, respectively. The band was cut into 1X1 mm pieces and placed in 1.5ml low bind tube (Axygen 1.7ml Cat# MCT-175-L-C). The gel slices were washed in 500ul of 100mM ammonium bicarbonate (Sigma-Aldridge Cat# 09830 Bio Ultra Grade) for 30min twice, and then incubated in 150ul of 100mM ammonium bicarbonate with 10ul of 50mM DTT (Astral Scientific Cat# C-1029) at 60°C for 30min. After cooling to room temperature (RT), 10ul of 100mM iodoacetamide (IAA) (BioRad Cat# 163-2109) was added to the gel slices and then incubated for 30min in the dark at RT. After incubation, the gel slices were washed twice in 500ul of 100mM ammonium bicarbonate with shaking for 30min each. In order to shrink the gel slices, 200ul of acetonitrile (Merck Cat# 100029) was then added. After 10-15min, the solvent was removed and the gel slices air-dried. When dry, the gel slices were completely covered by trypsin working solution (stock solution 1ug/ul from Promega Cat# V5280 Trypsin Gold Mass Spectrometry Grade, working solution 20ng/ul: 1/50 dilution in 100mM ammonium bicarbonate) on ice for 10-15min, followed by incubation at 37°C overnight for thorough digestion. On the following day, the tubes were briefly centrifuged and the trypsin solution containing digested tryptic peptides was transferred into mass spectrometry vials.

2.5.3 LC MS/MS

Extracts digested with Trypsin were analyzed using an AB Sciex TripleTOF 5600+ mass spectrometer fitted with a nanospray source (AB Sciex). Digested peptides were applied to a Polar 3 um precolumn (0.3 x 10 mm, SGE Analytical Science) and eluted onto a spraytip 5um C18 column (75mm x 150 mm with a bead pore size of 100Å) (Nikkyo Technos), using an Eksigent Ekspert 415 nanoLC. Peptides were eluted using a 35-minute gradient from 5% to 25% acetonitrile / 0.1% formic acid at a flow rate of 300 nl/minute over 35 minutes, followed by a second gradient to 40% acetonitrile / 0.1% formic acid over 7 minutes and a further step to 95% acetonitrile for 11 minutes. The mass spectrometer was operated in positive-ion mode with one MS scan of mass/charge (m/z) 350 – 1,500, followed by collision-induced dissociation fragmentation of +2 to +5 charge state ions that were greater than 10 counts per second for a maximum of 100 candidate ions. Exclusion of former target ions was performed for 30 seconds after 1 occurrence with a mass tolerance of 50 mDa. Rolling collision energy and dynamic accumulation were also applied. Product ion scans were from 100 to 1,500 Da in high sensitivity mode and an accumulation time of 0.01 seconds was used.

Spectra were searched using ProteinPilot (v4.5b, AB Sciex) using the Paragon search engine and the Uniprot human database (version 03-09-2014). The software was operated in biological and thorough ID modes, with the detected protein threshold set at 0.05. False discovery rate analysis was also performed.

The exported .wiff files from ProteinPilot™ were loaded into the PEAKS Studio 7.0 (build 20140912) software (Bioinformatics Solutions Inc.). Spectra were exported from ProteinPilot and analysed with PEAKS 7.0 (Bioinformatics Solutions Inc.). The data was refined with minimum charge of +2 and max charge of +6. Searches were made using the Uniprot human database with an error tolerance of 15 ppm for precursor ions and 0.02 Da for product ions. Carbamidomethylation was set as a fixed modification and oxidation of

methionines as a variable modification with a maximum of 2 variable PTMs per peptide. The digesting enzyme was set as Trypsin or GluC with a maximum missed cleavage of 1 and non-specific cleavage allowable at one end of the peptide.

2.6 Protein concentration assay

The protein concentrations of brain homogenates or purified Lewy bodies were measured using the EZQ protein quantification assay in order to load the same amount of protein onto the gel.

Chapter 3

Results

3.1 The specificity of the VAMP2 and α-synuclein antibodies for the detection of Lewy bodies and Lewy neurites.

At the beginning of this study, it was necessary to determine which antibodies that were available in the laboratory could be used to test the hypothesis. In order to optimize the antibodies to visualize Lewy bodies and Lewy neurites in this study, the specificity of different antibodies were tested on PD case tissue and compared to normal control brain tissue by using immunohistochemistry and immunoblot.

The morphology of classical Lewy bodies was initially demonstrated by using immunostaining with the tVAMP2 (truncated VAMP2) antibody. Figure 3-1 showed a clear picture of tVAMP2-stained Lewy bodies and Lewy neurites in a free-floating section of a PD+AD brain (SA0041). The classical Lewy body in the middle of the figure appeared as a spherical inclusion that displaced other cell components. It was composed of a dense core surrounded by a pale-stained halo of radiating fibrils. Lewy neurites were abnormal neurites containing granular material and abnormal filaments similar to those found in Lewy bodies. In figure 3-2 and 3-3, immunohistochemistry was conducted on free-floating and paraffin sections with a range of antibodies including one tVAMP2 antibody, one AtVAMP2 antibody that was purified from tVAMP2, both antibodies were kindly provided by Dr. Weiping Gai. In addition, two fVAMP2 (full-length VAMP2) antibodies purchased from Biochem and two α-synuclein antibodies (anti-sheep provided by Dr Weiping Gai and anti-mouse purchased from Elan) were also tested. The quality of each antibody was determined by the number of lesions per field counted under the light microscope with a magnification of 200X. The specificity of each antibody was determined by comparing a PD case (patient ID:

SA0015) with a normal case (patient ID: SA0036). In free-floating sections, tVAMP2 and AtVAMP2 antibodies (corresponding to amino acid residues 30-47) showed clear staining of Lewy bodies and Lewy neurites in the PD case but not in the normal brain (figure 3-2, a-d). Hence, it was concluded that tVAMP2 and AtVAMP2 antibodies were ideal for immunohistochemistry in the following study. However, the two fVAMP2 antibodies (corresponding to amino acid residues 2-17) showed poor staining of Lewy bodies and Lewy neurites but with strong staining in normal synapses, suggesting that these two antibodies were not useful pathological indicators (figure 3-2, e-h). As a gold standard for PD pathology, both α-synuclein antibodies detected Lewy bodies and Lewy neurites in PD. The sheep α-synuclein antibody stained more Lewy bodies in PD than mouse anti α-synuclein (figure 3-2, i-l).

To further test the quality of α-synuclein and tVAMP2 antibodies on paraffin sections, immunostaining was performed on sections of a DLB brain (patient ID: SA0046) (figure 3-3). Positively stained Lewy bodies and Lewy neurites were detected by all three antibodies (rabbit anti tVAMP2, rabbit anti AtVAMP2 and sheep anti α-synuclein). Notably, α-synuclein antibody produced very strong synaptic staining, making the background unclear compared with tVAMP2 antibodies (figure 3-3, c).

In order to further compare the quality of these three antibodies in staining Lewy bodies in PD and DLB, the numbers of positively stained Lewy bodies by each antibody in three independent cases were counted under 100X magnification (table 3-1, a-b) and analyzed using one-way anova to compare the mean of each group with the mean of every other group using Prism 6 software. Both tVAMP2 and AtVAMP2 stained significantly fewer Lewy bodies than α-synuclein-stained Lewy bodies ($p<0.05$) (figure 3-4, a-b).

Figure 3-1

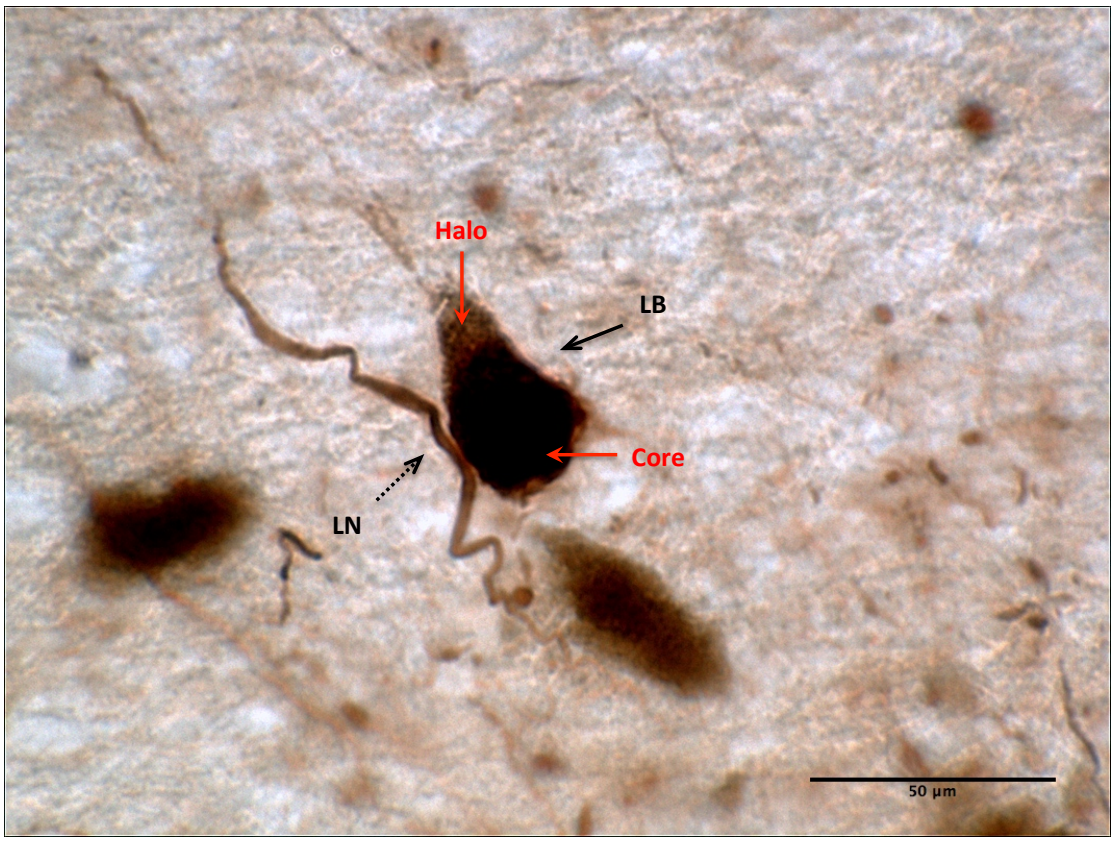

Figure 3-1: Morphology of Lewy bodies and Lewy neurites in Parkinson's disease. Immunostaining of tVAMP2 (1:2k) in the free-floating section of a PD+AD brain (SA0041) showed a clear picture of classical Lewy bodies and Lewy neurites. The observation was made using x1000 magnification with oil immersion lens. Scale bar is 50µm, solid arrow indicates Lewy body and dotted arrow indicates Lewy neurite. The core and surrounded halo of Lewy body are labeled with red arrows.

Figure 3-2, a-d

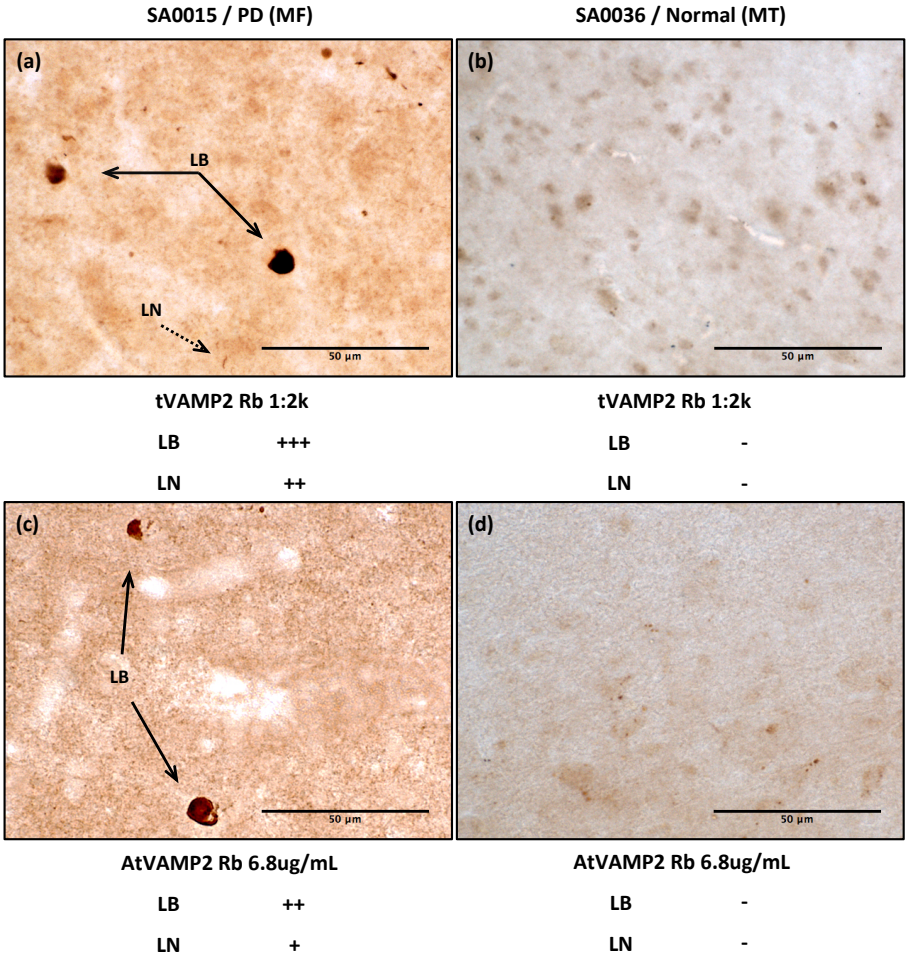

Figure 3-2 (a-d): Immunostaining with tVAMP2 and AtVAMP2 antibodies in free-floating sections of control and PD brains. Immunostaining with antibodies against tVAMP2 (rabbit, 1:2k), AtVAMP2 (rabbit, 6.8ug/ml) in free-floating sections of the mid-frontal region of a PD case (patient ID: SA0015) (left panels) and the mid-temporal region of a normal case (patient ID: SA0036) (right panels). Magnification of 400x using an Olympus BH-2 light microscope (Tokyo, Japan). The number of Lewy bodies and Lewy neurites was counted with a magnification of 200x. Scale bar is 50µm, solid arrows indicate Lewy bodies and dotted arrows indicate Lewy neurites.

LB: Lewy bodies, LN: Lewy neurites

- negative; + 1-5 inclusions/field; ++ 5-10 inclusions/field; +++ >10 inclusions/field

Figure 3-2, e-h

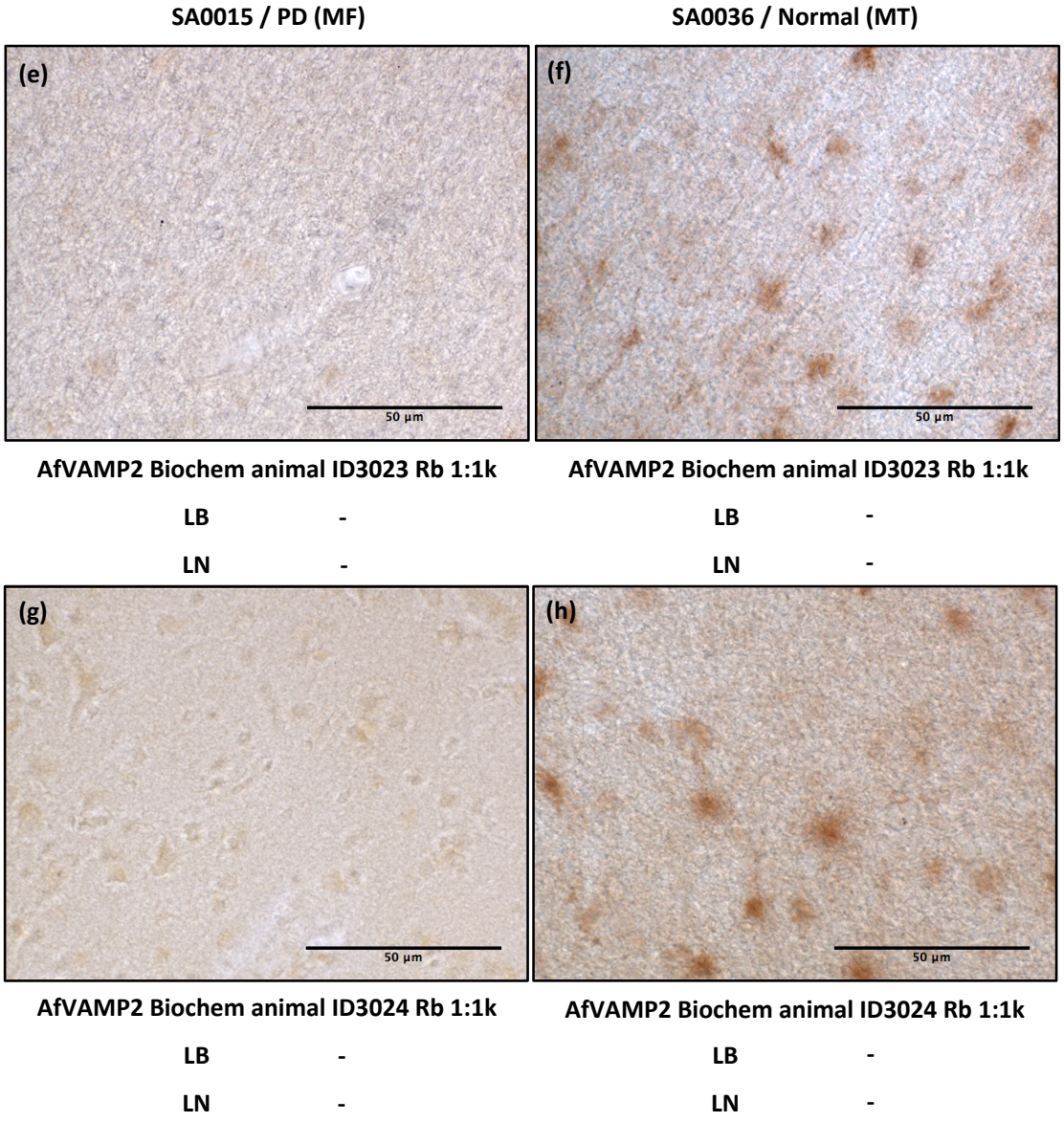

Figure 3-2 (e-h): Immunostaining with fVAMP2 antibodies in free-floating sections of control and PD brains. Immunostaining with antibodies against two fVAMP2 antibodies (Biochem, animal ID 3023 and 3024, rabbit, 1:1k) in free-floating sections of the mid-frontal region of a PD case (patient ID: SA0015) (left panels) and the mid-temporal region of a normal case (patient ID: SA0036) (right panels). Magnification of 400x using an Olympus BH-2 light microscope (Tokyo, Japan). Scale bar is 50µm.

Figure 3-2, i-l

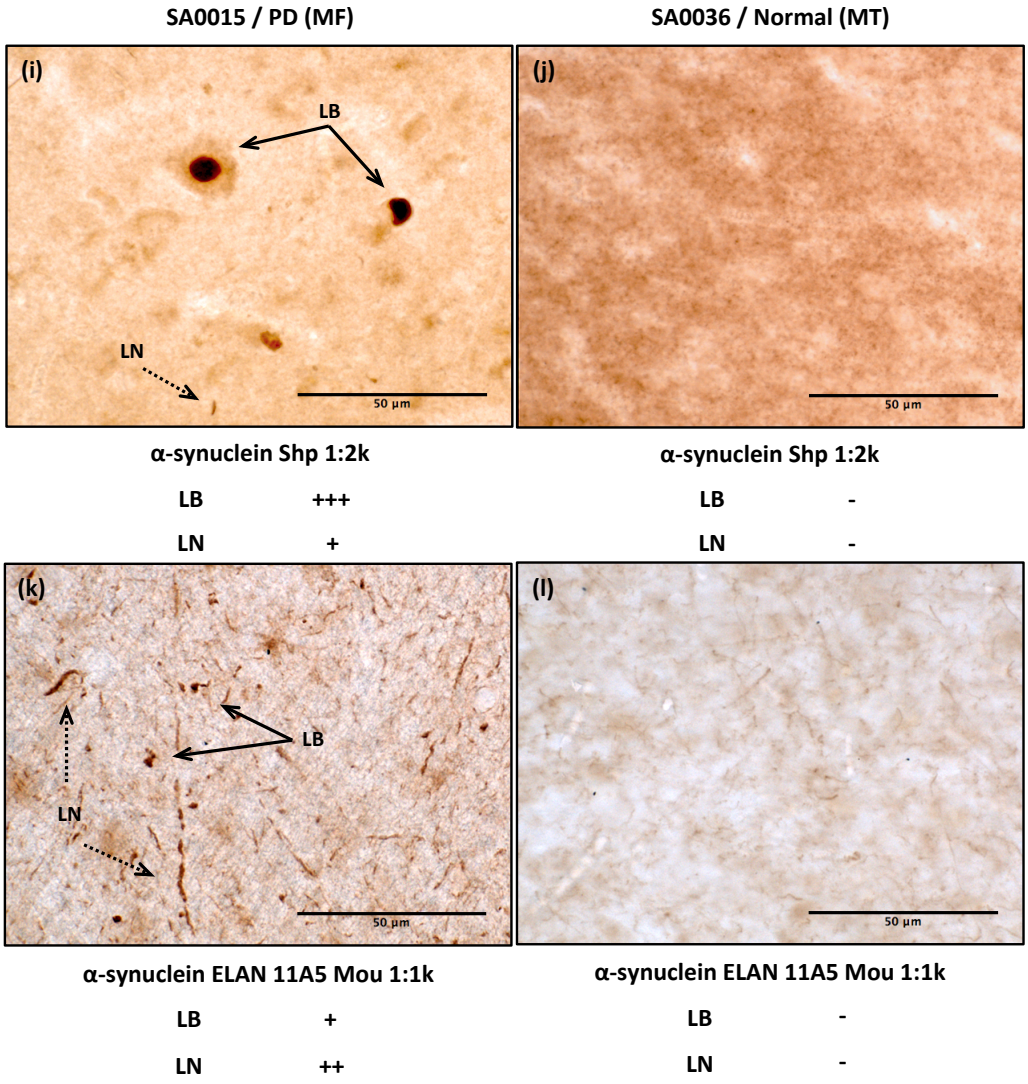

Figure 3-2 (i-l): Immunostaining with α-synuclein antibodies in free-floating sections of control and PD brains. Immunostaining with antibodies against α-synuclein (sheep, 1:2k) and α-synuclein (ELAN 11A5, mouse, 1:1k) in free-floating sections of the mid-frontal region of a PD case (patient ID: SA0015) (left panels) and the mid-temporal region of a normal case (patient ID: SA0036) (right panels). Magnification of 400x using an Olympus BH-2 light microscope (Tokyo, Japan). The number of Lewy bodies and Lewy neurites was counted with a magnification of 200x. Scale bar is 50µm, solid arrows indicate Lewy bodies and dotted arrows indicate Lewy neurites.

Figure 3-3

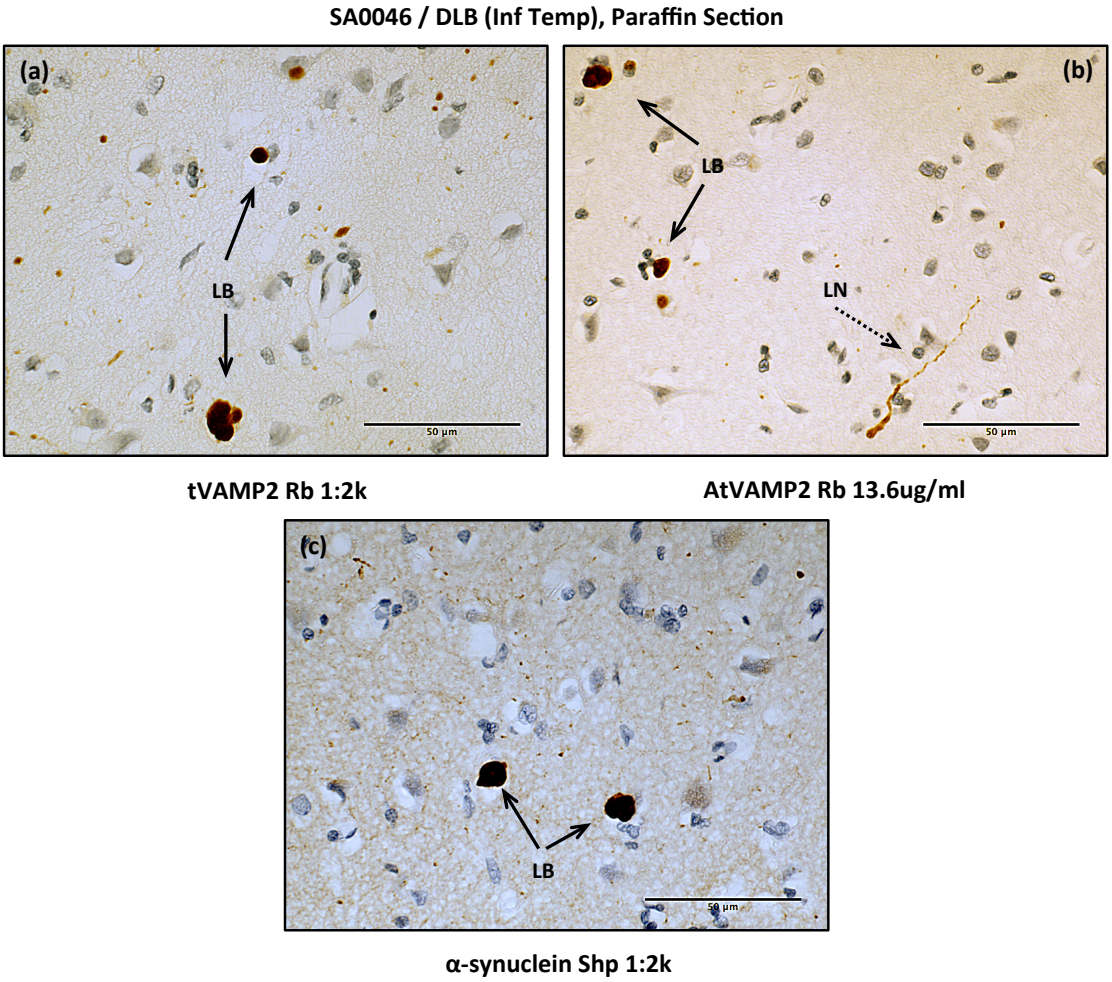

Figure 3-3: Immunostaining with tVAMP2, AtVAMP2 and α-synuclein antibodies in paraffin sections of a DLB brain. Immunostaining with antibodies against tVAMP2 (rabbit, 1:2k), AtVAMP2 (rabbit, 13.6ug/ml), α-synuclein (sheep, 1:2k) in paraffin sections of the inferior temporal region of a DLB case (patient ID: SA0046). Magnification of 400x using an Olympus BH-2 light microscope (Tokyo, Japan). Scale bar is 50µm, solid arrows indicate Lewy bodies and dotted arrows indicate Lewy neurites.

Table 3-1, a

	SA0083/DLB (MT)		SA0083/DLB (MF)		SA0015/PD (MF)	
Antibody	**Total Lewy body number**	**% of α-synuclein - stained Lewy body**	**Total Lewy body number**	**% of α-synuclein - stained Lewy body**	**Total Lewy body number**	**% of α-synuclein - stained Lewy body**
α-synuclein (1:2k)	1025	100	832	100	261	100
tVAMP2 (1:2k)	848	82.73	678	81.49	142	54.41
AtVAMP2 (6.8ug/ml)	637	62.15	668	80.29	182	69.73

Table 3-1, b

	Total Lewy body number		% of α-synuclein-stained Lewy body	
Antibody	**Mean**	**S.E.M**	**Mean**	**S.E.M**
α-synuclein (1:2k)	706	229.37	100	0
tVAMP2 (1:2k)	556	212.74	72.88	9.24
AtVAMP2 (6.8ug/ml)	495.67	157.09	70.72	5.26

Table 3-1, a-b: Counting of Lewy bodies that stained by tVAMP2, AtVAMP2 and α-synuclein antibodies in free-floating sections. (a) Immunostaining with antibodies against tVAMP2 (rabbit, 1:2k), AtVAMP2 (rabbit, 6.8ug/ml), α-synuclein (sheep, 1:2k) in three independent free-floating sections of the mid temporal region and the middle frontal region of a DLB case (SA0083) and the middle frontal region of a PD case (SA0015). (b) The total number of Lewy bodies stained by each antibody in every section was normalized by the number

of α-synuclein-stained Lewy bodies in the same case. Means and Standard Errors of the Mean (S.E.M) of total Lewy body number and percentage of α-synuclein-stained Lewy bodies were calculated accordingly.

Figure 3-4, a-b

(a) (b)

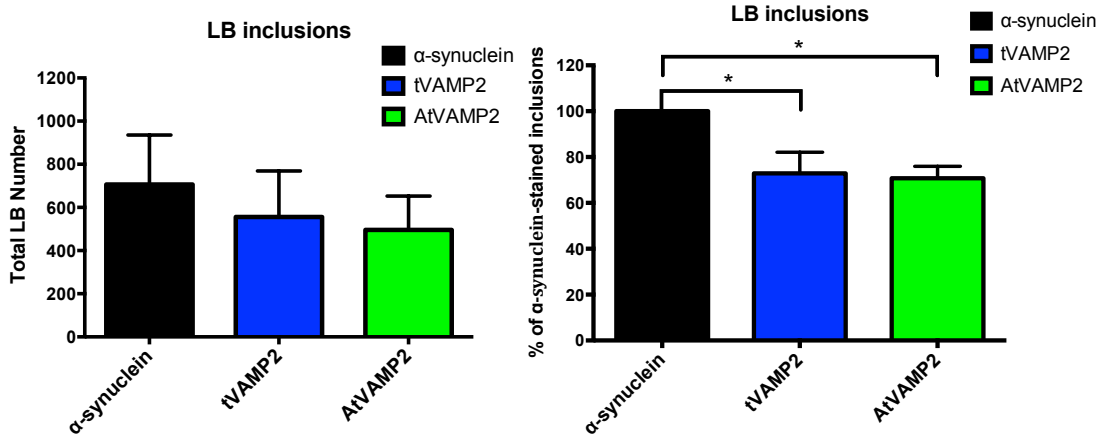

Figure 3-4, a-b: One-way Anova analysis of the total Lewy body numbers that stained by tVAMP2, AtVAMP2 and α-synuclein antibodies in free-floating sections. The total number of Lewy bodies and the normalized percentage of Lewy bodies were analyzed with one-way anova of multiple comparison in Prism 6. * indicates $p<0.05$.

Figure 3-4, c-d

(c)

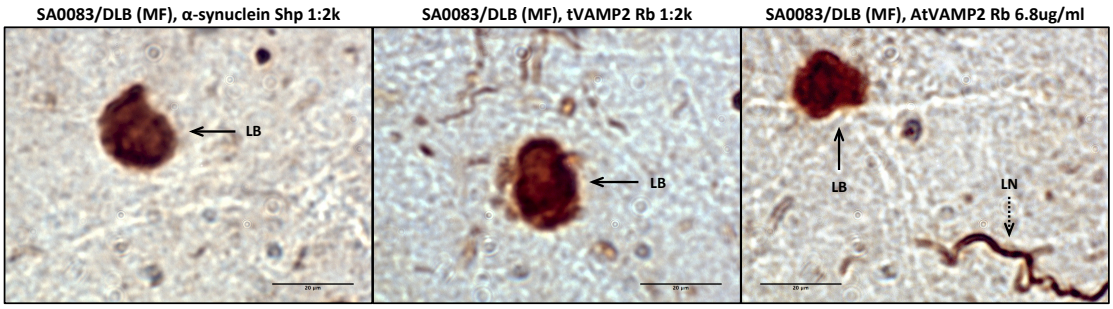

(d)

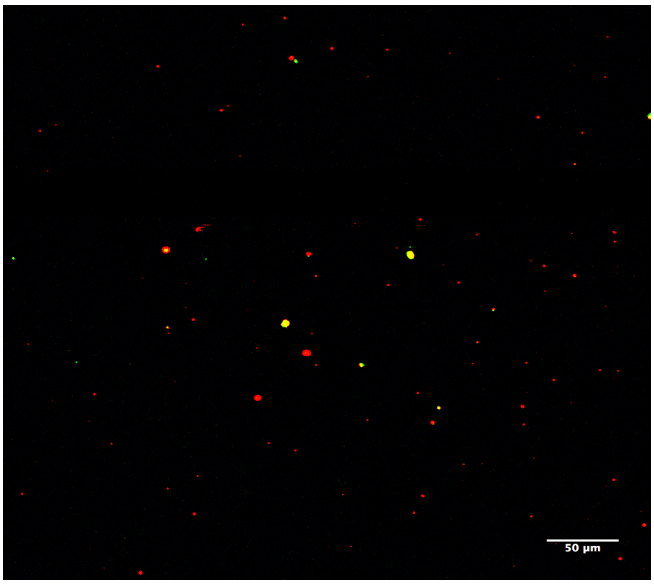

SA0274/PD, purified LB, α-synuclein shp 1:300–CY3 + tVAMP2 1:200- Alexa 488

Figure 3-4, c-d: Lewy bodies staining by tVAMP2, AtVAMP2 and α-synuclein antibodies in free-floating sections. (c) Morphology of positively stained Lewy bodies with α-synuclein (left), tVAMP2 (middle) and AtVAMP2 (right) antibodies under 1000x magnification in the free-floating sections of a DLB brain (SA0083) that were counted for analysis. Scale bar is 20µm, solid arrows indicate Lewy bodies and dotted arrows indicate Lewy neurites. (d) Positively stained Lewy bodies with antibodies of α-synuclein (red) or tVAMP2 (green) or both (yellow) under a confocal microscopy by double immunofluorescence staining. Scale bar is 50µm.

Purified Lewy bodies of a PD case (patient ID: SA0274) and normal tissue (patient ID: SA0230) was subjected to a Lewy body purification protocol. The samples were run on SDS-PAGE and immunoblotted with tVAMP2, AtVAMP2, fVAMP2 and Pan α-synuclein antibodies in order to: (1) compare specificity of each antibody by Western blot to identify whether each antibody detects a protein of the correct molecular weight; (2) examine the protein expression of truncated VAMP2 and α-synuclein in Lewy bodies of PD brain compared to control. In Western blot analysis (figure 3-5), in addition to the band for full-length VAMP2 monomer (at around 17kDa) and the bands with higher molecular weights for VAMP2 aggregates, there was another band at around 14kDa only detected by the truncated VAMP2 antibodies (tVAMP2 and AtVAMP2) which detect the 30-47 amino acid sequence (figure 3-5, e-f), but not by the full-length VAMP2 antibody (fVAMP2) which detects the 2-17 amino acid sequence (figure 3-5, g). The 14kDa band was only detected in purified Lewy bodies of PD but was absent in purified sample of normal case using the same protocol. This suggested that the 14kDa band was specific to Lewy pathologies. tVAMP2 antibody required a shorter exposure but contained a higher background with more non-specific bands (figure 3-5, b & f), whereas AtVAMP2 had a much clearer background but fainter bands (figure 3-5, a & e). α-synuclein antibody detected both monomer (around 20kDa) and aggregates in purified Lewy bodies (figure 3-5, h). All of these figures indicated the protein expression of both truncated VAMP2 and α-synuclein in Lewy bodies.

Figure 3-5, a'-d' & a-d

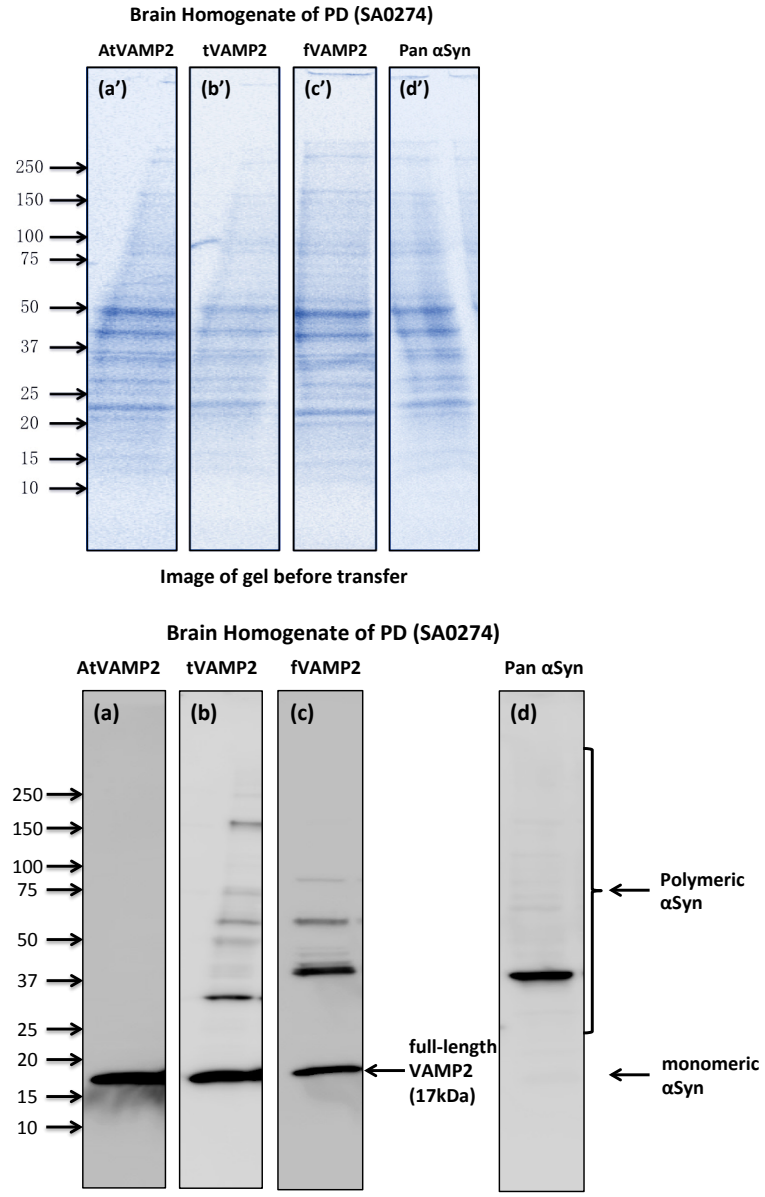

Figure 3-5, a'-d' & a-d: Western blot analysis of brain homogenate from a PD case using tVAMP2, AtVAMP2, fVAMP2 and Pan α-synuclein antibodies. Western blot of brain homogenate of a PD case (patient ID: SA0274) is shown in figure a-d. Brain homogenate was run on a 4-20% SDS-PAGE gel and blotted with antibodies against tVAMP2 (rabbit, 1:1k), AtVAMP2 (rabbit, 0.34ug/ml), fVAMP2 (rabbit, 1:1k) and Pan α-synuclein (rabbit, 1:2k). 15µg of protein was loaded for each sample. The corresponding image of each gel prior to transfer is shown in figure a'-d'. This experiment was repeated four times.

Figure 3-5, e'-h' & e-h

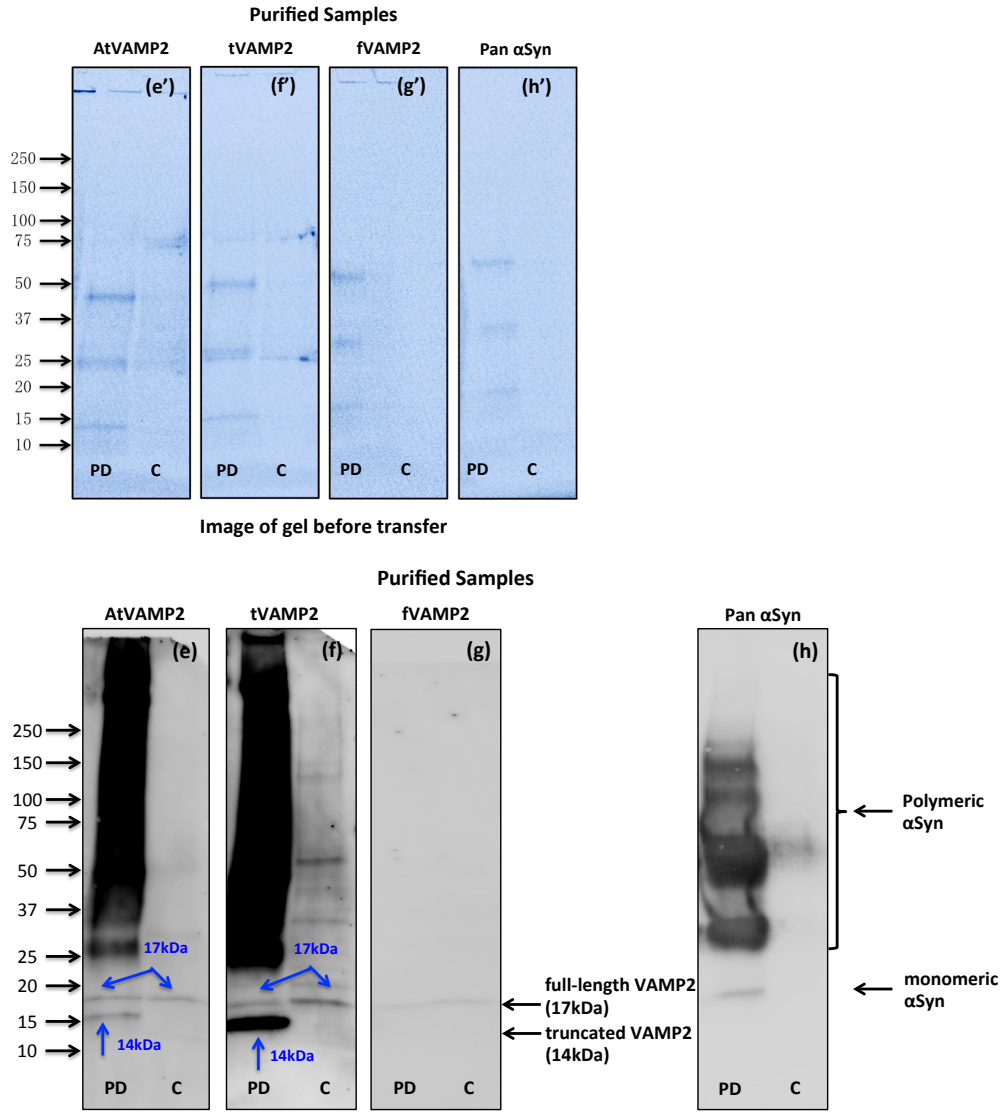

Figure 3-5, e'-h' & e-h: Western blot analysis of purified protein samples from a PD case and a normal case using tVAMP2, AtVAMP2, fVAMP2 and Pan α-synuclein antibodies. Western blot of purified protein from a PD case (patient ID: SA0274) and a normal case (C) (patient ID: SA0230) using the same protocol of Lewy body purification is shown in figure e-h. The purified proteins were run on a 4-20% SDS-PAGE gel and blotted with antibodies against tVAMP2 (rabbit, 1:1k), AtVAMP2 (rabbit, 0.34μg/ml), fVAMP2 (rabbit, 1:1k) and Pan α-synuclein (rabbit, 1:2k). 15μg of protein was loaded for each sample. The corresponding image of each gel prior to transfer is shown in figure e'-h'. This experiment was repeated four times.

3.2 Lewy bodies and Lewy neurites were detectable in various regions of PD brains while absent in normal brain by using immunostaining with tVAMP2 and α-synuclein antibodies.

Clinically, different distribution of Lewy bodies and Lewy neurites in brainstem and cortex will lead to various manifestations and symptoms in PD and DLB. Hence, an eligible pathological marker for PD and DLB should be able to detect Lewy bodies and Lewy neurites in different regions of brain. In 3.1, the antibodies of tVAMP2 (rabbit) and α-synuclein (sheep) and their dilutions were optimized in immunohistochemistry. The capability of these two antibodies to detect Lewy bodies and Lewy neurites in regions of neocortex and brainstem of PD or DLB brains was tested by using immunostaining on free-floating sections.

Firstly, the distribution of Lewy bodies in neocortex was identified via immunostaining with α-synuclein antibody. There are 6 classically recognized layers of the cortex (figure 3-6, a & b)[175]:

I: Outer plexiform (molecular) layer: sparse neurons and glia;

II: Outer granular layer: small pyramidal and stellate neurons;

III: Outer pyramidal layer: moderate sized pyramidal neurons;

IV: Inner granular layer: densely packed stellate neurons;

V: Ganglionic or inner pyramidal layer: large pyramidal neurons;

VI: Multiform cell layer: mixture of small pyramidal and stellate neurons.

It was reported that in DLB, Lewy pathology in the cerebral cortex affected layers V-VI initially, then accumulated in layer III, and finally layer II. The amygdala was first affected, then the limbic cortex, and finally the neocortex [176]. Our observation of immunostaining in the amygdala region of a DLB brain with α-synuclein showed that Lewy bodies are mainly distributed in layer V-VI (figure 3-6, c), consistent with the observations that were previously reported.

Then, to further explore the distribution of Lewy pathologies in different regions

of PD brainstem, we applied immunostaining on free-floating sections of two PD brains and compared to a normal case (figure 3-7). tVAMP2 positively stained Lewy bodies and Lewy neurites were detected in all the brainstem regions explored in the PD cases including Pons, Medulla, Rostral Medulla, Rostral Midbrain and Caudal Pons, and absent in the control case. Classical Lewy bodies and Lewy neurites were clearly shown in tVAMP2 stained free-floating sections of PD.

These results indicated that the optimized tVAMP2 and α-synuclein antibodies were validated in detecting Lewy bodies and Lewy neurites distributed in different regions of PD and DLB brains, suggesting their potential for use in pathological analysis for PD and DLB.

Figure 3-6

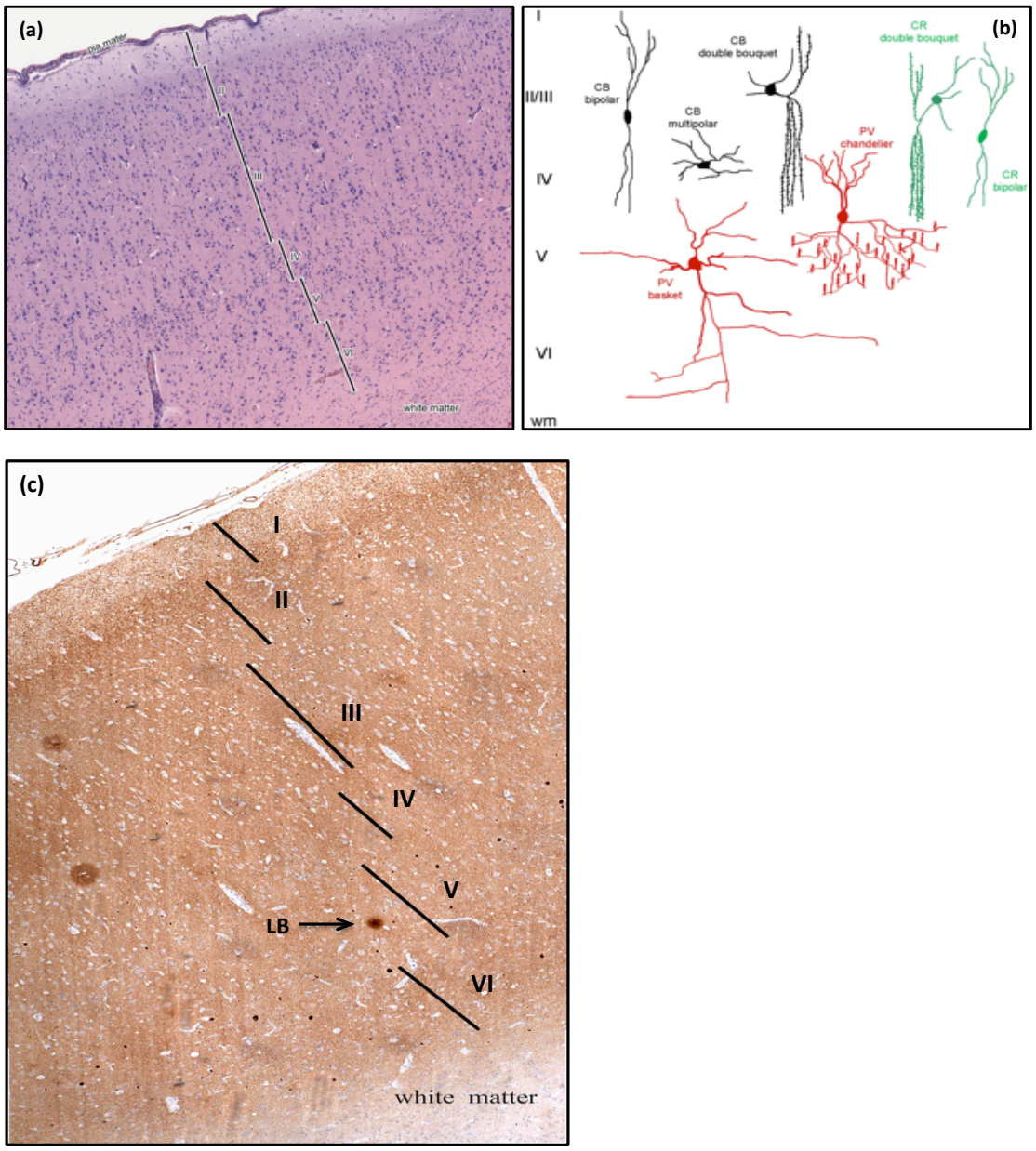

Figure 3-6: Lewy body distribution in neocortex layers. (a) & (b) Scheme of 6 classically recognized layers of the cortex[175]. (c) Immunostaining of α-synuclein in free-floating section of the amygdala region of a DLB brain (patient ID: SA0052). I: molecular layer; II: outer granular layer; III: outer pyramidal layer; IV: inner granular layer; V: inner pyramidal layer; VI: multiform cell layer.

Figure 3-7

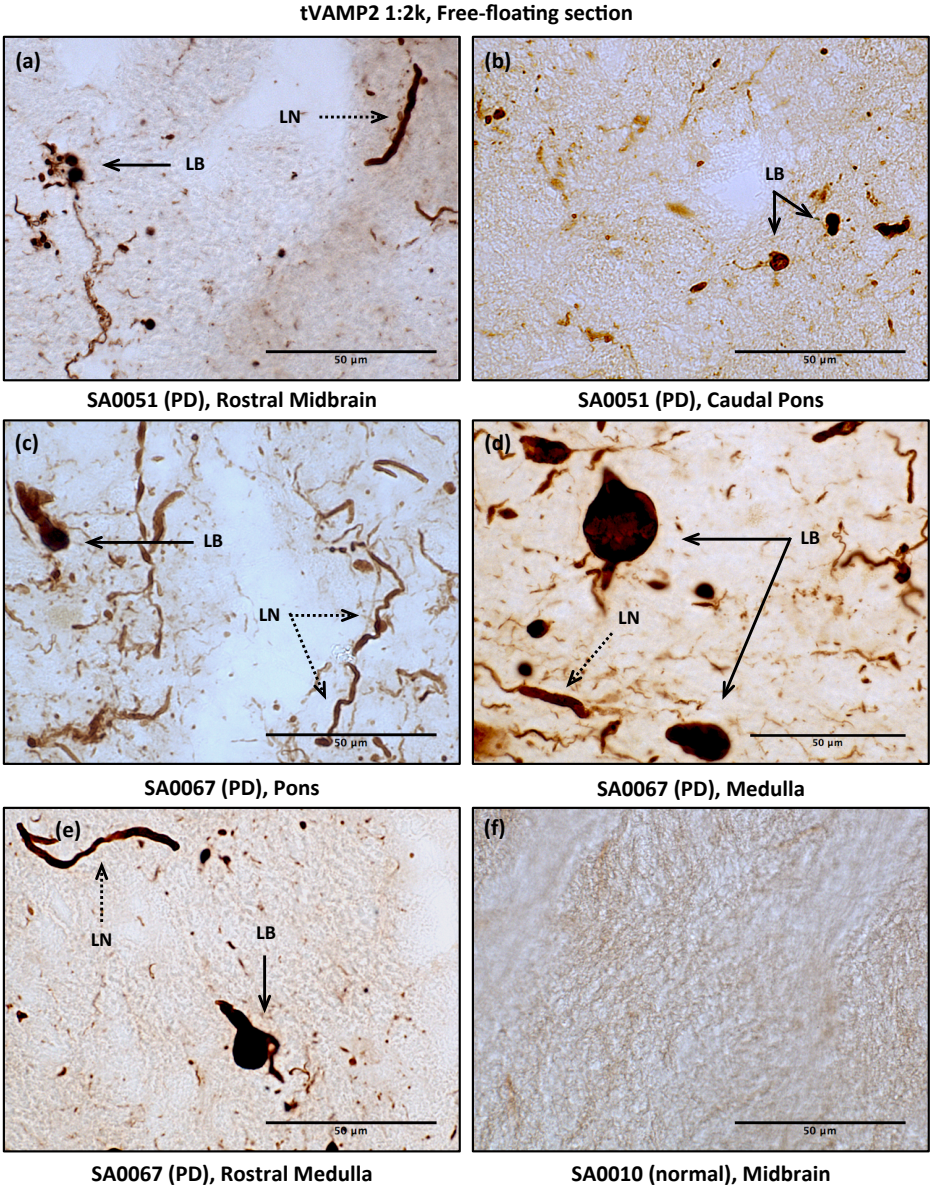

Figure 3-7: tVAMP2-stained Lewy pathologies distributed in various regions of PD brainstem. Immunostaining with an antibody against tVAMP2 (1:2k) in free-floating sections of different regions (Pons, Medulla, Rostral Medulla, Rotral Midbrain and Caudal Pons) of two PD brains (patient ID: SA0067 and SA0051) and the midbrain region of a normal brain (patient ID: SA0010) was observed under the magnification of 400x. Scale bar is 50µm, solid arrows indicate Lewy bodies and dotted arrows indicate Lewy neurites.

3.3 Co-localization of truncated VAMP2 and α-synuclein in Lewy bodies and Lewy neurites.

As shown above, both truncated VAMP2 and α-synuclein exist in Lewy bodies and Lewy neurites. The next question: Is there any relationship between truncated VAMP2 and α-synuclein in the formation of Lewy pathologies in PD and DLB? It is well-documented that α-synuclein is a major component of Lewy bodies and Lewy neurites [26], and that α-synuclein can act as a molecular chaperone of VAMP2 in stimulating SNARE complex assembly and neurotransmitter release [65], thus we hypothesized that the truncation of VAMP2 may play a role in α-synuclein-induced Lewy pathologies. In order to provide evidence for the hypothesis, we used double immunofluorescence staining with antibodies of tVAMP2 and α-synuclein.

It was demonstrated that the tVAMP2 antibody co-localized with α-synuclein in Lewy bodies (including early stage) and Lewy neurites on paraffin sections of DLB brains via double immunostaining with α-synuclein and tVAMP2 antibodies (figure 3-8 and 3-9) or with α-synuclein and AtVAMP2 antibodies (figure 3-10). Mouse anti α-synuclein also had the same pattern of staining as sheep anti α-synuclein (figure 3-9). This data is consistent with our hypothesis that tVAMP2 may form in the oligomers with α-synuclein in the formation of Lewy bodies and the development of the disease. Importantly, although overlapped with each other, tVAMP2 staining had the consistent tendency of a more central localization in Lewy bodies and Lewy neurites, while α-synuclein positive staining was more to the periphery. It was noteworthy that the tVAMP2 antibody detected many finer extensions from α-synuclein positive Lewy neurites (figure 3-9, j-l) and numerous additional swollen synapses that were not detectable by α-synuclein antibody (figure 3-9, m-o). This co-localization was further confirmed in purified Lewy bodies and Lewy neurites of PD (figure 3-11).

Figure 3-8, a-d

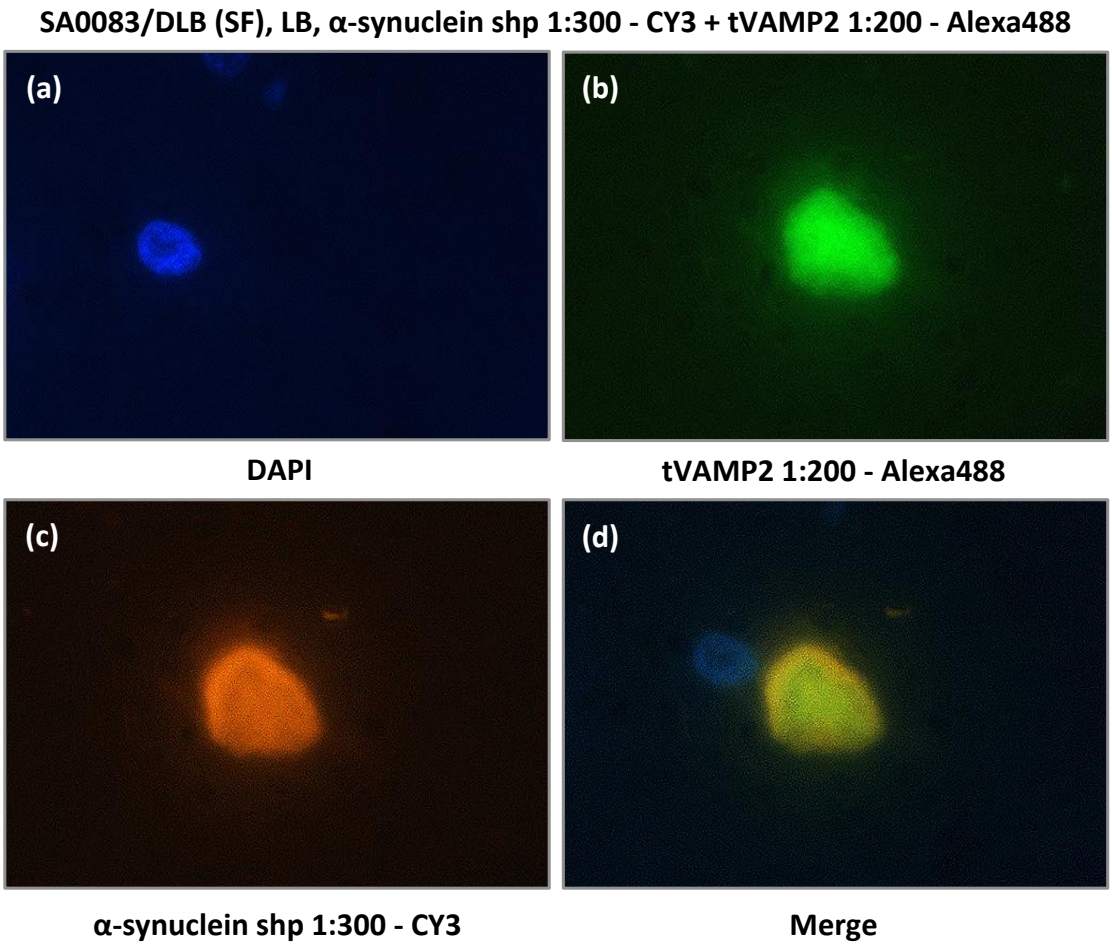

Figure 3-8, a-d: Co-localization of tVAMP2 and α-synuclein in Lewy bodies of DLB using fluorescence microscopy. Immunofluorescence double staining was performed on paraffin sections of a DLB brain (patient ID: SA0083). Primary antibodies: sheep anti α-synuclein, rabbit anti tVAMP2; fluorescence labeled Secondary antibodies: Cy3 donkey anti-sheep, Alexa 488 donkey anti-rabbit. tVAMP2 (b, in green) was overlapped with α-synuclein (c, in red) in Lewy bodies, with tVAMP2 localized more central than α-synuclein (d, merge).

Figure 3-8, e-h

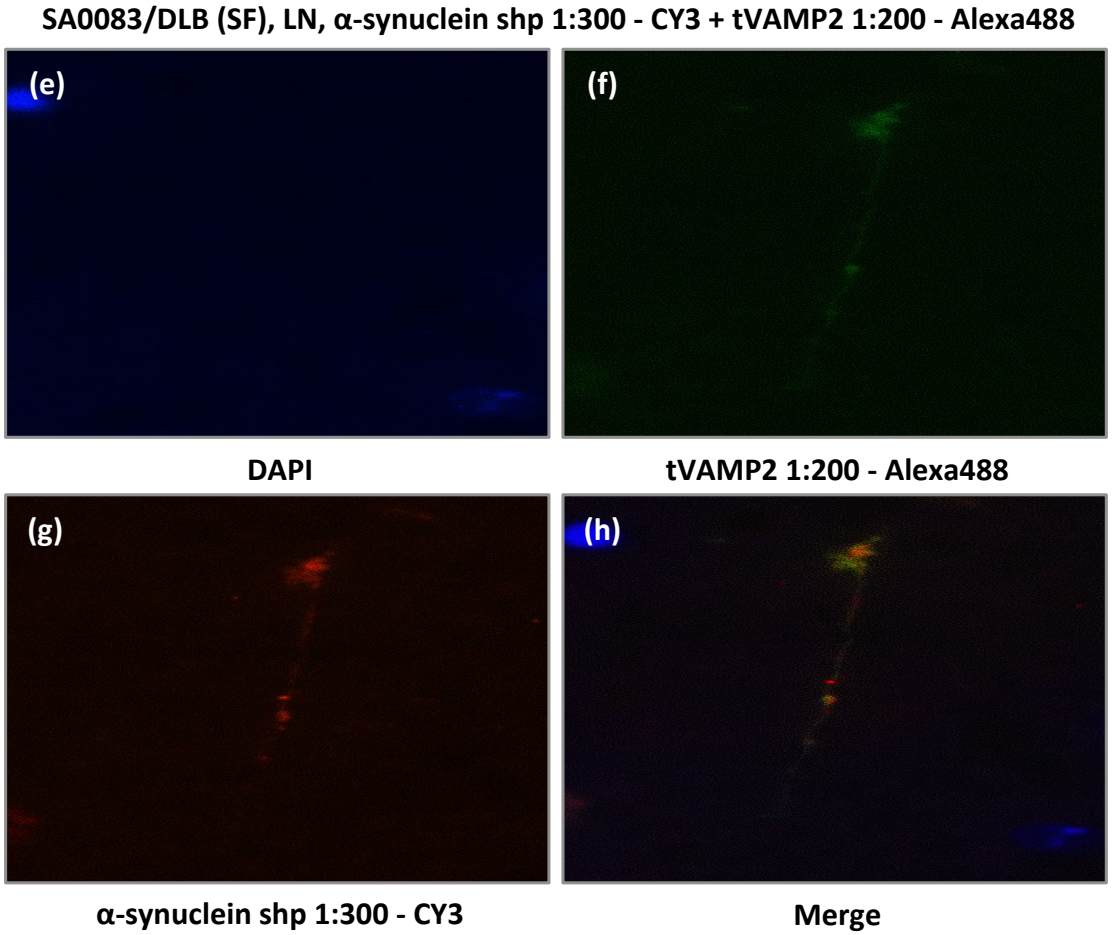

Figure 3-8, e-h: Co-localization of tVAMP2 and α-synuclein in Lewy neurites of DLB using fluorescence microscopy. Immunofluorescence double staining was performed on paraffin sections of a DLB brain (patient ID: SA0083). Primary antibodies: sheep anti α-synuclein, rabbit anti tVAMP2; fluorescence labeled Secondary antibodies: Cy3 donkey anti-sheep, Alexa 488 donkey anti-rabbit. tVAMP2 (f, in green) was overlapped with α-synuclein (g, in red) in Lewy neurites.

Figure 3-9, a-i

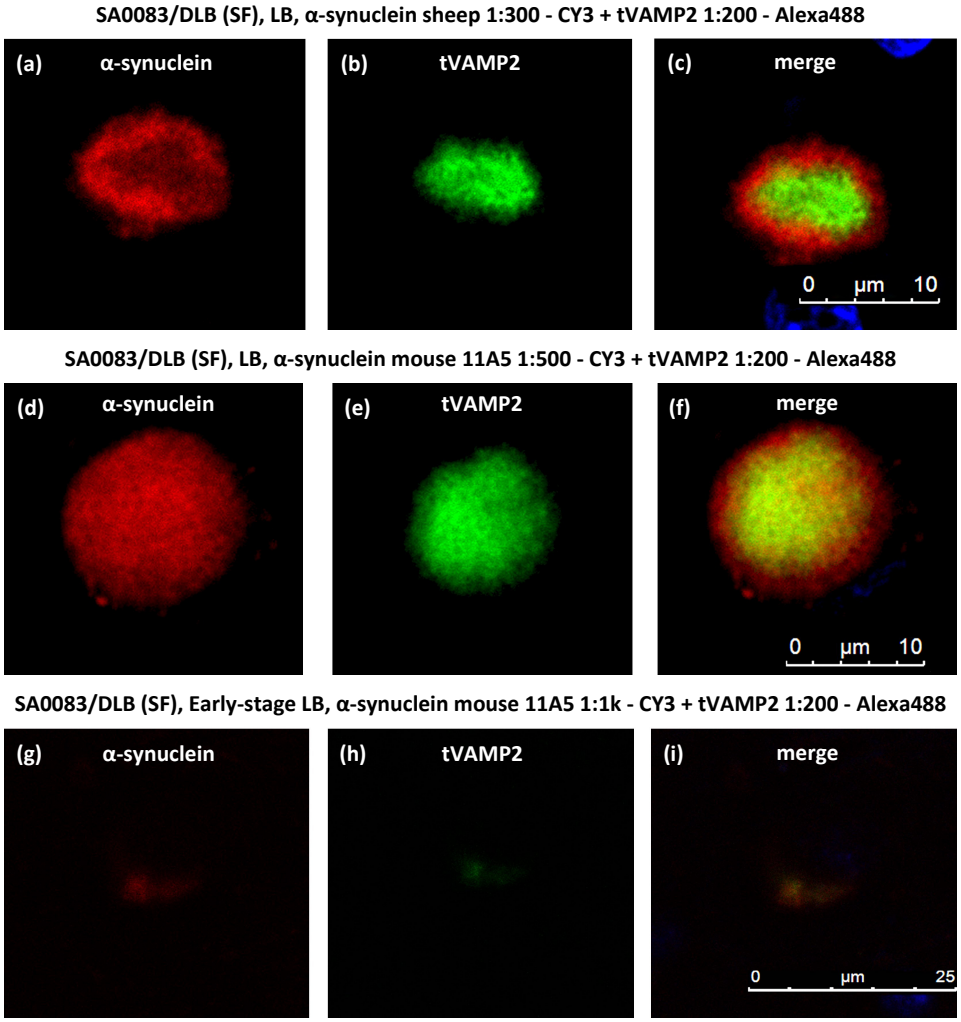

Figure 3-9, a-i: Co-localization of tVAMP2 and α-synuclein in Lewy bodies of DLB using confocal microscopy. Immunofluorescence double staining was performed on paraffin sections of a DLB brain (patient ID: SA0083). (a)~(c): Primary antibodies: sheep anti α-synuclein 1:300, rabbit anti tVAMP2 1:200; fluorescence labeled Secondary antibodies: Cy3 donkey anti-sheep (red), Alexa488 donkey anti-rabbit (green); (d)~(f): Primary antibodies: mouse anti 11A5 α-synuclein 1:500, rabbit anti tVAMP2 1:200; fluorescence labeled Secondary antibodies: Cy3 donkey anti-mouse, Alexa488 donkey anti-rabbit; (g)~(i): early-stage Lewy body, Primary antibodies: mouse anti 11A5 α-synuclein 1:1k, rabbit anti tVAMP2 1:200; fluorescence labeled Secondary antibodies: Cy3 donkey anti-mouse, Alexa488 donkey anti-rabbit.

Figure 3-9, j-o

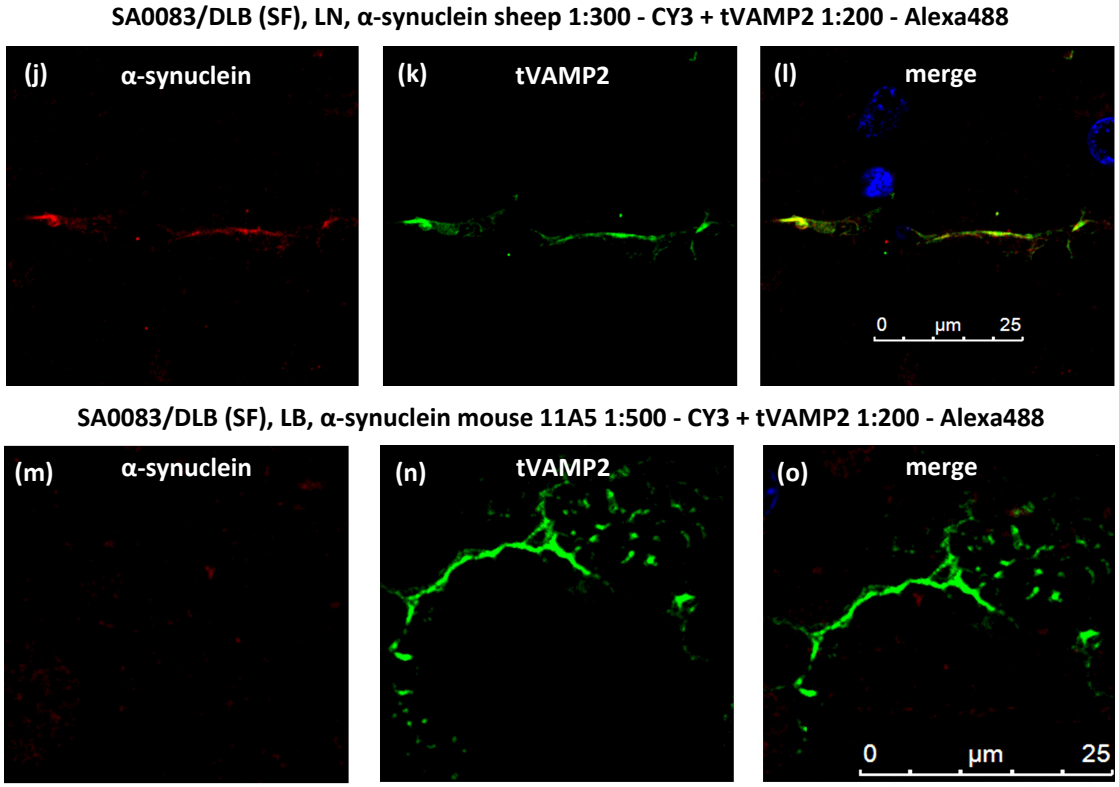

Figure 3-9, j-o: Co-localization of tVAMP2 and α-synuclein in Lewy neurites of DLB using confocal microscopy. Immunofluorescence double staining was performed on paraffin sections of a DLB brain (patient ID: SA0083). (j)~(l): Primary antibodies: sheep anti α-synuclein 1:300, rabbit anti tVAMP2 1:200; fluorescence labeled Secondary antibodies: Cy3 donkey anti-sheep (red), Alexa488 donkey anti-rabbit (green); (m)~(o): Primary antibodies: mouse anti 11A5 α-synuclein 1:500, rabbit anti tVAMP2 1:200; fluorescence labeled Secondary antibodies: Cy3 donkey anti-mouse, Alexa488 donkey anti-rabbit.

Figure 3-10

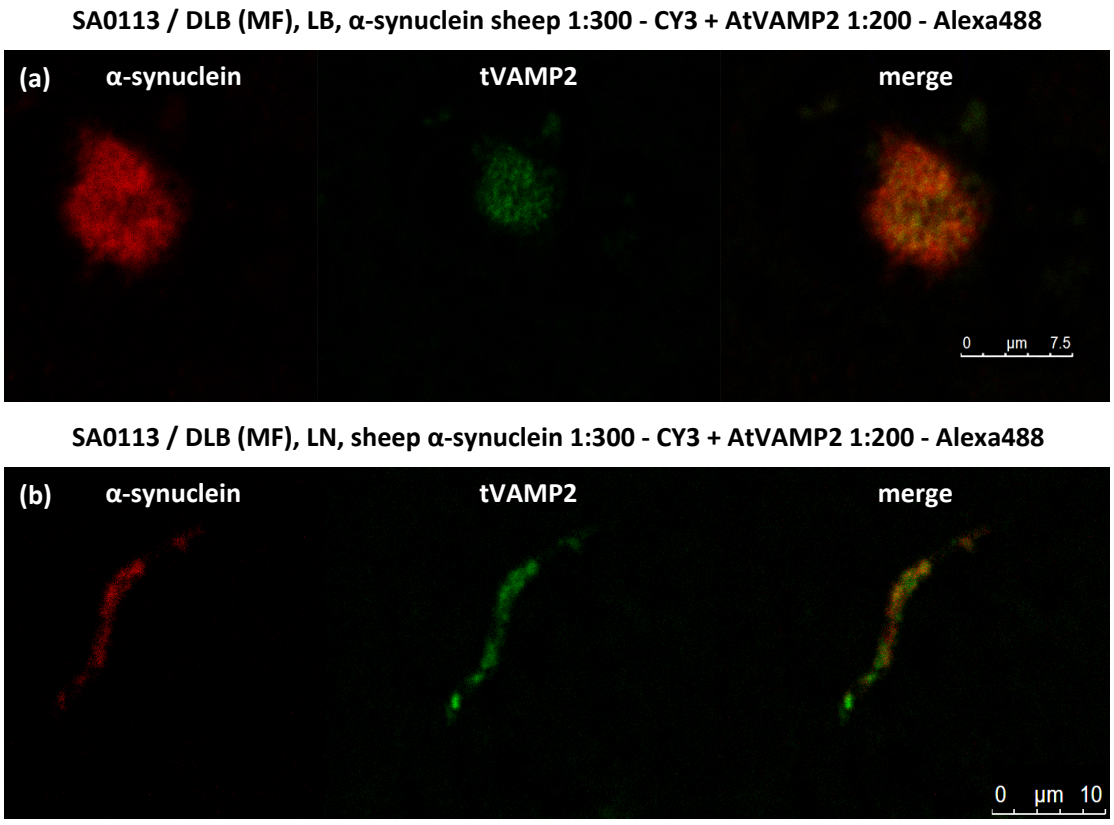

Figure 3-10: Co-localization of AtVAMP2 and α-synuclein in Lewy pathologies of DLB using confocal microscopy. Immunofluorescence double staining was performed on paraffin sections of the middle frontal region of a DLB brain (patient ID: SA0113). Primary antibodies: sheep anti α-synuclein 1:300, rabbit anti AtVAMP2 1:200; fluorescence labeled Secondary antibodies: Cy3 donkey anti-sheep (red), Alexa488 donkey anti-rabbit (green). (a): Lewy body; (b): Lewy neurite.

Figure 3-11

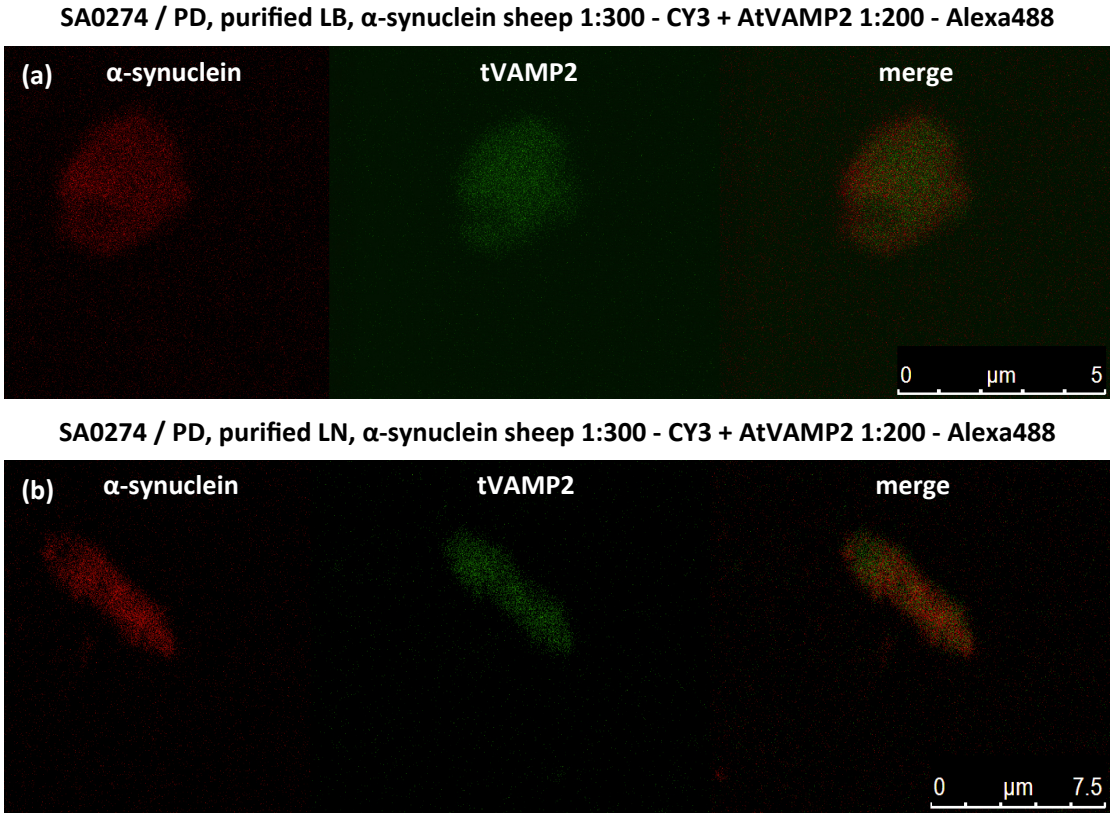

Figure 3-11: Co-localization of AtVAMP2 and α-synuclein in purified Lewy pathologies of PD using fluorescence microscopy. Immunofluorescence double staining was performed on purified Lewy bodies of a PD brain (patient ID: SA0274). Primary antibodies: sheep anti α-synuclein 1:300, rabbit anti AtVAMP2 1:200; fluorescence labeled Secondary antibodies: Cy3 donkey anti-sheep (red), Alexa488 donkey anti rabbit (green). (a): Lewy body; (b): Lewy neurite.

3.4 Truncated VAMP2 was specific for staining synucleinopathies inclusions without labeling AD pathologies.

It was demonstrated that tVAMP2 antibody co-localized with α-synuclein in Lewy bodies and Lewy neurites, however, whether tVAMP2 reactivity was specific for PD and DLB but not for other neurological diseases remained to be elucidated.

In order to determine the specificity of tVAMP2 staining on pathological inclusions of various neurodegenerative diseases, we immunostained free-floating sections of PD, DLB, MSA (Multiple System Atrophy) and AD (Alzheimer's Disease) brains and compared to a control case using tVAMP2 antibody (figure 3-12) or α-synuclein antibody (figure 3-13). tVAMP2 or α-synuclein antibodies positively stained Lewy bodies and Lewy neurites in PD and DLB brains, in contrast, immunoreactivity was absent in AD and normal brain. Notably, glial cytoplasmic inclusions (GCI), the hallmark of MSA, were also stained by both tVAMP2 and α-synuclein antibodies (figure 3-12, c and 3-13, c). These results suggested that tVAMP2 and α-synuclein was specific for staining inclusions of synucleinopathies but not for pathologies of AD. Moreover, the pathological observations were similar when using tVAMP2 and α-synuclein antibodies in immunohistochemistry, confirming that both antibodies were suitable for detecting Lewy bodies and Lewy neurites. Hyperphosphorylated Tau is important in the pathogenesis of neurodegenerative diseases including AD and frontotemporal dementia [93-95]. In figure 3-14, it was demonstrated that the Tau antibody (AF Tau, sheep, Antibody Technology Australia) stained neurofibrillary tangles of AD brain, but failed to stain Lewy pathologies and GCIs. VAMP1/2/3 antibody however did not stain any inclusions of these neurodegenerative diseases (figure 3-15).

When using immunohistochemistry with the tVAMP2 antibody on paraffin

sections of PD, AD, DLB and MSA brains (figure 3-16), it showed similar results to that found for free-floating sections in that Lewy bodies and Lewy neurites in PD and DLB brains and GCIs in MSA brain were positively stained by tVAMP2 antibody. However, there were no inclusions detected in AD brain by tVAMP2 antibody, which further confirmed that tVAMP2 was specific for staining synucleinopathies inclusions without labeling AD pathologies.

Figure 3-12

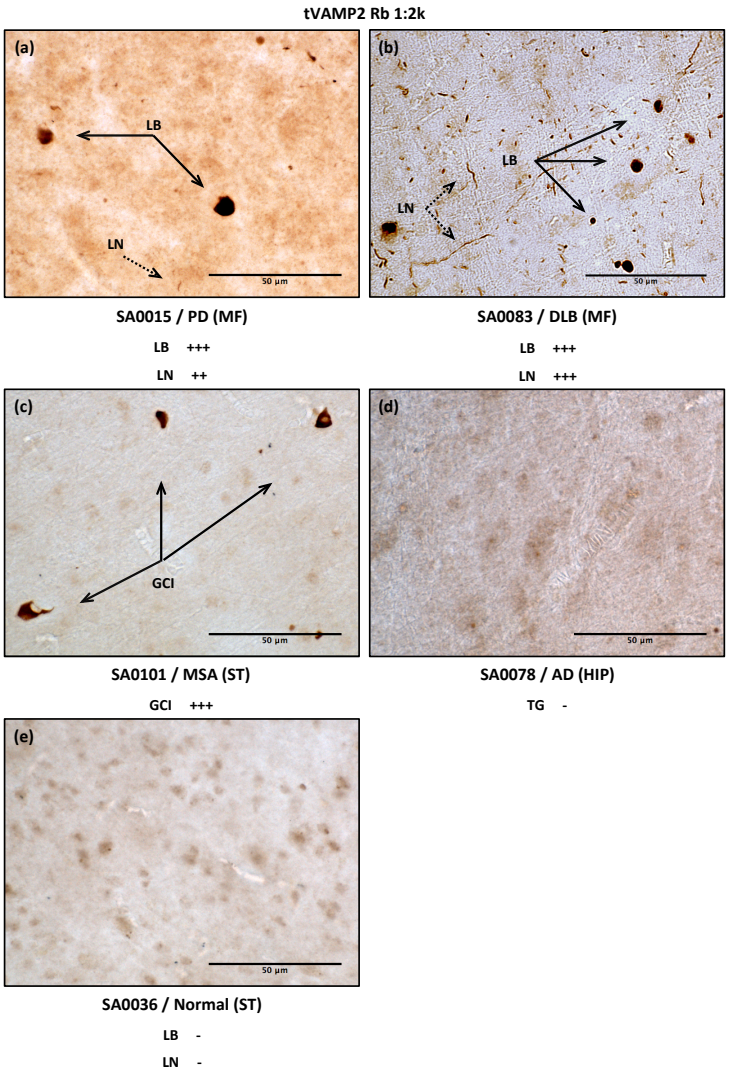

Figure 3-12: Immunostaining of tVAMP2 in free-floating sections of different neurodegenerative diseases compared to control. Immunostaining with an antibody against tVAMP2 (Rb, 1:2k) in free-floating sections of different neurodegenerative diseases and a normal brain. Sections: (a) mid-frontal of PD (SA0015), (b) mid-frontal of DLB (SA0083), (c) superior temporal of MSA (SA0101), (d) hippocampus of AD (SA0078) and (e) superior temporal of normal control (SA0036). Magnification of 400x under an Olympus BH-2 light microscope (Tokyo, Japan) is shown in the figure. Scale bar is 50µm. Lewy bodies, Lewy neurites and Glial Cytoplasmic Inclusions (GCIs) are indicated with arrows.

Figure 3-13

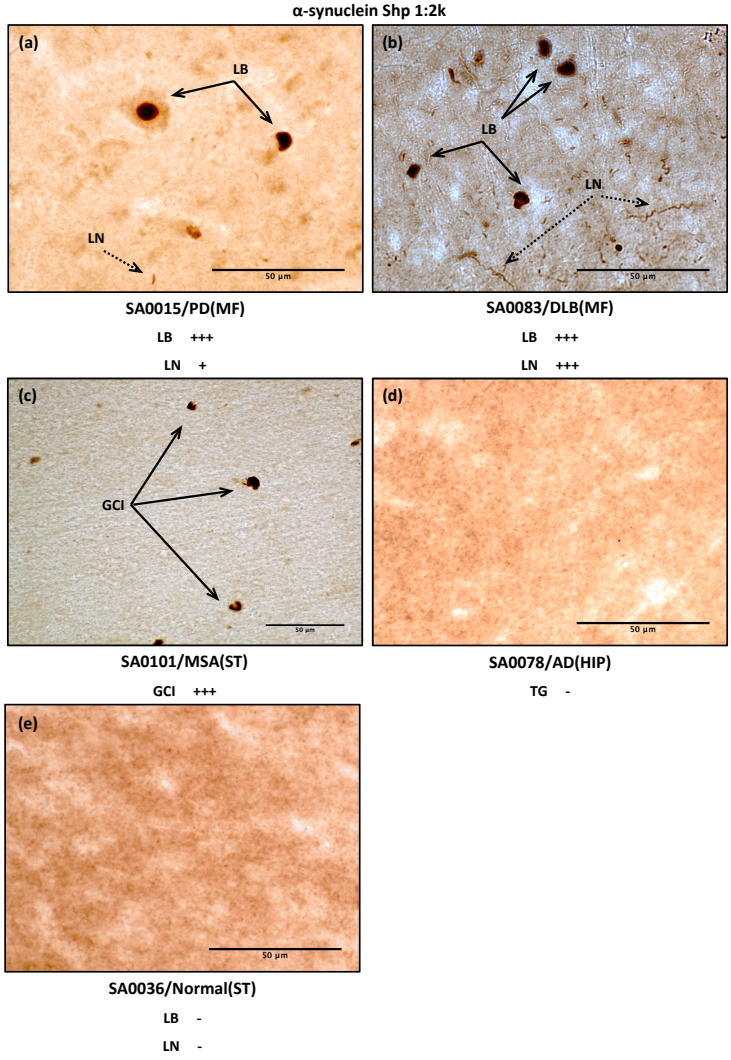

Figure 3-13: Immunostaining of α-synuclein in free-floating sections of different neurodegenerative diseases compared to control. Immunostaining with an antibody against α-synuclein (Shp, 1:2k) in free-floating sections of different neurodegenerative diseases and a normal brain. Sections: (a) mid-frontal of PD (SA0015), (b) mid-frontal of DLB (SA0083), (c) superior temporal of MSA (SA0101), (d) hippocampus of AD (SA0078) and (e) superior temporal of normal control (SA0036). Magnification of 400x under an Olympus BH-2 light microscope (Tokyo, Japan) is shown in the figure. Scale bar is 50µm. Lewy bodies, Lewy neurites and Glial Cytoplasmic Inclusions (GCIs) are indicated with arrows.

Figure 3-14

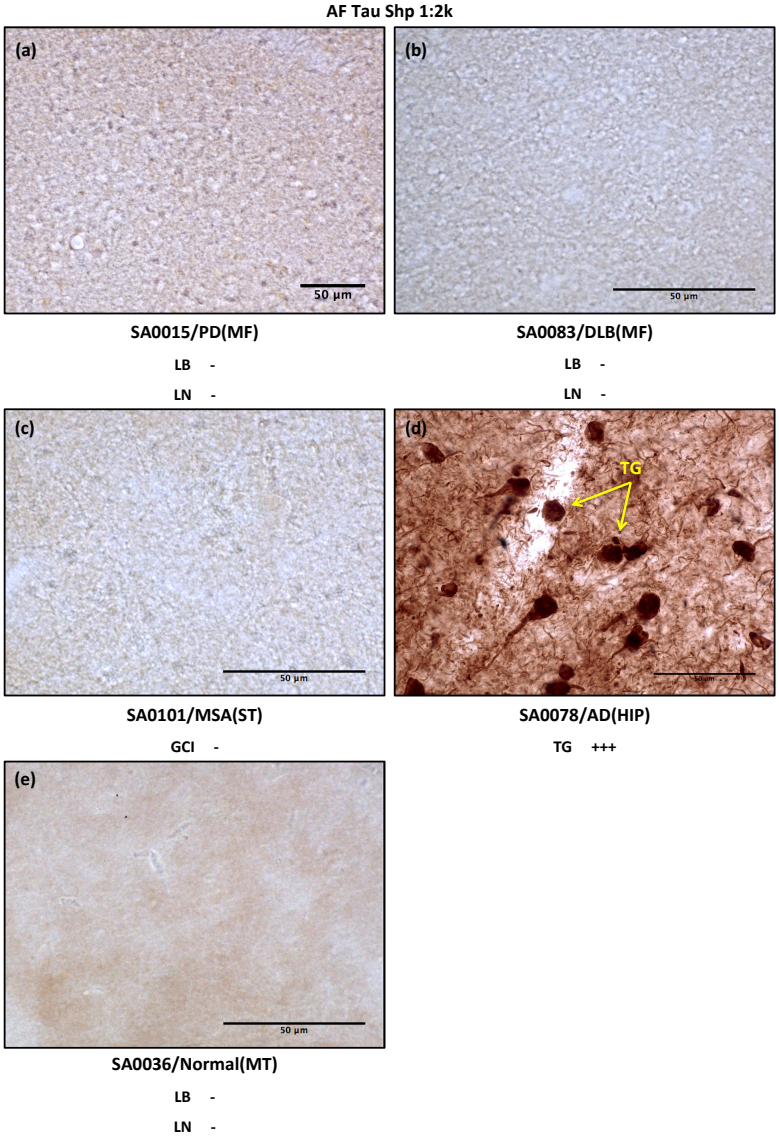

Figure 3-14: Immunostaining of Tau in free-floating sections of different neurodegenerative diseases compared to control. Immunostaining with an antibody against AF Tau (Shp, 1:2k) in free-floating sections of different neurodegenerative diseases and a normal brain. Sections: (a) mid-frontal of PD (SA0015), (b) mid-frontal of DLB (SA0083), (c) superior temporal of MSA (SA0101), (d) hippocampus of AD (SA0078) and (e) superior temporal of normal control (SA0036). Magnification of 400x under an Olympus BH-2 light microscope (Tokyo, Japan) is shown in the figure. Scale bar is 50µm. Neurofibrillary tangles are indicated with arrows.

Figure 3-15

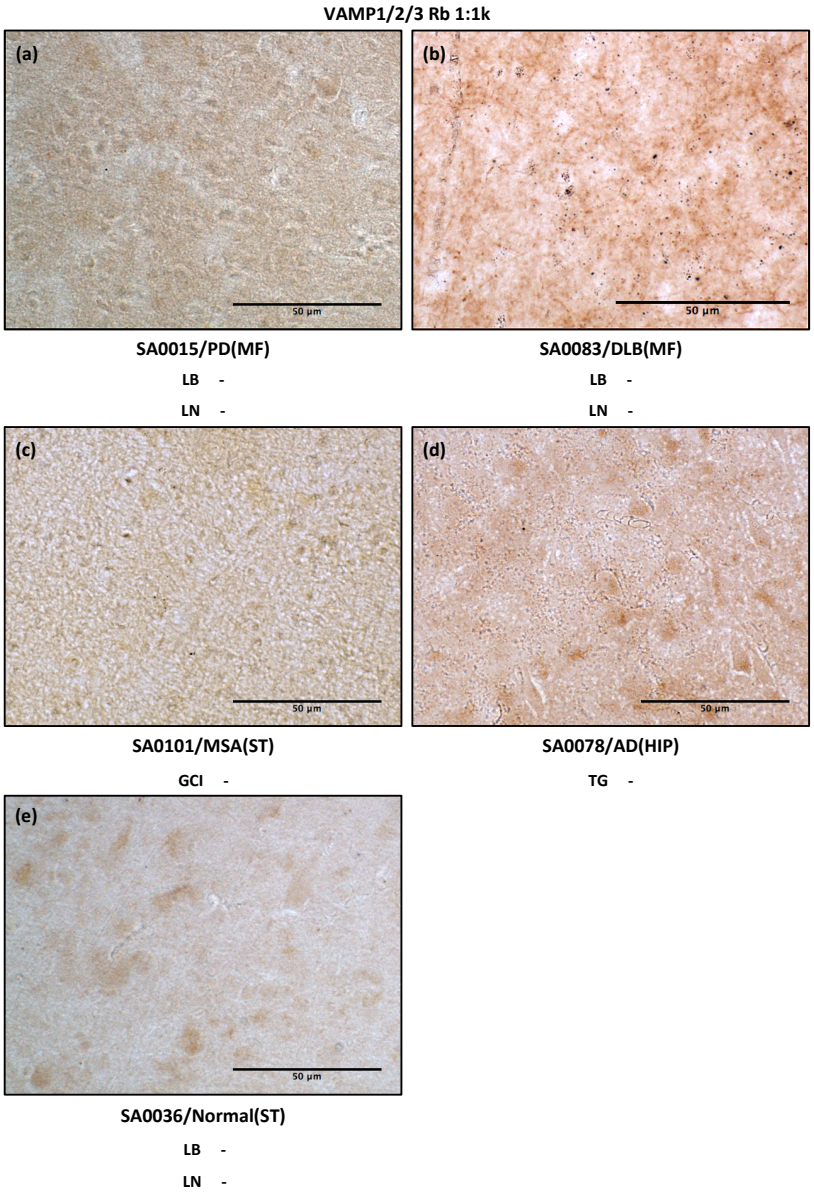

Figure 3-15: Immunostaining of VAMP1/2/3 in free-floating sections of different neurodegenerative diseases compared to control. Immunostaining with an antibody against VAMP1/2/3 (Rb, 1:1k) in free-floating sections of different neurodegenerative diseases and a normal brain. Sections: (a) mid-frontal of PD (SA0015), (b) mid-frontal of DLB (SA0083), (c) superior temporal of MSA (SA0101), (d) hippocampus of AD (SA0078) and (e) superior temporal of normal control (SA0036). Magnification of 400x under an Olympus BH-2 light microscope (Tokyo, Japan) is shown in the figure. Scale bar is 50µm.

Figure 3-16

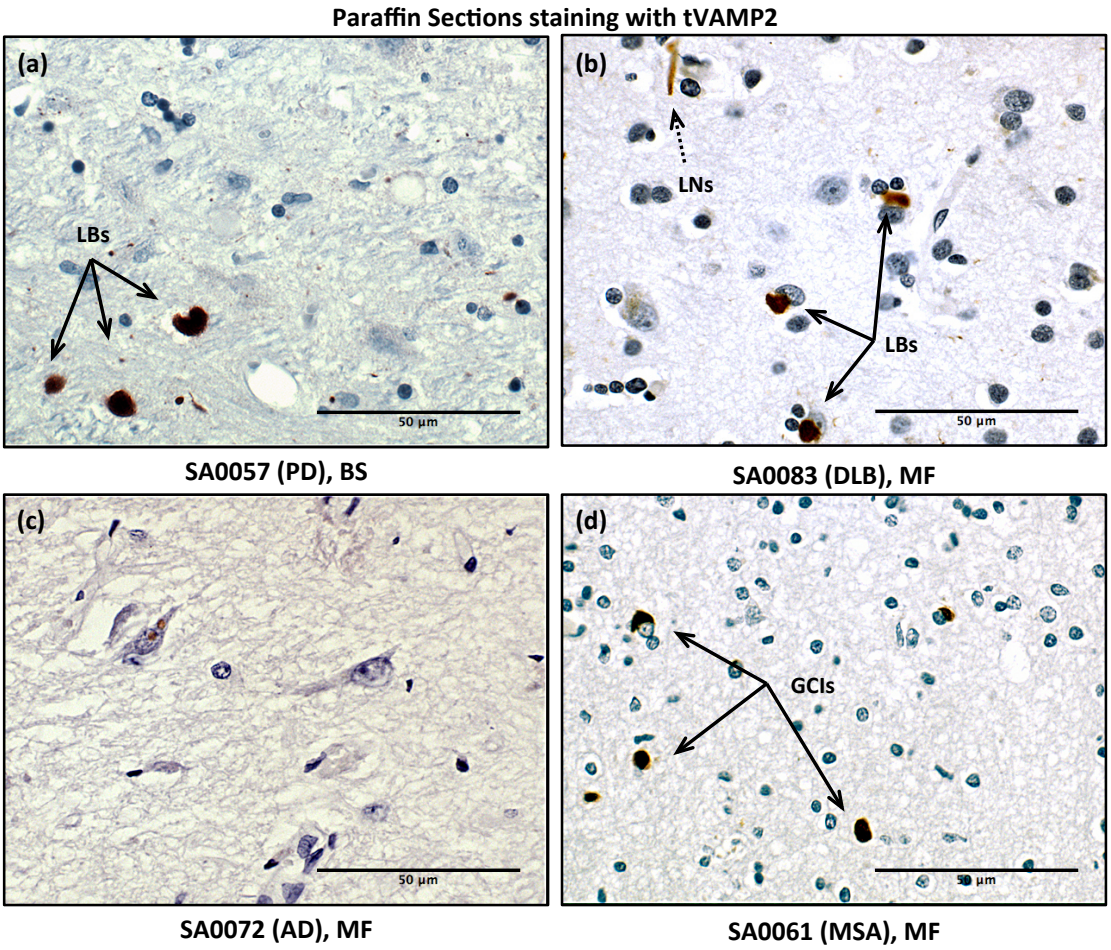

Figure 3-16: Immunostaining of tVAMP2 in the paraffin sections of different neurodegenerative diseases. Immunostaining with an antibody against tVAMP2 (Rb, 1:2k) in paraffin sections of different neurodegenerative diseases. Sections: (a) brainstem of PD (SA0057), (b) mid-frontal of DLB (SA0083), (c) mid-frontal of AD (SA0072) and (d) mid-frontal of MSA (SA0061). Magnification of 400x under an Olympus BH-2 light microscope (Tokyo, Japan) is shown in the figure. Scale bar is 50µm. Lewy bodies, Lewy neurites and Glial Cytoplasmic Inclusions (GCIs) are indicated with arrows.

3.5 Truncated VAMP2 was identified in purified Lewy bodies from PD and DLB.

In order to confirm the existence of truncated VAMP2 in Lewy bodies and its truncation site, 2D electrophoresis and mass spectrometry were performed on purified Lewy bodies from homogenate of PD (SA0274) and DLB (SA0249) brains. The purified proteins were then analyzed by 2D western blot using the α-synuclein and AtVAMP2 antibodies (figure 3-17, a-b). Four spots at around 14kDa with PIs of 5.7, 5.3, 5.0 and 4.7 suggesting truncated VAMP2 has four isoforms and three spots at around 28kDa which could be suggesting dimers of truncated VAMP2, and one band at around 17kDa corresponding to full-length VAMP2 on 1D gel were detected in purified Lewy bodies of PD (figure 3-17, b). The four spots could represent tVAMP2 with multiple phosphorylation sites. Four sites have previously been reported [177]. The AtVAMP2 antibody also reacted with high molecular weight (HMW) aggregates of 30-250kDa with a PI of a range of 4 to 6.5 (figure 3-17, b). Furthermore, one band at around 17kDa indicating monomer of α-synuclein and several bands with same PI and higher molecular weight indicating aggregates of α-synuclein were detected in purified Lewy bodies of DLB (figure 3-17, a).

The purified Lewy bodies of these two cases were further prepared for mass spectrometry analysis. Mass spectrometry was employed to attempt to identify the truncation site of tVAMP2. Purified Lewy bodies were used as the source of tVAMP2 due to their enrichment in synucleinopathy inclusions. Purified inclusions were solubilized and digested with the protease Trypsin and in a separate experiment, Glu C. Digestion of intact proteins to smaller peptides is necessary to bring the peptides into the mass range of the nanospray qTOF mass spectrometer. Four micrograms of purified proteins of each case was first loaded onto a 1D gel, after running and staining with coomassie blue, the area of interest

on the gel was divided and cut into small pieces (figure 3-18, a) and digested by trypsin for preparation for mass spectrometry. Importantly, peptides corresponding to aa32-47 and aa60-83 of human VAMP2 were identified in purified Lewy bodies of PD and DLB with a confidence above 95% (figure 3-18, b, in green), hence, a total of 34.5% amino acid sequence was identified (40 out of 116 AAs). Notably, a large peptide corresponding to N-terminal aa1-31 of human VAMP2 was not detected in purified Lewy bodies of PD and DLB (figure 3-18, b, in grey). The presence of the truncated peptide LLQQTQAQVDEVVDIMR suggested that the truncation point could be at arginine 31 (R31). However as digestion with trypsin which cleaves at lysine and arginine residues was used to prepare the samples for mass spectrometry, the presence of this peptide may be a consequence of this trypsin digestion. Therefore, a repeat experiment was performed using GluC to prepare the samples for mass spectrometry, thereby avoiding the possibility of arginine cleavage. GluC cleaves at glutamic acid residues (E) and at a much lower rate, at aspartic acid residues (D).

Theoretically, digestion with Glu C should generate 6 peptides corresponding to amino acids 1-16 (1); 17-41 (2); 42-55(3); 56-62 (4); 63-78 (5) and 79-116 (6). Peptides corresponding to peptides 3, 4 and 5 of VAMP2 were identified. Peptides 1 and 6 were not detected. While peptide 6 was too large to be detected by a mass spectrometer using standard conditions, peptide 1 should have been identified if it was present. Its lack of detection suggested that full length VAMP2 was not present in sufficient quantity to allow detection of the N-terminal peptide. Peptide 2 was also not detected although the mass of peptide 2 was on the edge of the detection limit for the mass spectrometer, so it was not surprising that it was not identified. However, fragments of peptide 2 were identified, corresponding to amino acids 31-41 (RLQQTQAQVDE) identified 6 times and the 1 amino acid shorter peptide 32-41 (LQQTQAQVDE) identified twice (figure 3-19).

Figure 3-17, a-b

(a)

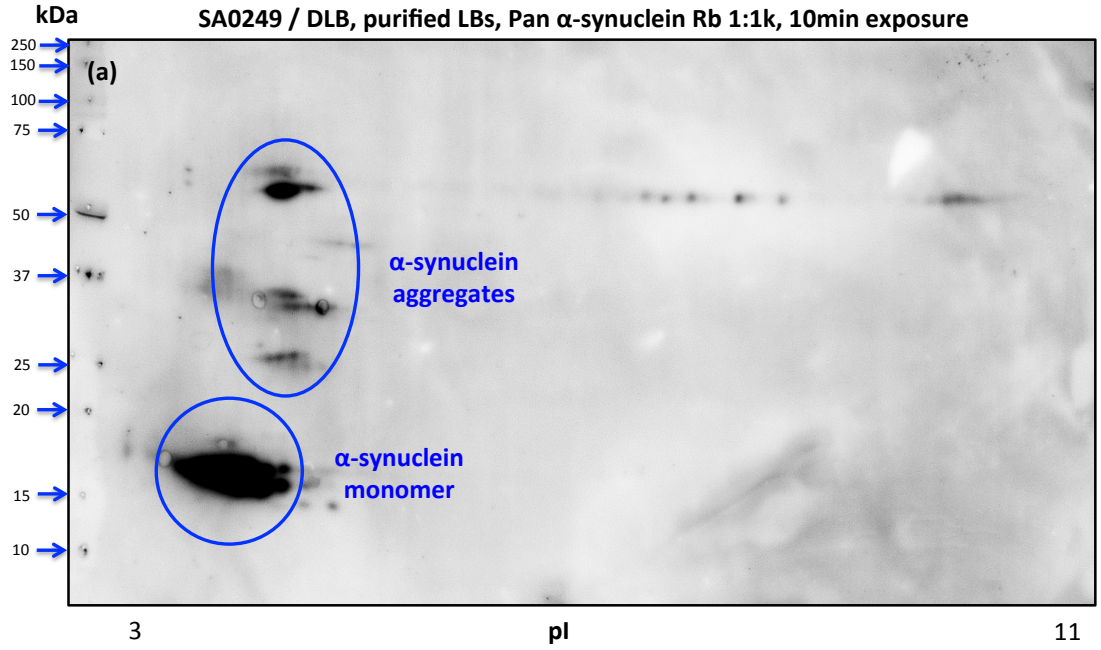

(b)

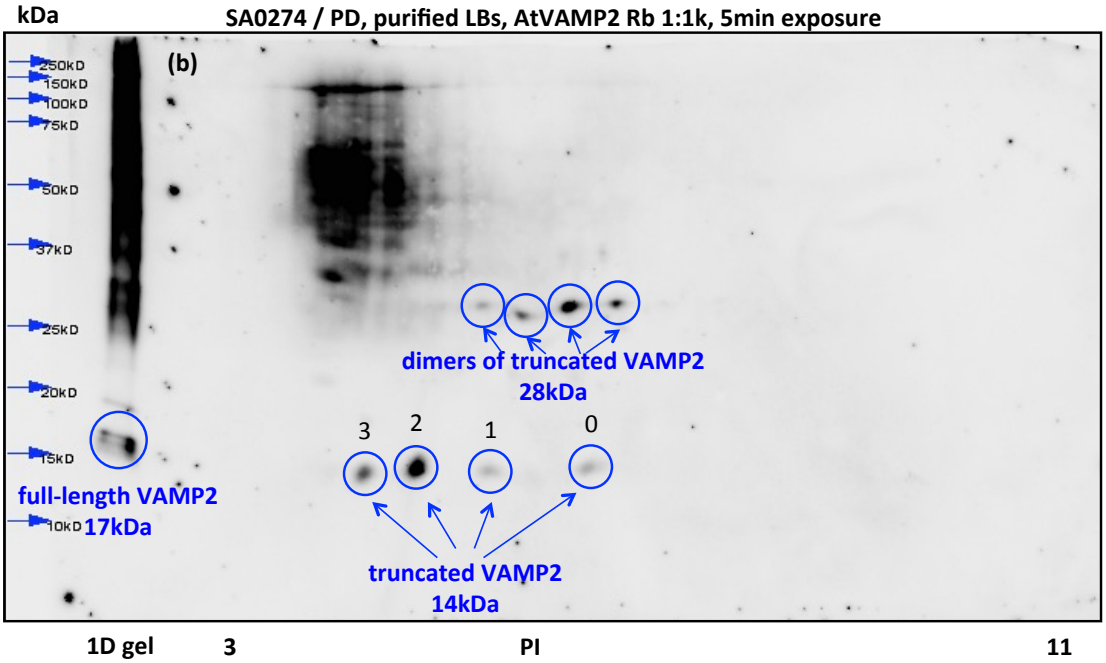

Figure 3-17, a-b: 2D electrophoresis of purified Lewy bodies from a DLB

case (SA0249) using α-synuclein antibody (a) and a PD case (SA0274) using AtVAMP2 antibody (b). The purified inclusions (70µg) focused on a 13cm strip (PI 3-11), separated by SDS PAGE, and transferred to a PVDF membrane and blotted with antibodies against: (a) Pan α-synuclein (rabbit, 1:1k); (b) AtVAMP2 (rabbit, 1:1k). In figure b, 8.5µg of purified inclusions was loaded on 1D gel. This experiment was repeated three times. Figures are representative of the three independent experiments.

Figure 3-18, a

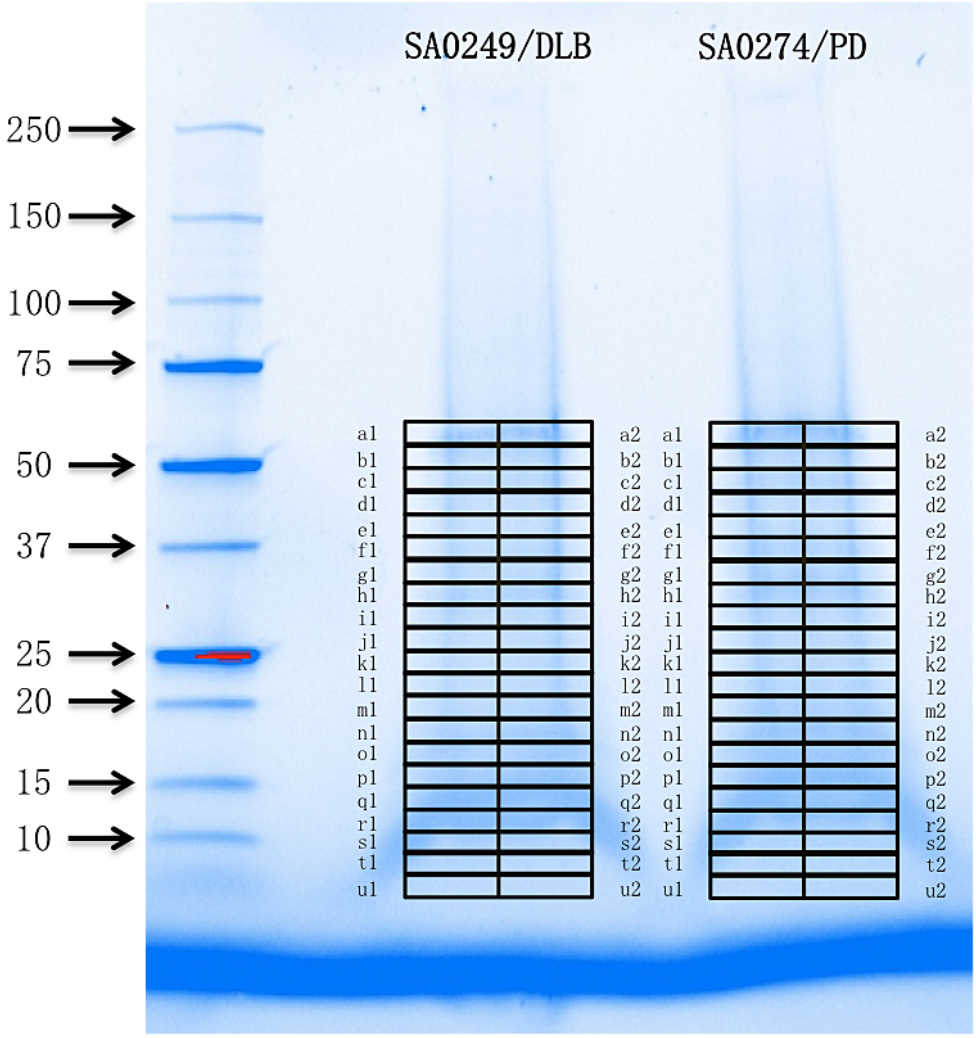

Figure 3-18, a: Sample Preparation for Mass spectrometry. Purified Lewy bodies from a DLB case (SA0249, left) and a PD case (SA0274, right) were run on the 1D gel and stained in Coomassie solution afterwards. Four micrograms protein of each sample was loaded. After staining, the specific part on the gel of interest was divided into 21 equal parts and cut into small pieces as shown on the figure and digested by trypsin for preparation of mass spectrometry.

Figure 3-18, b

VAMP2 sequence detected in purified LBs from SA0274 (PD)

MSATAATAPPAAPAGEGGPPAPPPNLTSNRR**LQQTQAQVDEVVDIMR**VNVDKVLERDQK**LSELDDRADALQAGASQ FETSAAK**LKRKYWWKNLKMMIILGVICAIILIIIIVYFST

Contrib	Conf	Sequence	Modifications	ΔMass	Prec MW	z
0.00	99	ADALQAGASQFETSAAK		-0.0011	1664.79	2
2.00	99	ADALQAGASQFETSAAK		0.0079	1664.80	2
0.00	99	ADALQAGASQFETSAAK		-0.0081	1664.79	2
0.00	99	LQQTQAQVDEVVDIMR	Oxidation(M)@15	-0.0063	1887.92	3
0.00	99	LQQTQAQVDEVVDIMR	Oxidation(M)@15	0.0036	1887.93	3
0.00	99	LQQTQAQVDEVVDIMR	Oxidation(M)@15	0.0107	1887.94	3
2.00	99	LQQTQAQVDEVVDIMR	Oxidation(M)@15	0.0003	1887.93	3
0.00	98.9	LSELDDR		0.0012	846.4097	2
1.39	98.9	LSELDDR		0.0006	846.4091	2
0.00	98.7	LSELDDR		0.0012	846.4097	2
0.00	98.4	LSELDDR		-0.0018	846.4065	2
0.00	98	LSELDDR		-0.0002	846.4083	2
0.00	97.2	ADALQAGASQFETSAAK		-0.0053	1664.79	2
0.00	97.2	LQQTQAQVDEVVDIMR	Oxidation(M)@15	-0.0072	1887.92	3
0.00	95.7	LQQTQAQVDEVVDIMR	Oxidation(M)@15	-0.0001	1887.93	3

SA0274 (PD)

LQQTQAQVDEVVDIMR

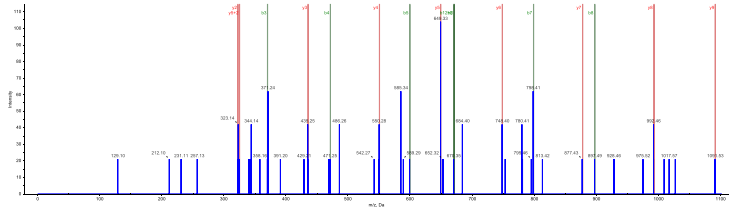

LSELDDR

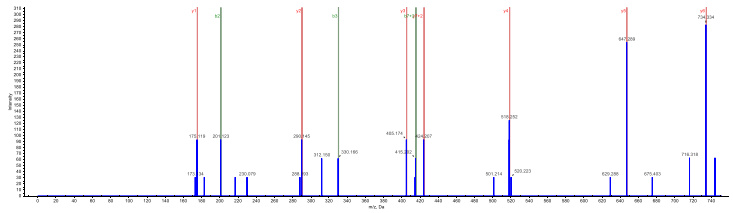

ADALQAGASQFETSAAK

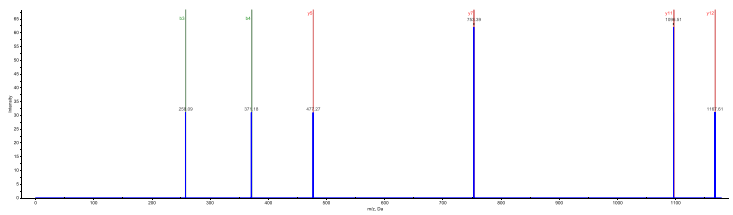

VAMP2 sequence detected in purified LBs from SA0249 (DLB)

MSATAATAPPAAPAGEGGPPAPPPNLTSNRR**LQQTQAQVDEVVDIMR**VNVDKVLERDQK**LSELDDRADALQAGASQ FETSAAK**LKRKYWWKNLKMMIILGVICAIILIIIIVYFST

Contrib	Conf	Sequence	Modifications	ΔMass	Prec MW	z
2.00	99	ADALQAGASQFETSAAK		0.9905	1665.79	3
0.00	99	ADALQAGASQFETSAAK		0.0050	1664.80	2
0.00	99	ADALQAGASQFETSAAK		-0.0001	1664.80	2
0.00	99	LQQTQAQVDEVVDIMR	Oxidation(M)@15	-0.0043	1887.93	3
2.00	99	LQQTQAQVDEVVDIMR	Oxidation(M)@15	0.0314	1887.96	3
0.00	99	LQQTQAQVDEVVDIMR	Oxidation(M)@15	0.0213	1887.95	3
2.00	99	LSELDDR		-0.0022	846.4061	2
0.00	97.9	ADALQAGASQFETSAAK		-0.0019	1664.79	2
0.00	97.2	ADALQAGASQFETSAAK		0.0101	1664.81	2
0.00	96	LSELDDR		0.0008	846.4091	2

SA0249 (DLB)

LQQTQAQVDEVVDIMR

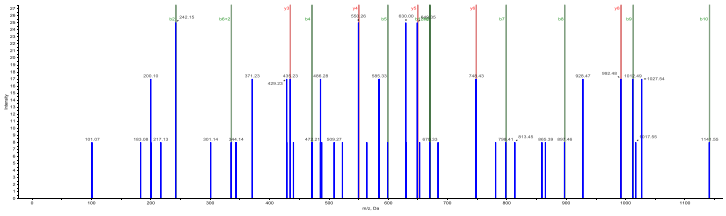

LSELDDR

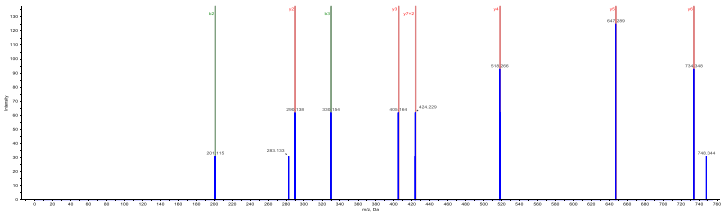

ADALQAGASQFETSAAK

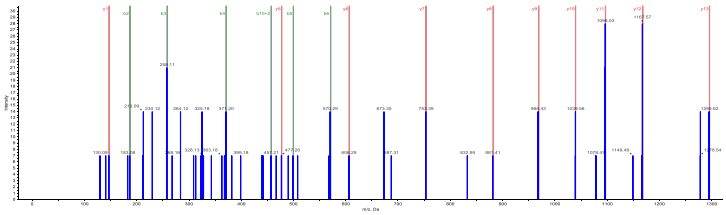

Figure 3-18, b: Peptide Sequence Detected by Mass spectrometry when using Trypsin as the designated protease. Amino acid sequences in green were detected in purified Lewy bodies with the confidence above 95%, whereas sequence in grey was not detected. Peptides with conf. > 95% are listed in tables. Spectros for 3 peptides (peptide 1: LQQTQAQVDEVVDIMR; peptide 2: LSELDDR; peptide 3: ADALQAGASQFETSAAK) are shown under the tables.

Figure 3-19

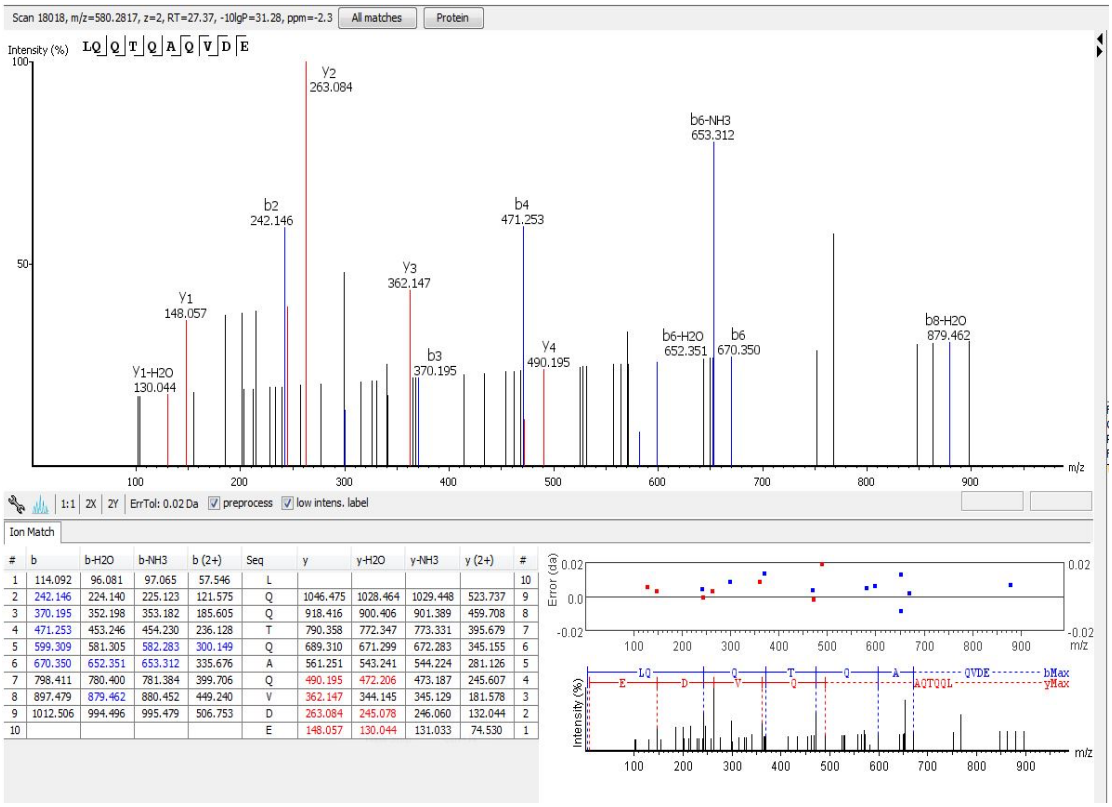

#	b	b-H2O	b-NH3	b (2+)	Seq	y	y-H2O	y-NH3	y (2+)	#
1	114.092	96.081	97.065	57.546	L					10
2	242.146	224.140	225.123	121.575	Q	1046.475	1028.464	1029.448	523.737	9
3	370.195	352.198	353.182	185.605	Q	918.416	900.406	901.389	459.708	8
4	471.253	453.246	454.230	236.128	T	790.358	772.347	773.331	395.679	7
5	599.309	581.305	582.283	300.149	Q	689.310	671.299	672.283	345.155	6
6	670.350	652.351	653.312	335.676	A	561.251	543.241	544.224	281.126	5
7	798.411	780.400	781.384	399.706	Q	490.195	472.206	473.187	245.607	4
8	897.479	879.462	880.452	449.240	V	362.147	344.145	345.129	181.578	3
9	1012.506	994.496	995.479	506.753	D	263.084	245.078	246.060	132.044	2
10					E	148.057	130.044	131.033	74.530	1

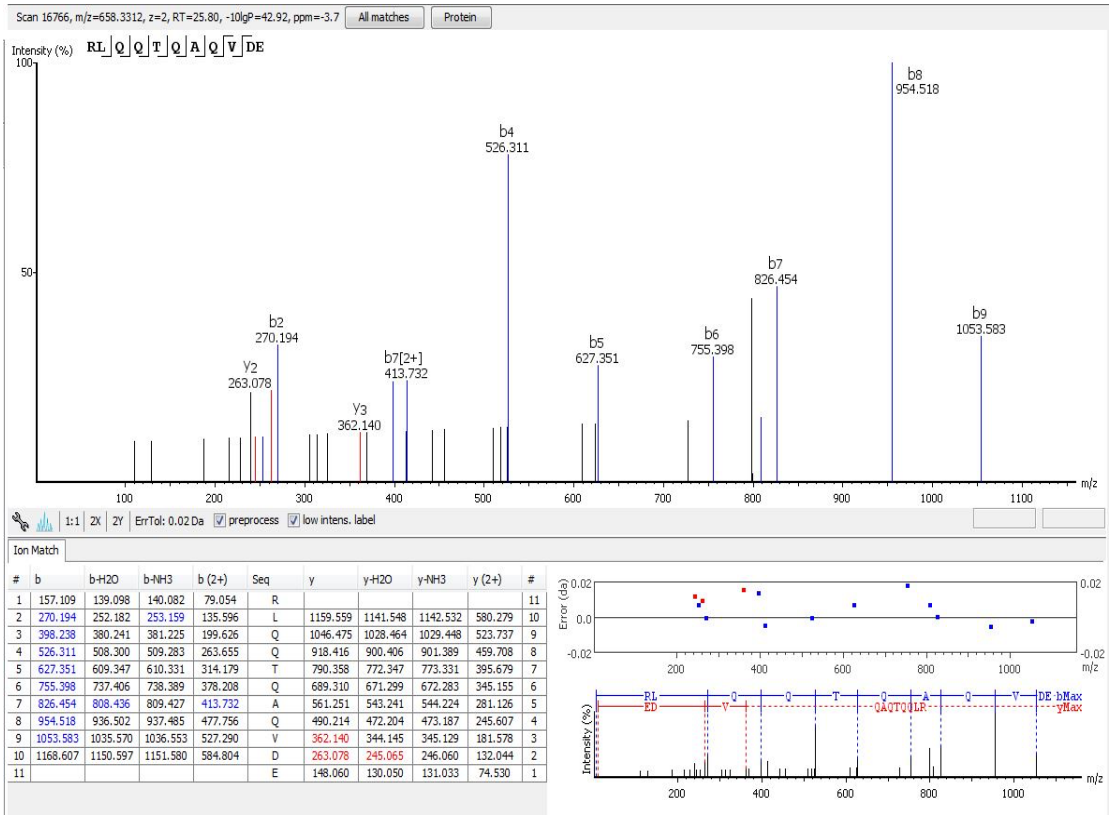

#	b	b-H2O	b-NH3	b (2+)	Seq	y	y-H2O	y-NH3	y (2+)	#
1	157.109	139.098	140.082	79.054	R					11
2	270.194	252.182	253.159	135.596	L	1159.559	1141.548	1142.532	580.279	10
3	398.238	380.241	381.225	199.626	Q	1046.475	1028.464	1029.448	523.737	9
4	526.311	508.300	509.283	263.655	Q	918.416	900.406	901.389	459.708	8
5	627.351	609.347	610.331	314.179	T	790.358	772.347	773.331	395.679	7
6	755.398	737.406	738.389	378.208	Q	689.310	671.299	672.283	345.155	6
7	826.454	808.436	809.427	413.732	A	561.251	543.241	544.224	281.126	5
8	954.518	936.502	937.485	477.756	Q	490.214	472.204	473.187	245.607	4
9	1053.583	1035.570	1036.553	527.290	V	362.140	344.145	345.129	181.578	3
10	1168.607	1150.597	1151.580	584.804	D	263.078	245.065	246.060	132.044	2
11					E	148.060	130.050	131.033	74.530	1

Figure 3-19: Peptide Sequence Detected by Mass spectrometry when using

Glu C as the designated protease. Purified Lewy bodies from a DLB case (Patient ID: SA0069) was run on the 1D gel and stained in Coomassie solution afterwards. 4ug protein of each sample was loaded. After staining, the specific part on the gel of interest was divided into 21 equal parts and cut into small pieces and digested by Glu C for preparation of mass spectrometry. Amino acids 31-41 (RLQQTQAQVDE) were identified 6 times and amino acids 32-41 (LQQTQAQVDE) were identified twice.

Chapter 4

Discussion and Conclusion

VAMP2 (vesicle associated membrane protein 2, also known as synaptobrevin-2) is a single transmembrane synaptic vesicle anchored SNARE protein, which assembles with presynaptic plasma membrane anchored SNARE proteins (such as syntaxin-1 and SNAP-25) into SNARE complexes for membrane fusion and neurotransmitter release. VAMP2 is composed of a cytoplasmic proline-rich N-terminal domain (residues 1-31), a SNARE motif (residues 32-84) followed by a transmembrane (TM) domain (residues 95-116)[102]. It is suggested that VAMP2 is involved in neurotransmitter release at a stage between docking and fusion, chaperoned by α-synuclein, a neuronal protein which is composed of 140 amino acids. In the formation of SNARE complexes in presynaptic terminals, the 40-residue highly acidic C-terminus binding domain of α-synuclein binds to the N-terminal 28 amino acids sequence of VAMP2, and the 100-residue positively-charged N-terminus binding domain of α-synuclein binds to the phospholipids of the plasma membrane simultaneously [67]. The N-terminally truncated VAMP2, which lacks 28 N-terminal residues, does not bind α-synuclein, and diminishes the effect on SNARE complex assembly, which is essential for neurotransmitter release. α-synuclein is identified as the prominent component of Lewy bodies and Lewy neurites, the pathological characteristic of PD and other neurodegenerative diseases [26]. However, the role of VAMP2 in the aggregation of α-synuclein and the formation of Lewy bodies and Lewy neurites and in the progress of PD and other synucleinopathies remains to be elucidated, especially in the vast majority of sporadic PD cases without genetic abnormalities associated with α-synuclein. What is the tVAMP2 neuropathology in PD and DLB? What is the N-terminal truncation site of the Lewy body-associated VAMP2 fragment? Will the increase in truncated VAMP2 be able to stimulate α-synuclein aggregation and hence participate in the formation of

Lewy bodies and Lewy neurites? Is tVAMP2 pathology specific to PD and DLB? In order to answer these questions, we used several antibodies to different regions of human VAMP2 sequence. They were tVAMP2 antibodies against aa30-47 and fVAMP2 antibodies against aa2-17. Two fVAMP2 antibodies were purchased from Biochem (animal ID3023 and 3024). They were synthetic peptides (aa 2-17 in rabbit synaptobrevin-2) coupled to key-hole limpet hemocyanin via an added N-terminal cysteine residue. They were able to recognize VAMP2 from different species including human, and were specific for VAMP2 and showed no cross-reactivity to VAMP1 and VAMP3. tVAMP2 antibody was provided by Dr Weiping Gai. It was raised against aa30-47 of rabbit VAMP2 and showed no cross-reactivity to VAMP1 and VAMP3. AtVAMP2 was affinity purified antibody from tVAMP2 serum using the immunizing peptide. This study revealed the protein expression of tVAMP2 (the peptide correspond to amino acid 30-47) with a band around 14kDa in purified Lewy bodies from postmortem samples of PD brain using Western blot, whereas this 14kDa band was absent in purified samples of normal brain (figure 3-5, e-f). The presence of the 14kDa tVAMP2 fragment in purified Lewy bodies suggested the possibility that VAMP2 proteolysis could be associated with Lewy body formation. In order to confirm this phenomenon and determine the truncation site, large quantities of purified Lewy bodies were required so mass spectrometry and neoepitope mapping strategy could be used for peptide sequencing, a similar strategy that was used previously to determine α-synuclein fragments [178]. More importantly, tVAMP2 antibody appears to react only with Lewy bodies and Lewy neurites, while α-synuclein – a gold standard for PD and DLB neuropathological diagnosis, stained in both Lewy bodies and normal synapses (figure 3-2 and 3-3). Hence, the specificity of tVAMP2 antibody could have unique value for neuropathological diagnoses for PD and DLB. DLB is a Parkinsonism with early development of dementia, often accompanied by prominent visual hallucinations

and fluctuations in arousal, and pathologically showing widespread α-synuclein deposition predominantly involving the neocortex[179]. However, the number of Lewy bodies that stained by α-synuclein was higher than tVAMP2 and AtVAMP2 with statistical significance (figure 3-4, a-b). Furthermore, it remains to be elucidated whether the VAMP2 pathology applies to all sporadic and familial PD and DLB cases, and whether it is specific to Lewy body diseases or appears in other human neurodegenerative diseases such as Alzheimer's Disease, and multiple system atrophy. Using immunohistochemistry, there was predominant positive staining of tVAMP2 throughout the brainstem including Pons, Medulla, Rostral Medulla, Rostral Midbrain and Caudal Pons in PD brains, while absent in control brain (figure 3-7). In addition, tVAMP2 was also detected in glial cytoplasmic inclusions in MSA brain but absent in neurofibrillary tangles in AD brain (figure 3-12, 3-16). These pathologies were also observed with α-synuclein antibody staining (figure 3-13). Notably, co-localization of tVAMP2 and α-synuclein to Lewy bodies and Lewy neurites was observed in PD and DLB (figure 3-8 to 3-11), suggesting that truncated VAMP2 may be involved in the pathology of PD and other neurodegenerative diseases. This specific VAMP2 molecular pathology may have unique value in both understanding the pathogenesis and pathological diagnosis of PD and DLB. Furthermore, tVAMP2 positively stained fine extensions of the Lewy neurite and abnormal synapses which were not detected by α-synuclein antibodies (figure 3-9, j-o), and it co-localized with α-synuclein in the early-stage Lewy body (figure 3-9, g-i), indicating that tVAMP2 could be used as an early marker of Lewy body pathologies in PD and DLB.

4.1 Truncated VAMP2 but not full-length VAMP2 was relevant to the pathogenesis of Lewy bodies and Lewy neurites in PD and DLB.

The immunohistochemistry studies revealed that tVAMP2 positively-stained Lewy bodies and Lewy neurites were clearly present in PD and DLB, in contrast, fVAMP2 only stained a small number of Lewy bodies in PD and DLB with normal synapses strongly stained as well (figure 3-2). Since the binding site of VAMP2 and α-synuclein was its N-terminal 28 amino acids sequence, and our antibodies were specific to VAMP2 lacking those 28 N-terminal residues, suggesting the possibility that the N-terminal truncation of VAMP2 may play a significant role in the aggregation of α-synuclein in the formation of Lewy pathologies, however, the mechanism remained to be elucidated. The correlation between truncated VAMP2 and α-synuclein was also reported in a recent study by Burre et al., which showed that α-synuclein had no effect on SNARE complex assembly in the presence of N-terminally 28-residues truncated VAMP2 by co-expressing truncated VAMP2 on HEK293 cells [68].

After counting positively immunostained Lewy bodies with different antibodies in three independent cases of PD and DLB, it was demonstrated that tVAMP2 and AtVAMP2 antibodies stained similar amount of inclusions, which was significantly less than that of α-synuclein ($p<0.05$) (figure 3-4). In our hypothesis, the aggregation of α-synuclein could be influenced by the truncation of VAMP2, however, other factors may also be involved in its mechanism. For example, α-synuclein dimerization was shown to play an important part in conformational transition and aggregation of α-synuclein with consequent neurotoxicity [180]. The dimerization of α-synuclein was reported to be induced by intramolecular oxidative cross-linking of tyrosine residues[181], and its existence was demonstrated during the conversion of α-synuclein from monomer to oligomer in in-vitro experiments[182]. In addition, it was reported that the influence of hydrophobic interfacial area had an impact on the acceleration of α-synuclein aggregation [183], however, the reason was not clear.

When testing purified Lewy bodies from a PD brain in Western blot, the tVAMP2

and AtVAMP2 antibodies against aa30-47 residues detected full-length (17kDa), higher molecular weight (HMW) aggregates, and a strong 14kDa band for truncated VAMP2 fragment, whereas fVAMP2 antibody against aa2-17 residues only detected full-length 17kDa band (figure 3-5, e-g). Thus, the 3kDa molecular mass indicated the difference between full-length and truncated VAMP2. The 14kDa band was not detected by fVAMP2 antibody and could suggest that the aa2-17 residue was cleaved from the full-length VAMP2 and was missing in truncated VAMP2 in the formation of Lewy bodies, however, we could not exclude the possibility that fVAMP2 antibody had lower affinity to the protein of VAMP2 than tVAMP2 antibody. This 14kDa band was absent in purified samples of normal brain (figure 3-5, e-f), suggesting that it was involving and participating in two Lewy body pathologies. Meanwhile, this 14kDa band of VAMP2 and monomeric α-synuclein were absent in samples of brain homogenate, whereas the 17kDa band and the HMW aggregates of VAMP2 and polymeric α-synuclein could be detected. As discussed above, the 17kDa band represents full-length VAMP2 which is a vSNARE protein and exists in normal brain tissue, however, the 14kDa band corresponding to truncated VAMP2 only appears in pathological conditions such as Lewy bodies and Lewy neurites. It was reported that a large number of genes (n=13298) were found to be expressed in human brain[184], hence, the amount of Lewy inclusions that loaded onto the gel might not be sufficient to observe truncated VAMP2 and monomeric α-synuclein. Another possible explanation is that the trypsinization during Lewy body purification causes conformational change of the protein which exposes the truncated site and makes it detectable. Thus, purification of Lewy inclusions from PD and DLB brain tissue is a critical method in the research of truncated VAMP2. The experiment needs to be repeated in order to perform statistical analysis on the 14kDa band of VAMP2 when comparing control and PD cases.

4.2 The regional specificity of VAMP2 neuropathology in PD and DLB.

The brain regional involvement of VAMP2 pathology in PD (figure 3-7) was shown via immunohistochemistry. tVAMP2-stained Lewy bodies and Lewy neurites were distributed in different regions of brainstem (Pons, Medulla, Rostral Medulla, Rostral Midbrain and Caudal Pons). According to 6 major stages of PD pathology proposed by Braak et al[31], Lewy bodies and Lewy neurites are found within the medulla and pons in early stages (1-2), and substantia nigra will not be affected until stage 3, while supratentorial compartment and cerebral cortex will be involved in late stages (4-6). In neocortex, Lewy bodies were mainly and initially distributed in the inner pyramidal layer (V) and multiform cell layer (VI), as was observed in figure 3-6. Further study could be performed to test the consistency of tVAMP2 staining of pathologies in different stages of PD by co-studying the medical history of each patient. For example, the motor symptoms usually result from the death of dopaminergic cells in the substantia nigra especially the ventral part of the pars compacta [15]. The cognition is controlled by caudate nucleus. It was reported that the mild cognitive impairment (MCI) of PD exhibited increased atrophy and changes in the bilateral occipital, left temporal, and frontal cortices compared with healthy controls [185]. The REM sleep behavior disorder is associated with structural lesions in the dorsal midbrain and pons [186]. Loss of sense of smell may involve the olfactory epithelium, olfactory bulb/tract, primary olfactory cortices, and their secondary targets [187]. Interestingly, it was revealed that worse olfaction was associated with poorer memory and executive performance, indicating that the olfactory dysfunction could be a biomarker of additional extranigral disease [188].

4.3 Truncated VAMP2 was co-localized with α-synuclein in Lewy bodies and Lewy neurites, suggesting their synergetic effect in PD pathology.

In results of double immunofluorescence staining, it showed the neuronal co-localization of VAMP2 and α-synuclein in DLB (figure 3-8 to 3-11), providing strong evidence to our hypothesis. It was detected that recombinant and native α-synuclein purified from mouse brain promoted clustering of synaptic vesicles, and this kind of "clustering" was dependent on specific interactions of α-synuclein with VAMP2 as well as anionic lipids, and it could be disrupted by one of the Parkinson's disease-related point mutants of α-synuclein, A30P, which was the lipid-binding deficient mutation[146]. Burre et al. revealed a direct protein interaction between α-synuclein and VAMP2 and demonstrated that this interaction was critical for maintaining normal functions of SNARE complex assembly and preventing neurodegeneration especially under stress conditions [67]. Our results provided new insights in the interaction between VAMP2 and α-synuclein in the pathogenesis of PD and DLB. Further research on this interaction is needed to bring the mechanism of α-synuclein aggregation to light, particularly in the majority of sporadic cases without genetic abnormalities associated with α-synuclein.

Interestingly, the tVAMP2 antibody detected many finer extensions from α-synuclein positive Lewy neurites that were not detected by the α-synuclein antibody (figure 3-9, j-o). These tVAMP2 positive/α-synuclein negative structures could be the earliest sign of pathogenesis of Lewy bodies and Lewy neurites, indicating that tVAMP2 could be an early marker for synaptic abnormalities prior to accumulating detectable α-synuclein aggregates. It has already been widely considered that Lewy body pathology in PD, as revealed by α-synuclein staining, may be initiated in the medulla oblongata located dorsal motor nucleus of the vagus nerve and propagated rostrally to the substantia

nigra and eventually neocortex [189]. Our observation (figure 3-9) suggested that the antibody to tVAMP2 might be able to detect early stage of degenerating neurites even before the accumulating aggregates were detectable by α-synuclein antibody. Also, it was observed that tVAMP2 co-localized with α-synuclein in the early-stage Lewy body (figure 3-9, g-i). It was noteworthy that tVAMP2 staining had the consistent tendency of a more central localization in Lewy bodies and Lewy neurites, while α-synuclein positive staining was more to the periphery. It was reported that the mechanism of Lewy body formation involved several steps of α-synuclein aggregation and propagation: unfolded monomer ➔ propagating dimer ➔ oligomers ➔ small amyloid fibrils ➔ amyloid fibrils, and the accumulation of these amyloid fibrils eventually led to the formation of Lewy bodies [190]. Hence, it was possible that α-synuclein fibrils enwrapped tVAMP2 in Lewy bodies and Lewy neurites, especially when truncation of VAMP2 was an early event in the process. Further research is needed to image more neurons with tVAMP2 antibodies as well as neuronal specific markers such as MAP2 or NeuN to demonstrate reliability of co-localization and authenticity and neuronal cells. In addition, it is necessary to compare VAMP2 pathology with α-synuclein pathology in a large inventory of Lewy body cases and in different brain regions to confirm if VAMP2 is really an early event during Lewy neurodegeneration and if VAMP2 pathology precedes α-synuclein changes. Furthermore, the mechanism by which tVAMP2 might initiate α-synuclein aggregation is unclear. It is possible that the presence of full-length VAMP2 might prevent α-synuclein aggregation and that the absence of full-length VAMP2 through N-terminal truncation could initiate α-synuclein aggregation. To provide evidence to this hypothesis, further in-vivo or in-vitro studies are necessary to examine if stimulation of tVAMP2 or attenuation of fVAMP2 is capable of inducing α-synuclein aggregation, electron and atomic force microscopies could be used to observe the morphology of aggregates after

incubating with varying ratios of recombinant α-synuclein and tVAMP2 or silencing fVAMP2 under in vitro condition, or immunoblot and immunofluorescence double labeling could be used after transient co-transfection with various tVAMP2 fragments and α-synuclein or siRNA against fVAMP2 on SY5Y cells, a human neuroblastoma derived cell line widely used for α-synuclein research, or even on rats. On the other hand, the toxicity of tVAMP2 alone in the normal α-synuclein expression level and its effect on SNARE complex assembly should also be taken into account. SY5Y cell line or primary rat neurons could be used to test the toxicity of tVAMP2 by transfecting tVAMP2 plasmid into the cells or neurons.

Also, will the increase of tVAMP2 lead to the decrease in SNARE assembly? In order to test this, we could transfect rat neurons with tVAMP2 vector and measure the SNARE complexes assembly level by Western blot. We should note that the SNARE complexes are SDS resistant in the absence of boiling.

4.4 The disease specificity of tVAMP2 neuropathology.

Besides Lewy bodies and Lewy neurites in PD and DLB, tVAMP2 antibodies also positively stained Glial Cytoplasmic Inclusion (GCIs), the hallmark of MSA (figure 3-12 and 3-16), which are identical to the α-synuclein staining (figure 3-13). These disorders are collectively called synucleinopathies. MSA is a neurodegenerative disorder with cell loss and gliosis or a proliferation of astrocytes in damaged areas of the central nervous system. Currently, a confirmed diagnosis of MSA is largely based on the post-mortem pathological diagnosis, which shows Glial Cytoplasmic Inclusion (GCIs) in damaged areas.

However, the inclusions of Alzheimer's disease (AD) which is caused by Tau protein and so-called tauopathy, was not detectable by these two antibodies in immunohistochemistry, indicating that tVAMP2 antibody has as high disease

specificity as the traditional biomarker, α-synuclein, in detecting inclusions of synucleinopathies. AD is always characterized by the loss of neurons and synapses in the cerebral cortex and certain subcortical regions. Except neurofibrillary tangles, amyloid plaques are another kind of neuropathologic characterization visible by microscopy. The antibody of Tau protein is an ideal marker to detect tangles, as seen in figure 3-14. Tau is a neuronal microtubule-associated protein which can aggregate to form intracytoplasmic pathologic inclusions associated with neurodegeneration such as neurofibrillary tangles in AD[191]. In AD, the brain accumulates Tau protein in the form of neurofibrillary tangles, which can be positively stained by Tau antibody (figure 3-12). It is important to note that α-synuclein stained normal synapses simultaneously with Lewy bodies and Lewy neurites, which pollutes the background of the staining (figure 3-13), whereas tVAMP2 advantageously avoided this problem, providing tVAMP2 a superior position as a PD marker. However, it could not be excluded that the deep background staining by α-synuclein was caused by technical problems or quality of the antibodies. Hence, the immunohistochemical experiments with different α-synuclein antibodies on free-floating sections need to be repeated to improve the images. However, VAMP1/2/3, an antibody detecting full-length VAMP1, VAMP2 and VAMP3, failed to stain all the inclusions mentioned above (figure 3-15).

The pathological discrimination between PD and DLB still remains unclear. In our study, both tVAMP2 and α-synuclein antibodies successfully detected Lewy bodies and Lewy neurites in both of these two diseases. Besides loss of dopaminergic cells as seen in PD, DLB also features the loss of acetylcholine-producing neurons like AD, and is often accompanied by AD. Further research should be conducted to verify the value of truncated VAMP2 as a target for PD and other synucleinopathies by knockout studies using either siRNA or animal knockout models.

4.5 Detection of isoforms of tVAMP2

2D gel electrophoresis revealed four spots at around 14kDa with pIs of 5.7, 5.3, 5.0 and 4.7 suggesting that the shortened truncated form of VAMP2 has 4 isoforms. (figure 3-17, b). VAMP2 has a theoretical PI of 7.8, and the theoretical pI of truncated VAMP2 is 6.4. It was reported that four serine residues within VAMP2 could serve as potential phosphorylation sites[175]. A single phosphorylation will reduce the theoretical pI of full length VAMP2 to 6.08, while two, three and four phosphorylations will reduce the theoretical pI to 5.28, 4.95 and 4.73 respectively (calculated using the Isoelectric Point Calculator – VAMP2 (human) - http://isoelectric.ovh.org). As tVAMP2 has a lower pI when compared to intact VAMP2, the four spots could correspond to phosphorylated tVAMP2 with one to four phosphorylations. Alternatively, the spots could correspond to isoforms with between zero and three phosphorylations. To determine which of these scenarios is correct, the spots could be excised from a high capacity 2D gel and the spots analysed by mass spectrometry to determine the phosphorylation sites. However, it should be noted that the mass spectrometry analysis performed later did not identify any phosphorylated peptides. Therefore, it is also possible that other post translational modifications could be responsible for the charge shift.

4.6 Truncated VAMP2 is a component of Lewy bodies in both PD and DLB.

In order to determine the exact truncation site of VAMP2 in Lewy body pathologies, qTOF mass spectrometry was used to characterize protein compositions of purified Lewy bodies. Through immunoprecipitation of the tVAMP2 using the antibody, the eluted tVAMP2 could be applied for peptide

sequencing mass spectrometry to determine the truncation site. The peptide sequence of human VAMP2 is already known (figure 1-4). Alternatively, the neoepitope mapping strategy could be used to define the truncation site by testing various antibodies overlapping different VAMP2 fragments. Once the antibodies are generated, we can use Western blot of purified Lewy bodies to identify those that only recognize tVAMP2.

Digestion with Trypsin revealed two peptides corresponding to aa32-47 and aa60-83 of human VAMP2 in purified Lewy bodies of PD and DLB with a confidence level above 95% by mass spectrometry (figure 3-18b, in green). These amino acids covered a total of 34.5% human VAMP2 sequence (40 out of 116 AAs), providing clear evidence for the presence of VAMP2 in Lewy bodies of PD and DLB. Notably, a large peptide corresponding to N-terminal aa1-31 of human VAMP2 was not detected by mass spectrometry (figure 3-18b, in grey). The presence of two truncated peptides with cleavage sites at Arg30 and at Arg31 suggested the potential for a protease with Trypsin-like activity to be responsible for the cleavage. As Lewy body purification involved two very short Trypsin steps to release Lewy bodies from the cytoskeleton, there remained the possibility that the cleavage was due to the activity of Trypsin. While this could not be excluded, a number of observations suggested this was unlikely. First, the tVAMP2 was located at the center of the relatively dense Lewy bodies, and not at the periphery (figure 3-8 to 3-11), which made access to VAMP2 by trypsin difficult in the very short time frame of the two trypsin incubations: the first incubation was less than 10 seconds, and the second one was 5 minutes. Control experiments were performed by the developers of the purification technique (Dr Tim Chataway and Dr Amy McCormack) that demonstrated that it took 15 minutes of incubation with Trypsin before any reduction in size of Lewy bodies could be seen. Secondly, if Trypsin was active, there should be a number of other truncated peptides observed. The data file which was originally searched using

Glu C as the digesting enzyme was re-searched using trypsin as the digesting enzyme as well as a third enzyme Asp N as a control to determine if a significant number of Tryptic peptides were present. Despite three Glu C peptides being identified in the purified Lewy body preparation, the only two Tryptic peptides that were identified were the Arg 30 and Arg 31 peptides, suggesting that Trypsin was not active and was not responsible for the 2 Arginine cleavage sites. Finally, re-searching the data generated by the Glu C digestion using Trypsin as the designated protease identified only 6 proteins out of the one hundred proteins sequenced: Tubulin, GFAP, Creatine Kinase B, histone H3, Dynamin-1 and Myelin Basic Protein. Each of these proteins contained a very small number of Tryptic peptides. These proteins were likely to be adherent proteins associated with the exterior of the Lewy bodies and have generated Tryptic peptides as a consequence of their location. Hence, this very small number of proteins suggested that Trypsin was not active against core Lewy body proteins. Therefore, the absence of aa1-31 and the presence of aa32-47 detected by mass spectrometry provides evidence of VAMP2 truncation during the formation of Lewy body pathology, which would be greatly supportive to our hypothesis. Furthermore, as shown in figure 3-5, the tVAMP2 antibody was designed to recognize aa30-47 of VAMP2 sequence, and it successfully detected a 14kDa band in Western blot which was considered as the truncated VAMP2. Taking both of these results into consideration, the truncation site of VAMP2 is highly possible at the 30th and 31st amino acid of the sequence.

The lack of presence of the N-terminal 1-16 peptide suggested that full length VAMP2 was not present in sufficient quantity to allow detection of the peptide by mass spectrometry. However, an important control would be to sequence recombinant VAMP2 to ensure that the N-terminal peptide does indeed ionize and fragment, and could therefore be detectable by mass spectrometry. Unfortunately, we were not able to obtain any recombinant VAMP2 within the

time frame of this study. While the tVAMP2 cleavage is likely to be caused by proteolysis, it cannot be excluded that tVAMP2 is the result of an alternate RNA splicing isoform. However, this is unlikely as this specific isoform must then be specifically incorporated into Lewy bodies. A more plausible explanation is that a protease acts on VAMP2 to generate tVAMP2.

Furthermore, in order to identify the truncation site, we need to use additional enzymes other than trypsin for LB purification. Specific cleavage is critical for determining the truncation site; for example, trypsin cleaves peptide chains mainly at the carboxyl side of lysine or arginine; proline-endopeptidase preferentially cleaves at proline site; endoproteinase Glu C specifically cleaves peptide chains at glutamate; and Asp-N hydrolyzes peptide bonds at the amino side of aspartate and cysteic acid residues. However, the source of human brain tissue was highly restricted to us, and there was not sufficient tissue for us to repeat the purification experiment. The output rate of purification was quite low, for instance, 59 grams of grey matter yielded 56.7ug of purified Lewy body inclusions in PD, and 33 grams of grey matter yielded 66ug of purified Lewy bodies in DLB. We used up all the purified inclusions from six independent purification experiments to develop and optimize the purification procedures and to repeat and ensure consistent results. Hence, further research could be done when brain tissue is available.

Conclusions

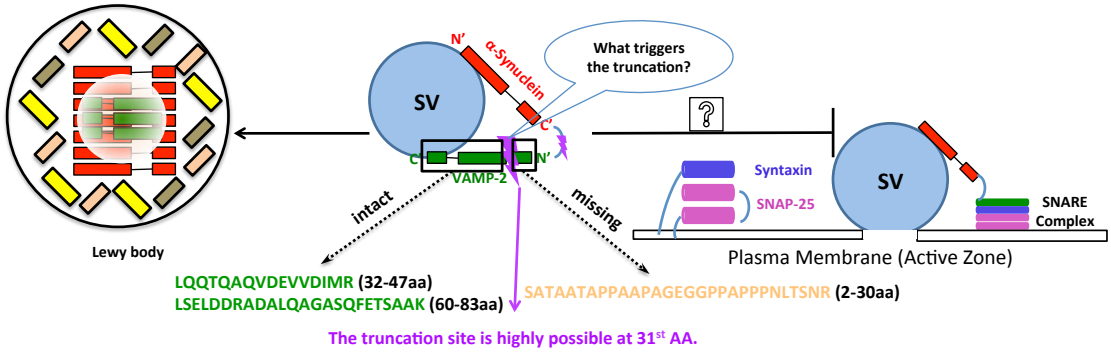

Figure 4-1: diagram of truncated VAMP2 in Lewy body formation. In PD and DLB, VAMP2 is truncated and fail to form SNARE complex with Syntaxin and SNAP-25 and hence inhibits neurotransmitter release. The truncation site is highly possible at the 31st AA of VAMP2 based on the peptide sequence detected by mass spectrometry. The absence of full-length VAMP2 caused by N-terminal truncation triggers the aggregation of α-synuclein. The aggregated α-synuclein localizes more to the edge of Lewy bodies and overlaps with truncated VAMP2 in the center of Lewy bodies. Both of these two proteins participate in the formation of Lewy bodies with other proteins. However, the factor that triggers the truncation of VAMP2 remains to be elucidated.

This study characterized a novel VAMP2 pathology in Parkinson's disease via the following findings:

1. Truncated VAMP2 existed in Lewy bodies and Lewy neurites in PD and DLB and co-localized with α-synuclein.
2. Truncated VAMP2 localized to the core of Lewy bodies and detected finer extensions of Lewy neurites when compared to α-synuclein, and truncated VAMP2 existed in early-stage Lewy bodies, indicating that it could be an early marker for pathologies of PD and DLB.

3. The tVAMP2 antibody corresponding to aa30-47 residues was an eligible antibody to detect Lewy pathologies. It was specific to synucleinopathies without detecting inclusions of Tauopathies.
4. Two peptide sequences of VAMP2 were detected by mass spectrometry from purified Lewy bodies, whereas the N-terminus was missing, highly suggesting that the truncation site was at 31st AA of VAMP2.

Reference

1. de Lau, L.M. and M.M. Breteler, *Epidemiology of Parkinson's disease.* Lancet Neurol, 2006. **5**(6): p. 525-35.
2. Van Den Eeden, S.K., C.M. Tanner, A.L. Bernstein, R.D. Fross, et al., *Incidence of Parkinson's disease: variation by age, gender, and race/ethnicity.* Am J Epidemiol, 2003. **157**(11): p. 1015-22.
3. Djaldetti, R., N. Lev, and E. Melamed, *Lesions outside the CNS in Parkinson's disease.* Mov Disord, 2009. **24**(6): p. 793-800.
4. Beach, T.G., C.H. Adler, L.I. Sue, L. Vedders, et al., *Multi-organ distribution of phosphorylated alpha-synuclein histopathology in subjects with Lewy body disorders.* Acta Neuropathol, 2010. **119**(6): p. 689-702.
5. Braak, H. and K. Del Tredici, *Invited Article: Nervous system pathology in sporadic Parkinson disease.* Neurology, 2008. **70**(20): p. 1916-25.
6. Fumimura, Y., M. Ikemura, Y. Saito, R. Sengoku, et al., *Analysis of the adrenal gland is useful for evaluating pathology of the peripheral autonomic nervous system in lewy body disease.* J Neuropathol Exp Neurol, 2007. **66**(5): p. 354-62.
7. Ikemura, M., Y. Saito, R. Sengoku, Y. Sakiyama, et al., *Lewy body pathology involves cutaneous nerves.* J Neuropathol Exp Neurol, 2008. **67**(10): p. 945-53.
8. Orimo, S., T. Uchihara, A. Nakamura, F. Mori, et al., *Axonal alpha-synuclein aggregates herald centripetal degeneration of cardiac sympathetic nerve in Parkinson's disease.* Brain, 2008. **131**(Pt 3): p. 642-50.
9. Wakabayashi, K., F. Mori, K. Tanji, S. Orimo, et al., *Involvement of the peripheral nervous system in synucleinopathies, tauopathies and other neurodegenerative proteinopathies of the brain.* Acta Neuropathol, 2010. **120**(1): p. 1-12.
10. Braak, H., M. Sastre, J.R. Bohl, R.A. de Vos, et al., *Parkinson's disease: lesions in dorsal horn layer I, involvement of parasympathetic and sympathetic pre- and postganglionic neurons.* Acta Neuropathol, 2007. **113**(4): p. 421-9.
11. Dickson, D.W., H. Fujishiro, C. Orr, A. DelleDonne, et al., *Neuropathology of non-motor features of Parkinson disease.* Parkinsonism Relat Disord, 2009. **15 Suppl 3**: p. S1-5.
12. Shino, M.Y., V. McGuire, S.K. Van Den Eeden, C.M. Tanner, et al., *Familial aggregation of Parkinson's disease in a multiethnic community-based case-control study.* Mov Disord, 2010. **25**(15): p. 2587-94.
13. Elbaz, A., J.H. Bower, B.J. Peterson, D.M. Maraganore, et al., *Survival study of Parkinson disease in Olmsted County, Minnesota.* Arch Neurol, 2003. **60**(1): p. 91-6.
14. Hawkes, C.H., *The prodromal phase of sporadic Parkinson's disease: does it exist and if so how long is it?* Mov Disord, 2008. **23**(13): p. 1799-807.
15. Rodriguez-Oroz, M.C., M. Jahanshahi, P. Krack, I. Litvan, et al., *Initial*

clinical manifestations of Parkinson's disease: features and pathophysiological mechanisms. Lancet Neurol, 2009. **8**(12): p. 1128-39.
16. Jankovic, J., *Parkinson's disease: clinical features and diagnosis.* J Neurol Neurosurg Psychiatry, 2008. **79**(4): p. 368-76.
17. Barichella, M., E. Cereda, and G. Pezzoli, *Major nutritional issues in the management of Parkinson's disease.* Mov Disord, 2009. **24**(13): p. 1881-92.
18. Caballol, N., M.J. Marti, and E. Tolosa, *Cognitive dysfunction and dementia in Parkinson disease.* Mov Disord, 2007. **22 Suppl 17**: p. S358-66.
19. Hely, M.A., J.G. Morris, W.G. Reid, and R. Trafficante, *Sydney Multicenter Study of Parkinson's disease: non-L-dopa-responsive problems dominate at 15 years.* Mov Disord, 2005. **20**(2): p. 190-9.
20. Davie, C.A., *A review of Parkinson's disease.* Br Med Bull, 2008. **86**: p. 109-27.
21. Spillantini, M.G., J.R. Murrell, M. Goedert, M.R. Farlow, et al., *Mutation in the tau gene in familial multiple system tauopathy with presenile dementia.* Proc Natl Acad Sci U S A, 1998. **95**(13): p. 7737-41.
22. Gallagher, C.L., T.R. Oakes, S.C. Johnson, M.K. Chung, et al., *Rate of 6-[18F]fluorodopa uptake decline in striatal subregions in Parkinson's disease.* Mov Disord, 2011. **26**(4): p. 614-20.
23. Porritt, M.J., P.E. Batchelor, A.J. Hughes, R. Kalnins, et al., *New dopaminergic neurons in Parkinson's disease striatum.* Lancet, 2000. **356**(9223): p. 44-5.
24. San Sebastian, W., J. Guillen, M. Manrique, S. Belzunegui, et al., *Modification of the number and phenotype of striatal dopaminergic cells by carotid body graft.* Brain, 2007. **130**(Pt 5): p. 1306-16.
25. Mundinano, I.C., M.C. Caballero, C. Ordonez, M. Hernandez, et al., *Increased dopaminergic cells and protein aggregates in the olfactory bulb of patients with neurodegenerative disorders.* Acta Neuropathol, 2011. **122**(1): p. 61-74.
26. Spillantini, M.G., M.L. Schmidt, V.M. Lee, J.Q. Trojanowski, et al., *Alpha-synuclein in Lewy bodies.* Nature, 1997. **388**(6645): p. 839-40.
27. Healy, D.G., P.M. Abou-Sleiman, A.J. Lees, J.P. Casas, et al., *Tau gene and Parkinson's disease: a case-control study and meta-analysis.* J Neurol Neurosurg Psychiatry, 2004. **75**(7): p. 962-5.
28. Gan-Or, Z., N. Giladi, U. Rozovski, C. Shifrin, et al., *Genotype-phenotype correlations between GBA mutations and Parkinson disease risk and onset.* Neurology, 2008. **70**(24): p. 2277-83.
29. Zabetian, C.P., A. Samii, A.D. Mosley, J.W. Roberts, et al., *A clinic-based study of the LRRK2 gene in Parkinson disease yields new mutations.* Neurology, 2005. **65**(5): p. 741-4.
30. Jellinger, K.A., *Neuropathology of sporadic Parkinson's disease: evaluation*

and changes of concepts. Mov Disord, 2012. **27**(1): p. 8-30.
31. Braak, H., K. Del Tredici, U. Rub, R.A. de Vos, et al., *Staging of brain pathology related to sporadic Parkinson's disease.* Neurobiol Aging, 2003. **24**(2): p. 197-211.
32. Savica, R., B.R. Grossardt, J.H. Bower, B.F. Boeve, et al., *Incidence of dementia with Lewy bodies and Parkinson disease dementia.* JAMA Neurol, 2013. **70**(11): p. 1396-402.
33. Fujishiro, H., H. Umegaki, D. Isojima, H. Akatsu, et al., *Depletion of cholinergic neurons in the nucleus of the medial septum and the vertical limb of the diagonal band in dementia with Lewy bodies.* Acta Neuropathol, 2006. **111**(2): p. 109-14.
34. Colloby, S.J., S. McParland, J.T. O'Brien, and J. Attems, *Neuropathological correlates of dopaminergic imaging in Alzheimer's disease and Lewy body dementias.* Brain, 2012. **135**(Pt 9): p. 2798-808.
35. Donaghy, P.C. and I.G. McKeith, *The clinical characteristics of dementia with Lewy bodies and a consideration of prodromal diagnosis.* Alzheimers Res Ther, 2014. **6**(4): p. 46.
36. Mayo, M.C. and Y. Bordelon, *Dementia with Lewy bodies.* Semin Neurol, 2014. **34**(2): p. 182-8.
37. Mori, E., M. Ikeda, K. Kosaka, and D.L.B.S.I. Donepezil, *Donepezil for dementia with Lewy bodies: a randomized, placebo-controlled trial.* Ann Neurol, 2012. **72**(1): p. 41-52.
38. Graff-Radford, J., B.F. Boeve, O. Pedraza, T.J. Ferman, et al., *Imaging and acetylcholinesterase inhibitor response in dementia with Lewy bodies.* Brain, 2012. **135**(Pt 8): p. 2470-7.
39. Vanacore, N., V. Bonifati, G. Fabbrini, C. Colosimo, et al., *Epidemiology of multiple system atrophy. ESGAP Consortium. European Study Group on Atypical Parkinsonisms.* Neurol Sci, 2001. **22**(1): p. 97-9.
40. Bjornsdottir, A., G. Gudmundsson, H. Blondal, and E. Olafsson, *Incidence and prevalence of multiple system atrophy: a nationwide study in Iceland.* J Neurol Neurosurg Psychiatry, 2013. **84**(2): p. 136-40.
41. Wenning, G.K., C. Colosimo, F. Geser, and W. Poewe, *Multiple system atrophy.* Lancet Neurol, 2004. **3**(2): p. 93-103.
42. Swan, L. and J. Dupont, *Multiple system atrophy.* Phys Ther, 1999. **79**(5): p. 488-94.
43. Watanabe, H., Y. Saito, S. Terao, T. Ando, et al., *Progression and prognosis in multiple system atrophy: an analysis of 230 Japanese patients.* Brain, 2002. **125**(Pt 5): p. 1070-83.
44. Tandon, R. and S. Pradhan, *Autonomic predominant multiple system atrophy in the context of Parkinsonian and cerebellar variants.* Clin Neurol Neurosurg, 2015. **130**: p. 110-3.
45. Lin, D.J., K.L. Hermann, and J.D. Schmahmann, *Multiple system atrophy of*

the cerebellar type: clinical state of the art. Mov Disord, 2014. **29**(3): p. 294-304.
46. Burn, D.J. and E. Jaros, *Multiple system atrophy: cellular and molecular pathology.* Mol Pathol, 2001. **54**(6): p. 419-26.
47. Papp, M.I., J.E. Kahn, and P.L. Lantos, *Glial cytoplasmic inclusions in the CNS of patients with multiple system atrophy (striatonigral degeneration, olivopontocerebellar atrophy and Shy-Drager syndrome).* J Neurol Sci, 1989. **94**(1-3): p. 79-100.
48. Wakabayashi, K., M. Yoshimoto, S. Tsuji, and H. Takahashi, *Alpha-synuclein immunoreactivity in glial cytoplasmic inclusions in multiple system atrophy.* Neurosci Lett, 1998. **249**(2-3): p. 180-2.
49. Wenning, G.K. and S. Braune, *Multiple system atrophy: pathophysiology and management.* CNS Drugs, 2001. **15**(11): p. 839-52.
50. Clayton, D.F. and J.M. George, *The synucleins: a family of proteins involved in synaptic function, plasticity, neurodegeneration and disease.* Trends Neurosci, 1998. **21**(6): p. 249-54.
51. Bellucci, A., L. Navarria, M. Zaltieri, C. Missale, et al., *alpha-Synuclein synaptic pathology and its implications in the development of novel therapeutic approaches to cure Parkinson's disease.* Brain Res, 2012. **1432**: p. 95-113.
52. George, J.M., *The synucleins.* Genome Biol, 2002. **3**(1): p. REVIEWS3002.
53. Hashimoto, M., E. Rockenstein, M. Mante, M. Mallory, et al., *beta-Synuclein inhibits alpha-synuclein aggregation: a possible role as an anti-parkinsonian factor.* Neuron, 2001. **32**(2): p. 213-23.
54. Ahmad, M., S. Attoub, M.N. Singh, F.L. Martin, et al., *Gamma-synuclein and the progression of cancer.* FASEB J, 2007. **21**(13): p. 3419-30.
55. Bayer, T.A., P. Jakala, T. Hartmann, R. Egensperger, et al., *Neural expression profile of alpha-synuclein in developing human cortex.* Neuroreport, 1999. **10**(13): p. 2799-803.
56. Beyer, K., *Alpha-synuclein structure, posttranslational modification and alternative splicing as aggregation enhancers.* Acta Neuropathol, 2006. **112**(3): p. 237-51.
57. Davidson, W.S., A. Jonas, D.F. Clayton, and J.M. George, *Stabilization of alpha-synuclein secondary structure upon binding to synthetic membranes.* J Biol Chem, 1998. **273**(16): p. 9443-9.
58. Chandra, S., X. Chen, J. Rizo, R. Jahn, et al., *A broken alpha -helix in folded alpha -Synuclein.* J Biol Chem, 2003. **278**(17): p. 15313-8.
59. Burre, J., S. Vivona, J. Diao, M. Sharma, et al., *Properties of native brain alpha-synuclein.* Nature, 2013. **498**(7453): p. E4-6; discussion E6-7.
60. Weinreb, P.H., W. Zhen, A.W. Poon, K.A. Conway, et al., *NACP, a protein implicated in Alzheimer's disease and learning, is natively unfolded.* Biochemistry, 1996. **35**(43): p. 13709-15.

61. Serpell, L.C., J. Berriman, R. Jakes, M. Goedert, et al., *Fiber diffraction of synthetic alpha-synuclein filaments shows amyloid-like cross-beta conformation.* Proc Natl Acad Sci U S A, 2000. **97**(9): p. 4897-902.
62. Waxman, E.A. and B.I. Giasson, *Molecular mechanisms of alpha-synuclein neurodegeneration.* Biochim Biophys Acta, 2009. **1792**(7): p. 616-24.
63. Conway, K.A., J.D. Harper, and P.T. Lansbury, *Accelerated in vitro fibril formation by a mutant alpha-synuclein linked to early-onset Parkinson disease.* Nat Med, 1998. **4**(11): p. 1318-20.
64. Ulmer, T.S. and A. Bax, *Comparison of structure and dynamics of micelle-bound human alpha-synuclein and Parkinson disease variants.* J Biol Chem, 2005. **280**(52): p. 43179-87.
65. Bonini, N.M. and B.I. Giasson, *Snaring the function of alpha-synuclein.* Cell, 2005. **123**(3): p. 359-61.
66. Schoch, S., F. Deak, A. Konigstorfer, M. Mozhayeva, et al., *SNARE function analyzed in synaptobrevin/VAMP knockout mice.* Science, 2001. **294**(5544): p. 1117-22.
67. Burre, J., M. Sharma, T. Tsetsenis, V. Buchman, et al., *Alpha-synuclein promotes SNARE-complex assembly in vivo and in vitro.* Science, 2010. **329**(5999): p. 1663-7.
68. Burre, J., M. Sharma, and T.C. Sudhof, *alpha-Synuclein assembles into higher-order multimers upon membrane binding to promote SNARE complex formation.* Proc Natl Acad Sci U S A, 2014. **111**(40): p. E4274-83.
69. Schulz-Schaeffer, W.J., *The synaptic pathology of alpha-synuclein aggregation in dementia with Lewy bodies, Parkinson's disease and Parkinson's disease dementia.* Acta Neuropathol, 2010. **120**(2): p. 131-43.
70. Calabresi, P., N.B. Mercuri, and M. Di Filippo, *Synaptic plasticity, dopamine and Parkinson's disease: one step ahead.* Brain, 2009. **132**(Pt 2): p. 285-7.
71. Polymeropoulos, M.H., C. Lavedan, E. Leroy, S.E. Ide, et al., *Mutation in the alpha-synuclein gene identified in families with Parkinson's disease.* Science, 1997. **276**(5321): p. 2045-7.
72. Kruger, R., W. Kuhn, T. Muller, D. Woitalla, et al., *Ala30Pro mutation in the gene encoding alpha-synuclein in Parkinson's disease.* Nat Genet, 1998. **18**(2): p. 106-8.
73. Zarranz, J.J., J. Alegre, J.C. Gomez-Esteban, E. Lezcano, et al., *The new mutation, E46K, of alpha-synuclein causes Parkinson and Lewy body dementia.* Ann Neurol, 2004. **55**(2): p. 164-73.
74. Kiely, A.P., Y.T. Asi, E. Kara, P. Limousin, et al., *alpha-Synucleinopathy associated with G51D SNCA mutation: a link between Parkinson's disease and multiple system atrophy?* Acta Neuropathol, 2013. **125**(5): p. 753-69.
75. Proukakis, C., C.G. Dudzik, T. Brier, D.S. MacKay, et al., *A novel alpha-synuclein missense mutation in Parkinson disease.* Neurology, 2013. **80**(11): p. 1062-4.

76. Singleton, A.B., M. Farrer, J. Johnson, A. Singleton, et al., *alpha-Synuclein locus triplication causes Parkinson's disease.* Science, 2003. **302**(5646): p. 841.
77. Chartier-Harlin, M.C., J. Kachergus, C. Roumier, V. Mouroux, et al., *Alpha-synuclein locus duplication as a cause of familial Parkinson's disease.* Lancet, 2004. **364**(9440): p. 1167-9.
78. Lesage, S. and A. Brice, *Parkinson's disease: from monogenic forms to genetic susceptibility factors.* Hum Mol Genet, 2009. **18**(R1): p. R48-59.
79. Fujiwara, H., M. Hasegawa, N. Dohmae, A. Kawashima, et al., *alpha-Synuclein is phosphorylated in synucleinopathy lesions.* Nat Cell Biol, 2002. **4**(2): p. 160-4.
80. Sugeno, N., A. Takeda, T. Hasegawa, M. Kobayashi, et al., *Serine 129 phosphorylation of alpha-synuclein induces unfolded protein response-mediated cell death.* J Biol Chem, 2008. **283**(34): p. 23179-88.
81. Hardy, J. and K. Gwinn-Hardy, *Genetic classification of primary neurodegenerative disease.* Science, 1998. **282**(5391): p. 1075-9.
82. Spillantini, M.G., R.A. Crowther, R. Jakes, M. Hasegawa, et al., *alpha-Synuclein in filamentous inclusions of Lewy bodies from Parkinson's disease and dementia with lewy bodies.* Proc Natl Acad Sci U S A, 1998. **95**(11): p. 6469-73.
83. Spillantini, M.G. and M. Goedert, *The alpha-synucleinopathies: Parkinson's disease, dementia with Lewy bodies, and multiple system atrophy.* Ann N Y Acad Sci, 2000. **920**: p. 16-27.
84. Masliah, E., E. Rockenstein, I. Veinbergs, Y. Sagara, et al., *beta-amyloid peptides enhance alpha-synuclein accumulation and neuronal deficits in a transgenic mouse model linking Alzheimer's disease and Parkinson's disease.* Proc Natl Acad Sci U S A, 2001. **98**(21): p. 12245-50.
85. Wakabayashi, K. and H. Takahashi, *Neuropathology of autonomic nervous system in Parkinson's disease.* Eur Neurol, 1997. **38 Suppl 2**: p. 2-7.
86. Solano, S.M., D.W. Miller, S.J. Augood, A.B. Young, et al., *Expression of alpha-synuclein, parkin, and ubiquitin carboxy-terminal hydrolase L1 mRNA in human brain: genes associated with familial Parkinson's disease.* Ann Neurol, 2000. **47**(2): p. 201-10.
87. Sharrad, D.F., W.P. Gai, and S.J. Brookes, *Selective coexpression of synaptic proteins, alpha-synuclein, cysteine string protein-alpha, synaptophysin, synaptotagmin-1, and synaptobrevin-2 in vesicular acetylcholine transporter-immunoreactive axons in the guinea pig ileum.* J Comp Neurol, 2013. **521**(11): p. 2523-37.
88. Sharrad, D.F., E. de Vries, and S.J. Brookes, *Selective expression of alpha-synuclein-immunoreactivity in vesicular acetylcholine transporter-immunoreactive axons in the guinea pig rectum and human colon.* J Comp Neurol, 2013. **521**(3): p. 657-76.

89. Asuni, A.A., K. Hilton, Z. Siskova, K. Lunnon, et al., *Alpha-synuclein deficiency in the C57BL/6JOlaHsd strain does not modify disease progression in the ME7-model of prion disease.* Neuroscience, 2010. **165**(3): p. 662-74.
90. Wilhelmus, M.M., R. Verhaar, G. Andringa, J.G. Bol, et al., *Presence of tissue transglutaminase in granular endoplasmic reticulum is characteristic of melanized neurons in Parkinson's disease brain.* Brain Pathol, 2011. **21**(2): p. 130-9.
91. Nath, S., J. Goodwin, Y. Engelborghs, and D.L. Pountney, *Raised calcium promotes alpha-synuclein aggregate formation.* Mol Cell Neurosci, 2011. **46**(2): p. 516-26.
92. Bellucci, A., G. Collo, I. Sarnico, L. Battistin, et al., *Alpha-synuclein aggregation and cell death triggered by energy deprivation and dopamine overload are counteracted by D2/D3 receptor activation.* J Neurochem, 2008. **106**(2): p. 560-77.
93. Alvarez-Erviti, L., Y. Couch, J. Richardson, J.M. Cooper, et al., *Alpha-synuclein release by neurons activates the inflammatory response in a microglial cell line.* Neurosci Res, 2011. **69**(4): p. 337-42.
94. Przedborski, S., *Inflammation and Parkinson's disease pathogenesis.* Mov Disord, 2010. **25 Suppl 1**: p. S55-7.
95. Duka, T., M. Rusnak, R.E. Drolet, V. Duka, et al., *Alpha-synuclein induces hyperphosphorylation of Tau in the MPTP model of parkinsonism.* FASEB J, 2006. **20**(13): p. 2302-12.
96. Duka, T. and A. Sidhu, *The neurotoxin, MPP+, induces hyperphosphorylation of Tau, in the presence of alpha-Synuclein, in SH-SY5Y neuroblastoma cells.* Neurotox Res, 2006. **10**(1): p. 1-10.
97. Duka, T., V. Duka, J.N. Joyce, and A. Sidhu, *Alpha-Synuclein contributes to GSK-3beta-catalyzed Tau phosphorylation in Parkinson's disease models.* FASEB J, 2009. **23**(9): p. 2820-30.
98. Qureshi, H.Y. and H.K. Paudel, *Parkinsonian neurotoxin 1-methyl-4-phenyl-1,2,3,6-tetrahydropyridine (MPTP) and alpha-synuclein mutations promote Tau protein phosphorylation at Ser262 and destabilize microtubule cytoskeleton in vitro.* J Biol Chem, 2011. **286**(7): p. 5055-68.
99. Fujishiro, H., Y. Tsuboi, W.L. Lin, H. Uchikado, et al., *Co-localization of tau and alpha-synuclein in the olfactory bulb in Alzheimer's disease with amygdala Lewy bodies.* Acta Neuropathol, 2008. **116**(1): p. 17-24.
100. Kloepper, T.H., C.N. Kienle, and D. Fasshauer, *An elaborate classification of SNARE proteins sheds light on the conservation of the eukaryotic endomembrane system.* Mol Biol Cell, 2007. **18**(9): p. 3463-71.
101. Sutton, R.B., D. Fasshauer, R. Jahn, and A.T. Brunger, *Crystal structure of a SNARE complex involved in synaptic exocytosis at 2.4 A resolution.* Nature, 1998. **395**(6700): p. 347-53.

102. Rizo, J. and T.C. Sudhof, *The membrane fusion enigma: SNAREs, Sec1/Munc18 proteins, and their accomplices--guilty as charged?* Annu Rev Cell Dev Biol, 2012. **28**: p. 279-308.
103. Sudhof, T.C., *The synaptic vesicle cycle.* Annu Rev Neurosci, 2004. **27**: p. 509-47.
104. Sudhof, T.C. and J.E. Rothman, *Membrane fusion: grappling with SNARE and SM proteins.* Science, 2009. **323**(5913): p. 474-7.
105. Jahn, R. and R.H. Scheller, *SNAREs--engines for membrane fusion.* Nat Rev Mol Cell Biol, 2006. **7**(9): p. 631-43.
106. Gray, B.C., Z. Siskova, V.H. Perry, and V. O'Connor, *Selective presynaptic degeneration in the synaptopathy associated with ME7-induced hippocampal pathology.* Neurobiol Dis, 2009. **35**(1): p. 63-74.
107. Fdez, E., M. Martinez-Salvador, M. Beard, P. Woodman, et al., *Transmembrane-domain determinants for SNARE-mediated membrane fusion.* J Cell Sci, 2010. **123**(Pt 14): p. 2473-80.
108. Walter, A.M., K. Wiederhold, D. Bruns, D. Fasshauer, et al., *Synaptobrevin N-terminally bound to syntaxin-SNAP-25 defines the primed vesicle state in regulated exocytosis.* J Cell Biol, 2010. **188**(3): p. 401-13.
109. Chapman, E.R., *Synaptotagmin: a Ca(2+) sensor that triggers exocytosis?* Nat Rev Mol Cell Biol, 2002. **3**(7): p. 498-508.
110. Blasi, J., E.R. Chapman, E. Link, T. Binz, et al., *Botulinum neurotoxin A selectively cleaves the synaptic protein SNAP-25.* Nature, 1993. **365**(6442): p. 160-3.
111. Blasi, J., E.R. Chapman, S. Yamasaki, T. Binz, et al., *Botulinum neurotoxin C1 blocks neurotransmitter release by means of cleaving HPC-1/syntaxin.* EMBO J, 1993. **12**(12): p. 4821-8.
112. Schiavo, G., O. Rossetto, S. Catsicas, P. Polverino de Laureto, et al., *Identification of the nerve terminal targets of botulinum neurotoxin serotypes A, D, and E.* J Biol Chem, 1993. **268**(32): p. 23784-7.
113. Simpson, L.L., J.A. Coffield, and N. Bakry, *Chelation of zinc antagonizes the neuromuscular blocking properties of the seven serotypes of botulinum neurotoxin as well as tetanus toxin.* J Pharmacol Exp Ther, 1993. **267**(2): p. 720-7.
114. Schiavo, G., M. Matteoli, and C. Montecucco, *Neurotoxins affecting neuroexocytosis.* Physiol Rev, 2000. **80**(2): p. 717-66.
115. Turton, K., J.A. Chaddock, and K.R. Acharya, *Botulinum and tetanus neurotoxins: structure, function and therapeutic utility.* Trends Biochem Sci, 2002. **27**(11): p. 552-8.
116. Dolly, J.O., J. Black, R.S. Williams, and J. Melling, *Acceptors for botulinum neurotoxin reside on motor nerve terminals and mediate its internalization.* Nature, 1984. **307**(5950): p. 457-60.
117. Montecucco, C. and G. Schiavo, *Structure and function of tetanus and*

botulinum neurotoxins. Q Rev Biophys, 1995. **28**(4): p. 423-72.
118. Gerst, J.E., *SNAREs and SNARE regulators in membrane fusion and exocytosis.* Cell Mol Life Sci, 1999. **55**(5): p. 707-34.
119. Hayashi, T., H. McMahon, S. Yamasaki, T. Binz, et al., *Synaptic vesicle membrane fusion complex: action of clostridial neurotoxins on assembly.* EMBO J, 1994. **13**(21): p. 5051-61.
120. Mayer, A., W. Wickner, and A. Haas, *Sec18p (NSF)-driven release of Sec17p (alpha-SNAP) can precede docking and fusion of yeast vacuoles.* Cell, 1996. **85**(1): p. 83-94.
121. Sollner, T., M.K. Bennett, S.W. Whiteheart, R.H. Scheller, et al., *A protein assembly-disassembly pathway in vitro that may correspond to sequential steps of synaptic vesicle docking, activation, and fusion.* Cell, 1993. **75**(3): p. 409-18.
122. Sollner, T., S.W. Whiteheart, M. Brunner, H. Erdjument-Bromage, et al., *SNAP receptors implicated in vesicle targeting and fusion.* Nature, 1993. **362**(6418): p. 318-24.
123. Hanson, P.I., R. Roth, H. Morisaki, R. Jahn, et al., *Structure and conformational changes in NSF and its membrane receptor complexes visualized by quick-freeze/deep-etch electron microscopy.* Cell, 1997. **90**(3): p. 523-35.
124. Weber, T., B.V. Zemelman, J.A. McNew, B. Westermann, et al., *SNAREpins: minimal machinery for membrane fusion.* Cell, 1998. **92**(6): p. 759-72.
125. Zhou, P., T. Bacaj, X. Yang, Z.P. Pang, et al., *Lipid-anchored SNAREs lacking transmembrane regions fully support membrane fusion during neurotransmitter release.* Neuron, 2013. **80**(2): p. 470-83.
126. Han, X., C.T. Wang, J. Bai, E.R. Chapman, et al., *Transmembrane segments of syntaxin line the fusion pore of Ca2+-triggered exocytosis.* Science, 2004. **304**(5668): p. 289-92.
127. Ngatchou, A.N., K. Kisler, Q. Fang, A.M. Walter, et al., *Role of the synaptobrevin C terminus in fusion pore formation.* Proc Natl Acad Sci U S A, 2010. **107**(43): p. 18463-8.
128. Margittai, M., H. Otto, and R. Jahn, *A stable interaction between syntaxin 1a and synaptobrevin 2 mediated by their transmembrane domains.* FEBS Lett, 1999. **446**(1): p. 40-4.
129. Stein, A., G. Weber, M.C. Wahl, and R. Jahn, *Helical extension of the neuronal SNARE complex into the membrane.* Nature, 2009. **460**(7254): p. 525-8.
130. Hata, Y., C.A. Slaughter, and T.C. Sudhof, *Synaptic vesicle fusion complex contains unc-18 homologue bound to syntaxin.* Nature, 1993. **366**(6453): p. 347-51.
131. Misura, K.M., R.H. Scheller, and W.I. Weis, *Three-dimensional structure of the neuronal-Sec1-syntaxin 1a complex.* Nature, 2000. **404**(6776): p.

355-62.
132. Dulubova, I., S. Sugita, S. Hill, M. Hosaka, et al., *A conformational switch in syntaxin during exocytosis: role of munc18.* EMBO J, 1999. **18**(16): p. 4372-82.
133. Ma, C., W. Li, Y. Xu, and J. Rizo, *Munc13 mediates the transition from the closed syntaxin-Munc18 complex to the SNARE complex.* Nat Struct Mol Biol, 2011. **18**(5): p. 542-9.
134. Xu, Y., L. Su, and J. Rizo, *Binding of Munc18-1 to synaptobrevin and to the SNARE four-helix bundle.* Biochemistry, 2010. **49**(8): p. 1568-76.
135. Schollmeier, Y., J.M. Krause, S. Kreye, J. Malsam, et al., *Resolving the function of distinct Munc18-1/SNARE protein interaction modes in a reconstituted membrane fusion assay.* J Biol Chem, 2011. **286**(35): p. 30582-90.
136. Yamaguchi, T., I. Dulubova, S.W. Min, X. Chen, et al., *Sly1 binds to Golgi and ER syntaxins via a conserved N-terminal peptide motif.* Dev Cell, 2002. **2**(3): p. 295-305.
137. Shen, J., D.C. Tareste, F. Paumet, J.E. Rothman, et al., *Selective activation of cognate SNAREpins by Sec1/Munc18 proteins.* Cell, 2007. **128**(1): p. 183-95.
138. Parisotto, D., M. Pfau, A. Scheutzow, K. Wild, et al., *An extended helical conformation in domain 3a of Munc18-1 provides a template for SNARE (soluble N-ethylmaleimide-sensitive factor attachment protein receptor) complex assembly.* J Biol Chem, 2014. **289**(14): p. 9639-50.
139. Brose, N., A.G. Petrenko, T.C. Sudhof, and R. Jahn, *Synaptotagmin: a calcium sensor on the synaptic vesicle surface.* Science, 1992. **256**(5059): p. 1021-5.
140. Geppert, M., Y. Goda, R.E. Hammer, C. Li, et al., *Synaptotagmin I: a major Ca2+ sensor for transmitter release at a central synapse.* Cell, 1994. **79**(4): p. 717-27.
141. Kummel, D., S.S. Krishnakumar, D.T. Radoff, F. Li, et al., *Complexin cross-links prefusion SNAREs into a zigzag array.* Nat Struct Mol Biol, 2011. **18**(8): p. 927-33.
142. Shao, X., C. Li, I. Fernandez, X. Zhang, et al., *Synaptotagmin-syntaxin interaction: the C2 domain as a Ca2+-dependent electrostatic switch.* Neuron, 1997. **18**(1): p. 133-42.
143. Giraudo, C.G., W.S. Eng, T.J. Melia, and J.E. Rothman, *A clamping mechanism involved in SNARE-dependent exocytosis.* Science, 2006. **313**(5787): p. 676-80.
144. Reim, K., M. Mansour, F. Varoqueaux, H.T. McMahon, et al., *Complexins regulate a late step in Ca2+-dependent neurotransmitter release.* Cell, 2001. **104**(1): p. 71-81.
145. Wang, D., D. Epstein, O. Khalaf, S. Srinivasan, et al., *Ca2+-Calmodulin*

regulates SNARE assembly and spontaneous neurotransmitter release via v-ATPase subunit V0a1. J Cell Biol, 2014. **205**(1): p. 21-31.
146. Diao, J., J. Burre, S. Vivona, D.J. Cipriano, et al., *Native alpha-synuclein induces clustering of synaptic-vesicle mimics via binding to phospholipids and synaptobrevin-2/VAMP2.* Elife (Cambridge), 2013. **2**: p. e00592.
147. Burre, J., M. Sharma, and T.C. Sudhof, *Systematic mutagenesis of alpha-synuclein reveals distinct sequence requirements for physiological and pathological activities.* J Neurosci, 2012. **32**(43): p. 15227-42.
148. Sharma, M., J. Burre, P. Bronk, Y. Zhang, et al., *CSPalpha knockout causes neurodegeneration by impairing SNAP-25 function.* EMBO J, 2012. **31**(4): p. 829-41.
149. Sharma, M., J. Burre, and T.C. Sudhof, *CSPalpha promotes SNARE-complex assembly by chaperoning SNAP-25 during synaptic activity.* Nat Cell Biol, 2011. **13**(1): p. 30-9.
150. Fernandez-Chacon, R., M. Wolfel, H. Nishimune, L. Tabares, et al., *The synaptic vesicle protein CSP alpha prevents presynaptic degeneration.* Neuron, 2004. **42**(2): p. 237-51.
151. Chandra, S., G. Gallardo, R. Fernandez-Chacon, O.M. Schluter, et al., *Alpha-synuclein cooperates with CSPalpha in preventing neurodegeneration.* Cell, 2005. **123**(3): p. 383-96.
152. Schmitz, F., L. Tabares, D. Khimich, N. Strenzke, et al., *CSPalpha-deficiency causes massive and rapid photoreceptor degeneration.* Proc Natl Acad Sci U S A, 2006. **103**(8): p. 2926-31.
153. Greten-Harrison, B., M. Polydoro, M. Morimoto-Tomita, L. Diao, et al., *alphabetagamma-Synuclein triple knockout mice reveal age-dependent neuronal dysfunction.* Proc Natl Acad Sci U S A, 2010. **107**(45): p. 19573-8.
154. Scott, D.A., I. Tabarean, Y. Tang, A. Cartier, et al., *A pathologic cascade leading to synaptic dysfunction in alpha-synuclein-induced neurodegeneration.* J Neurosci, 2010. **30**(24): p. 8083-95.
155. Garcia-Reitbock, P., O. Anichtchik, A. Bellucci, M. Iovino, et al., *SNARE protein redistribution and synaptic failure in a transgenic mouse model of Parkinson's disease.* Brain, 2010. **133**(Pt 7): p. 2032-44.
156. Lai, Y., S. Kim, J. Varkey, X. Lou, et al., *Nonaggregated alpha-Synuclein Influences SNARE-Dependent Vesicle Docking via Membrane Binding.* Biochemistry, 2014. **53**(24): p. 3889-96.
157. Conway, K.A., J.C. Rochet, R.M. Bieganski, and P.T. Lansbury, Jr., *Kinetic stabilization of the alpha-synuclein protofibril by a dopamine-alpha-synuclein adduct.* Science, 2001. **294**(5545): p. 1346-9.
158. Choi, B.K., M.G. Choi, J.Y. Kim, Y. Yang, et al., *Large alpha-synuclein oligomers inhibit neuronal SNARE-mediated vesicle docking.* Proc Natl Acad Sci U S A, 2013. **110**(10): p. 4087-92.
159. Nakamura, K., V.M. Nemani, F. Azarbal, G. Skibinski, et al., *Direct*

membrane association drives mitochondrial fission by the Parkinson disease-associated protein alpha-synuclein. J Biol Chem, 2011. **286**(23): p. 20710-26.

160. Banerjee, R., A.A. Starkov, M.F. Beal, and B. Thomas, *Mitochondrial dysfunction in the limelight of Parkinson's disease pathogenesis.* Biochim Biophys Acta, 2009. **1792**(7): p. 651-63.
161. Esteves, A.R., D.M. Arduino, D.F. Silva, C.R. Oliveira, et al., *Mitochondrial Dysfunction: The Road to Alpha-Synuclein Oligomerization in PD.* Parkinsons Dis, 2011. **2011**: p. 693761.
162. Manning, G., D.B. Whyte, R. Martinez, T. Hunter, et al., *The protein kinase complement of the human genome.* Science, 2002. **298**(5600): p. 1912-34.
163. Lu, G.W., J. Chen, L.A. Espinoza, S. Garfield, et al., *Protein kinase D 3 is localized in vesicular structures and interacts with vesicle-associated membrane protein 2.* Cellular Signalling, 2007. **19**(4): p. 867-879.
164. Arthur, C.P. and M.H. Stowell, *Structure of synaptophysin: a hexameric MARVEL-domain channel protein.* Structure, 2007. **15**(6): p. 707-14.
165. Becher, A., A. Drenckhahn, I. Pahner, M. Margittai, et al., *The synaptophysin-synaptobrevin complex: a hallmark of synaptic vesicle maturation.* J Neurosci, 1999. **19**(6): p. 1922-31.
166. Washbourne, P., G. Schiavo, and C. Montecucco, *Vesicle-associated membrane protein-2 (synaptobrevin-2) forms a complex with synaptophysin.* Biochem J, 1995. **305 (Pt 3)**: p. 721-4.
167. Khvotchev, M.V. and T.C. Sudhof, *Stimulus-dependent dynamic homo- and heteromultimerization of synaptobrevin/VAMP and synaptophysin.* Biochemistry, 2004. **43**(47): p. 15037-43.
168. Siddiqui, T.J., O. Vites, A. Stein, R. Heintzmann, et al., *Determinants of synaptobrevin regulation in membranes.* Mol Biol Cell, 2007. **18**(6): p. 2037-46.
169. Bonanomi, D., L. Rusconi, C.A. Colombo, F. Benfenati, et al., *Synaptophysin I selectively specifies the exocytic pathway of synaptobrevin 2/VAMP2.* Biochem J, 2007. **404**(3): p. 525-34.
170. Pennuto, M., D. Bonanomi, F. Benfenati, and F. Valtorta, *Synaptophysin I controls the targeting of VAMP2/synaptobrevin II to synaptic vesicles.* Mol Biol Cell, 2003. **14**(12): p. 4909-19.
171. Deak, F., S. Schoch, X.R. Liu, T.C. Sudhof, et al., *Synaptobrevin is essential for fast synaptic-vesicle endocytosis.* Nature Cell Biology, 2004. **6**(11): p. 1102-U21.
172. Gordon, S.L. and M.A. Cousin, *X-linked intellectual disability-associated mutations in synaptophysin disrupt synaptobrevin II retrieval.* J Neurosci, 2013. **33**(34): p. 13695-700.
173. Bao, H., R.W. Daniels, G.T. MacLeod, M.P. Charlton, et al., *AP180 maintains the distribution of synaptic and vesicle proteins in the nerve terminal and*

indirectly regulates the efficacy of Ca2+-triggered exocytosis. J Neurophysiol, 2005. **94**(3): p. 1888-903.
174. Koo, S.J., S. Markovic, D. Puchkov, C.C. Mahrenholz, et al., *SNARE motif-mediated sorting of synaptobrevin by the endocytic adaptors clathrin assembly lymphoid myeloid leukemia (CALM) and AP180 at synapses.* Proceedings of the National Academy of Sciences of the United States of America, 2011. **108**(33): p. 13540-13545.
175. Raghanti, M.A., M.A. Spocter, C. Butti, P.R. Hof, et al., *A comparative perspective on minicolumns and inhibitory GABAergic interneurons in the neocortex.* Front Neuroanat, 2010. **4**: p. 3.
176. Burn, D.J., *Cortical Lewy body disease.* J Neurol Neurosurg Psychiatry, 2004. **75**(2): p. 175-8.
177. Fritzius, T., A.D. Frey, M. Schweneker, D. Mayer, et al., *WD-repeat-propeller-FYVE protein, ProF, binds VAMP2 and protein kinase Czeta.* FEBS J, 2007. **274**(6): p. 1552-66.
178. Anderson, J.P., D.E. Walker, J.M. Goldstein, R. de Laat, et al., *Phosphorylation of Ser-129 is the dominant pathological modification of alpha-synuclein in familial and sporadic Lewy body disease.* J Biol Chem, 2006. **281**(40): p. 29739-52.
179. McKeith, I.G., D.W. Dickson, J. Lowe, M. Emre, et al., *Diagnosis and management of dementia with Lewy bodies: third report of the DLB Consortium.* Neurology, 2005. **65**(12): p. 1863-72.
180. Roostaee, A., S. Beaudoin, A. Staskevicius, and X. Roucou, *Aggregation and neurotoxicity of recombinant alpha-synuclein aggregates initiated by dimerization.* Mol Neurodegener, 2013. **8**: p. 5.
181. Krishnan, S., E.Y. Chi, S.J. Wood, B.S. Kendrick, et al., *Oxidative dimer formation is the critical rate-limiting step for Parkinson's disease alpha-synuclein fibrillogenesis.* Biochemistry, 2003. **42**(3): p. 829-37.
182. Iwata, A., M. Maruyama, T. Akagi, T. Hashikawa, et al., *Alpha-synuclein degradation by serine protease neurosin: implication for pathogenesis of synucleinopathies.* Hum Mol Genet, 2003. **12**(20): p. 2625-35.
183. Pronchik, J., X. He, J.T. Giurleo, and D.S. Talaga, *In vitro formation of amyloid from alpha-synuclein is dominated by reactions at hydrophobic interfaces.* J Am Chem Soc, 2010. **132**(28): p. 9797-803.
184. Naumova, O.Y., M. Lee, S.Y. Rychkov, N.V. Vlasova, et al., *Gene expression in the human brain: the current state of the study of specificity and spatiotemporal dynamics.* Child Dev, 2013. **84**(1): p. 76-88.
185. Hanganu, A., C. Bedetti, T. Jubault, J.F. Gagnon, et al., *Mild cognitive impairment in patients with Parkinson's disease is associated with increased cortical degeneration.* Mov Disord, 2013. **28**(10): p. 1360-9.
186. Boeve, B.F., M.H. Silber, C.B. Saper, T.J. Ferman, et al., *Pathophysiology of REM sleep behaviour disorder and relevance to neurodegenerative disease.*

Brain, 2007. **130**(Pt 11): p. 2770-88.
187. Attems, J., L. Walker, and K.A. Jellinger, *Olfactory bulb involvement in neurodegenerative diseases.* Acta Neuropathol, 2014. **127**(4): p. 459-75.
188. Morley, J.F., D. Weintraub, E. Mamikonyan, P.J. Moberg, et al., *Olfactory Dysfunction Is Associated with Neuropsychiatric Manifestations in Parkinson's Disease.* Movement Disorders, 2011. **26**(11): p. 2051-2057.
189. Braak, H., U. Rub, W.P. Gai, and K. Del Tredici, *Idiopathic Parkinson's disease: possible routes by which vulnerable neuronal types may be subject to neuroinvasion by an unknown pathogen.* J Neural Transm, 2003. **110**(5): p. 517-36.
190. Lashuel, H.A., C.R. Overk, A. Oueslati, and E. Masliah, *The many faces of alpha-synuclein: from structure and toxicity to therapeutic target.* Nat Rev Neurosci, 2013. **14**(1): p. 38-48.
191. Ballatore, C., V.M. Lee, and J.Q. Trojanowski, *Tau-mediated neurodegeneration in Alzheimer's disease and related disorders.* Nat Rev Neurosci, 2007. **8**(9): p. 663-72.